2003

IDENTIFICATION OF NATURAL ATTENUATION OF TRICHLOROETHENE AND TECHNETIUM-99 ALONG LITTLE BAYOU CREEK, McCRACKEN COUNTY, KENTUCKY

Abhijit Mukherjee
University of Kentucky, amukh2@uky.edu

ABSTRACT OF THESIS

IDENTIFICATION OF NATURAL ATTENUATION OF TRICHLOROETHENE AND TECHNETIUM-99 ALONG LITTLE BAYOU CREEK, McCRACKEN COUNTY, KENTUCKY

Natural attenuation of trichloroethene (TCE) and technetium (^{99}Tc) was studied for five consecutive seasons (from January 2002 to January 2003) in Little Bayou Creek. The stream receives ground water discharge from an aquifer contaminated by past waste disposal activities at the Paducah Gaseous Diffusion Plant (PGDP), a uranium enrichment facility near Paducah, Kentucky. Results from stream gaging, contaminant monitoring, tracer tests (with bromide, nitrate, rhodamine WT and propane) and simulation modeling indicate the TCE is naturally attenuated by volatilization and dilution, with volatilization rates related to the ambient temperature and surface discharge rate. The only apparent mechanism of ^{99}Tc attenuation is dilution. Travel times of non-gaseous tracers were found to be similar and have highest values in October and lowest in June. It was also estimated from modeling that the transport of the solutes in the stream was mostly one-dimensional with insignificant secondary storage.

Keywords: natural attenuation, trichloroethene, technetium, tracer test, Paducah

Abhijit Mukherjee

18 April 2003

IDENTIFICATION OF NATURAL ATTENUATION OF TRICHLOROETHENE AND TECHNETIUM-99 ALONG LITTLE BAYOU CREEK, McCRACKEN COUNTY, KENTUCKY

By

Abhijit Mukherjee

Alan E. Fryar
Director of Thesis and
Director of Graduate Studies

18 April 2003

RULES FOR THE USE OF THESIS

Unpublished theses submitted for the Master's degree and deposited in the University of Kentucky Library are as a rule open for inspection, but are to be used only with due regard to the rights of the authors. Bibliographical references may be noted, but quotations or summaries of parts may be published only with the permission of the author, and with the usual scholarly acknowledgements.

Extensive copying or publication of the thesis in whole or in part also requires the consent of the Dean of the Graduate School of the University of Kentucky.

THESIS

Abhijit Mukherjee

The Graduate School

University of Kentucky

2003

IDENTIFICATION OF NATURAL ATTENUATION OF TRICHLOROETHENE AND TECHNETIUM-99 ALONG LITTLE BAYOU CREEK, McCRACKEN COUNTY, KENTUCKY

THESIS

A thesis submitted in partial fulfillment
of the requirements for the degree of Master of Science in the
College of Arts and Sciences
at the University of Kentucky

By
Abhijit Mukherjee

Director: Dr. Alan E. Fryar, Associate Professor of Geological Sciences
Lexington, Kentucky
2003

This thesis is dedicated to my grandmother late Shefalika Devi and my parents Kajali and Barindra Lal Mukherjee

Acknowledgements

First of all, I would like to show my earnest gratitude and appreciation to my teacher and advisor Dr. Alan Fryar, through whom executing this research work and writing this thesis has become possible. His teachings of hydrogeology and the constant support he gave me both during laboratory analysis and field work were invaluable assets for doing this work. Furthermore, his patience in answering my endless questions and emotional support he gave me after traveling for the first time to a foreign country in the opposite hemisphere of the globe will remain as an unforgettable memory to me throughout my life.

I would also like to sincerely acknowledge the help I got from Dr. Elisa D'Angelo of the UK Department of Agronomy for the gas chromatograph analysis, Jim Currens and Randy Paylor of the Kentucky Geological Survey for fluorometry analysis, Milinda Hamilton of the UK Department of Forestry for nitrate and bromide analysis, Dr. Sue Rimmer for her support in planning the research, and Gaye Brewer and Brian Begley (Kentucky Division of Waste Management) for helping me in sampling during field work. I would also like to show my special thanks to my colleague Ravi Kanda and my lab mates Todd McFarland, Danita LaSage, Lee Gatterdam, Todd Aseltyne and Tom Reed for their help on various occasions.

I would like to thank the Commonwealth of Kentucky, the Graduate School of the University of Kentucky, the Brown-McFarlan Fund and the Southeastern Section of the Geological Society of America for providing funds for this thesis work. Thanks also to Pam Stephens and Mary Sue Johnson for providing me help with the official procedures.

Last but not least, I wish to show my heartiest gratitude to my parents, brothers Indrajit and Prosenjit, and other family members together with my beloved friends back home in India, and also my aunt, uncle and cousins in Pennsylvania, for their constant emotional support and good wishes during my long stay for higher studies in the USA. Finally, I would like to thank my fiancée Abira for her everlasting patience, inspiration and trust in me.

Table of Contents

List of Tables

List of Figures

List of Figures (*continued*)

List of Figures (*continued*)

List of Files

abmthesis.pdf

Chapter 1
Introduction

Contamination of ground water and surface water by organic and inorganic pollutants is one of the most formidable environmental crises of the contemporary world. Of these, the chlorinated hydrocarbons (CHCs), like polychlorinated biphenyls (PCBs) and chloroethenes, are among the most widely occurring aqueous contaminants at waste disposal sites (Plumb and Pitchford, 1985) and in water supply wells (Westrick et al., 1984; Chapelle, 1993) of industrially developed countries. Moreover, remediation processes for CHCs have been difficult and expensive, if at all possible.

Little Bayou Creek is a first-order tributary to the Ohio River. The stream receives a considerable amount of inflow from an aquifer contaminated by past waste disposal activities at the Paducah Gaseous Diffusion Plant (PGDP), a US Department of Energy (USDOE) uranium enrichment facility (Figure 1.1) in Mississippi Embayment area (Figure 1.2) of the McCracken County, Kentucky (Figure 1.3). These activities have resulted in contamination of surface water and ground water by trichloroethene (TCE), a suspected carcinogen, and technetium-99 (^{99}Tc), a radionuclide. The PGDP site is listed on the National Priority List (i.e., it is a Superfund site). The creek is also polluted by PCBs, which has resulted in its listing as a Clean Water Act 303(d) stream and also one of the 110 water bodies classified as first priority for Total Maximum Daily Load program development by the Kentucky Division of Water.

1.1 Object and Scope of Work

The primary objective of this study was to understand and quantify the degree and nature of natural attenuation of specific contaminants following seepage into surface flow. The processes of attenuation, including in-stream dilution, volatilization, and sorption to the stream sediments, for TCE and ^{99}Tc were studied in Little Bayou Creek. The seasonal (quarterly) measurement of 1) stream flow, 2) in-stream contaminant concentrations, and 3) transport of injected tracers in the stream helped to assess the qualitative and quantitative aspects of attenuation and its seasonal variability. In order to examine seasonal variability, measurements were taken during baseflow

conditions (i.e., in the absence of rainfall). Conservative, non-conservative and visual tracers were mixed with the stream water to measure attenuation. Stream flow was also gaged at pre-determined locations to estimate ground water inflow.

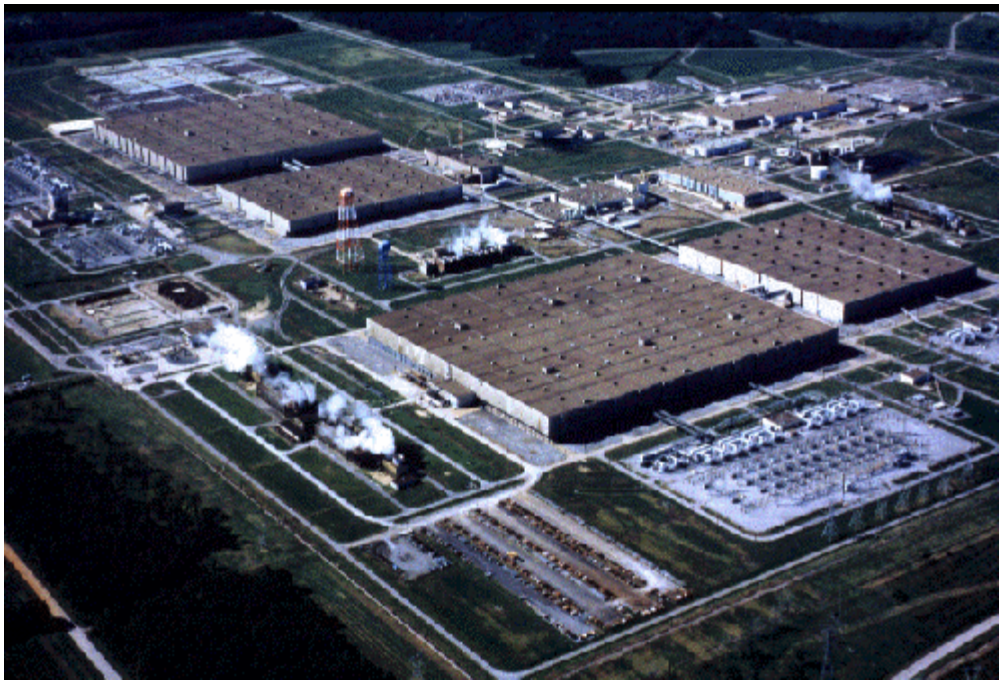

Figure 1.1: Aerial view of Paducah Gaseous Diffusion Plant.

1.2 Importance of the Work

Volatile organic compounds (VOCs) such as TCE, which are widespread contaminants, may discharge to streams under natural hydraulic gradients (Kim and Hemond, 1998). Hence the study of interactions between surface water and contaminated ground water can be crucial in understanding the fate and possible remediation of contaminants.

Contamination of Little Bayou Creek potentially poses a threat to the ecosystem of the surrounding West Kentucky Wildlife Management Area. Other workers have studied seepage of VOCs to streams elsewhere in North America (e.g., Kim and Hemond (1998) in Massachusetts, Conant (2001) in Ontario, Imbrigiotta et al. (1996) in New Jersey). However, none of these studies appears to have looked at the fate of the contaminant downstream from sites of seepage, and none has been undertaken in the Gulf Coastal Plain.

1.3 Previous Work

The geology and ground water resources of McCracken County and the surrounding area have been studied extensively by Davis et al. (1973) and reviewed by Carey and Stickney (2001). Further studies on the geology of the area, including the PGDP site, have been done by Olive (1966, 1980), Finch (1967), Kolata et al. (1981), and Davis (1996). Clausen et al. (1992), CH2M Hill Southeast, Inc. (1992), Jacobs Engineering Group Inc. (1995), Jacobs EM Team (1999) and several others have extensively studied the hydrogeology of the PGDP site and its vicinity. Evaldi and McClain (1989) measured temperature, specific conductance and stream flow in August 1989 along Little Bayou Creek. Fryar (1997) and Fryar et al. (2000) examined the fate of TCE and ^{99}Tc in ground water and surface water in the vicinity of the PGDP. Butler (1999) and Etienne (1999) studied the possibility of intrinsic biodegradation of TCE in the study area, while Sweat (2000) studied sorption of TCE to soils and sediments from the vicinity of the PGDP. LaSage and Fryar (2000) described the seasonal variability in stream flow, spring flow, contaminant concentrations and fate of contaminants along the flow path.

Characteristics and sampling methods for VOC-contaminated discharging ground water have been described by Fusillo et al. (1991). Samples were collected by minipiezometers immediately beneath the stream bed. Seepage meters were used to measure the VOC concentration in discharging ground water by Avery et al. (1991). Vroblesky et al. (1991) used vapor samplers as an alternative to traditional sampling mechanisms.

Various workers have studied the fate of VOCs and other solutes in stream and ground water by tracer techniques. Kilpatrick and Cobb (1985) and Kilpatrick et al. (1987) discussed technologies of working with tracers and methods of measuring gaseous exchange rates between stream water and the ambient atmosphere. Methods of working with steady state tracer gas have also been described by Yotsukura et al. (1983). Genereux and Hemond (1990) used in-stream gaseous and solute tracers in Walker Branch, on the Oak Ridge Reservation in Tennessee, to measure the levels of ^{222}Rn, a hydrological flow-path indicator under steady stream-flow conditions. Similar studies with gaseous tracers have also been done by Grant and Skavroneck (1980), who used ethylene and propane in Wisconsin; Genereux and Hemond (1992), who used

liquidified petroleum gas (mainly propane) in Walker Branch, Tennessee, and Wanninkhof et al. (1990), who used SF_6 in Tennessee. Kim and Hemond (1998) studied the attenuation of VOCs in the Aberjona River in Massachusetts by introduction of a conservative and a volatile tracer in the stream water and subsequent solving of mass-balance equations for tracers and VOCs along the reach. Kimball et al. (2001) quantified mine-drainage inflows in a creek in Utah by tracer injections and simultaneous synoptic sampling.

1.4 Description of the Study Area

Location

Little Bayou Creek flows for about 11 km from its source, through the West Kentucky Wildlife Management Area (WKWMA), an 11.25 km^2 preserve, to its confluence with Bayou Creek, which drains to the Ohio River (Figure 1.4). The watershed of the creek encompasses an area of about 14.9 km^2. The PGDP is situated on the divide between the watersheds of Bayou Creek and Little Bayou Creek, approximately 14 km west of the city of Paducah (37° 07' 25" north latitude and 88° 48' 59" west longitude). The site is situated within the U.S. Geological Survey (USGS) 7.5 minute Heath and Joppa quadrangle topographic maps.

General Physiography

The study area lies within the northern tip of the Mississippi Embayment portion of the Gulf Coastal Plain province (Figure 1.2). Topographically, McCracken County is generally a rolling plain. The surface of the uplands is rolling but there are large areas of level land present between some of the streams, including the flood plains of the Clarks, Ohio, and Tennessee Rivers. In the Ohio River flood plain the normal elevation is about 91 m above MSL.

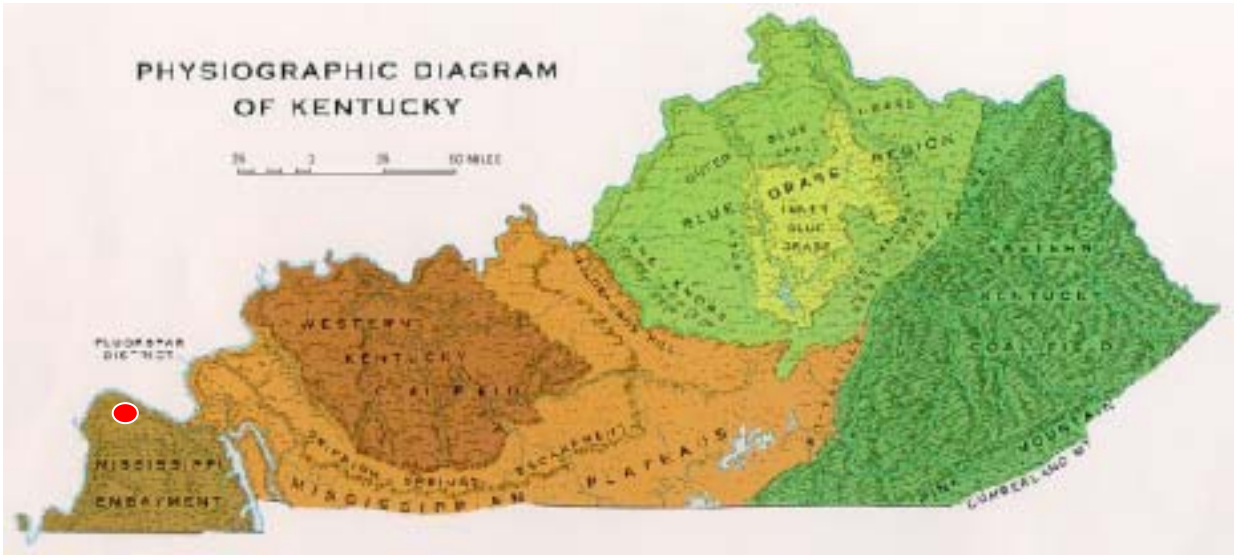

Figure 1.2: Physiographic map of Kentucky.
(Source http://www.uky.edu/KG/coal/webgeoky/pages/physiographic.html)

The highest elevation, about 150 m above MSL, is found along the Tennessee Valley divide near St. Johns in the southern part of the county. High elevations are also present in the uplands between Mayfield Creek and the West Fork of Massac Creek in the southwestern part (McGrain and Currens, 1978).

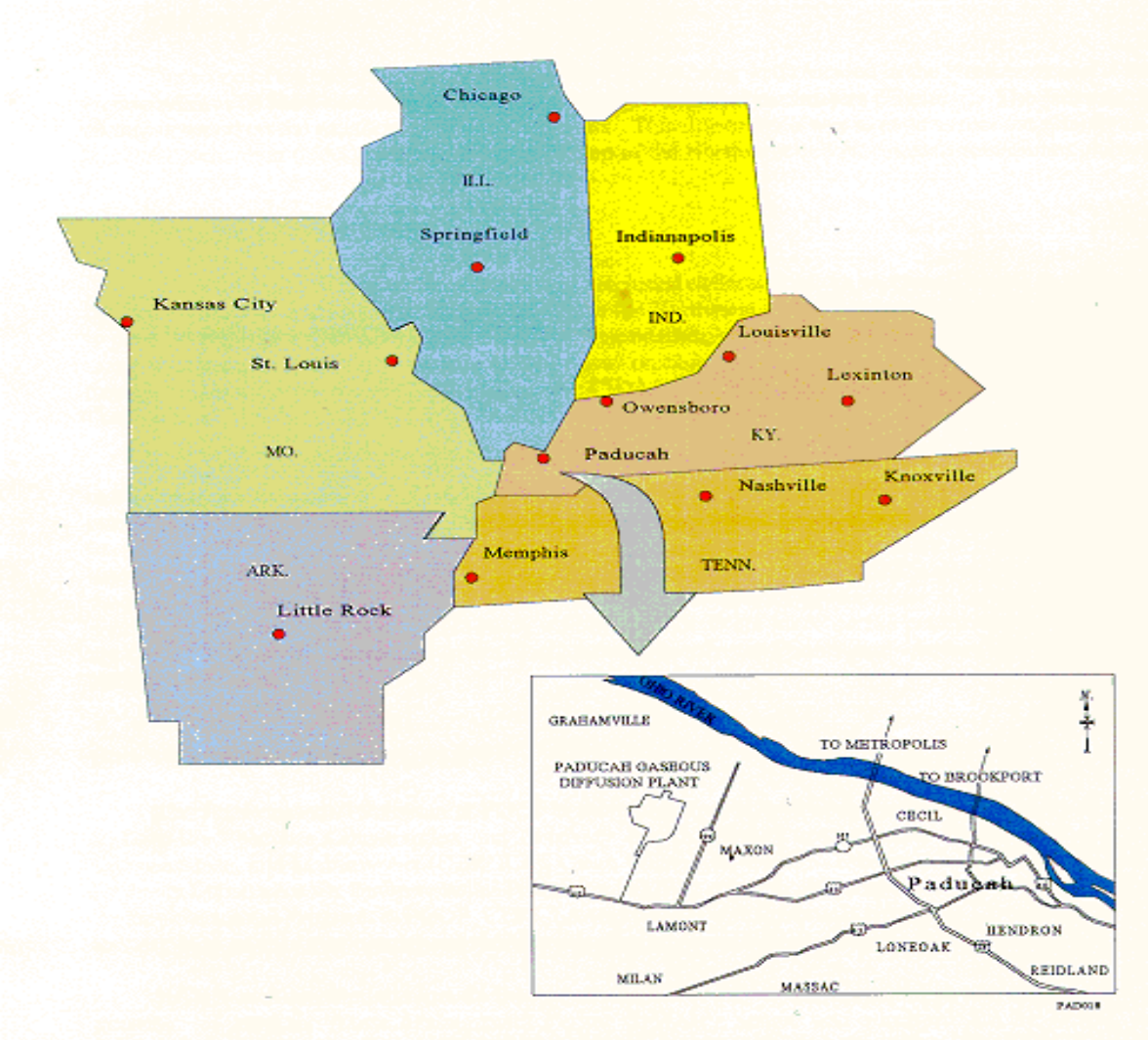

Figure 1.3: Location of Kentucky and Paducah with respect to the neighboring states (Clausen et al., 1997).

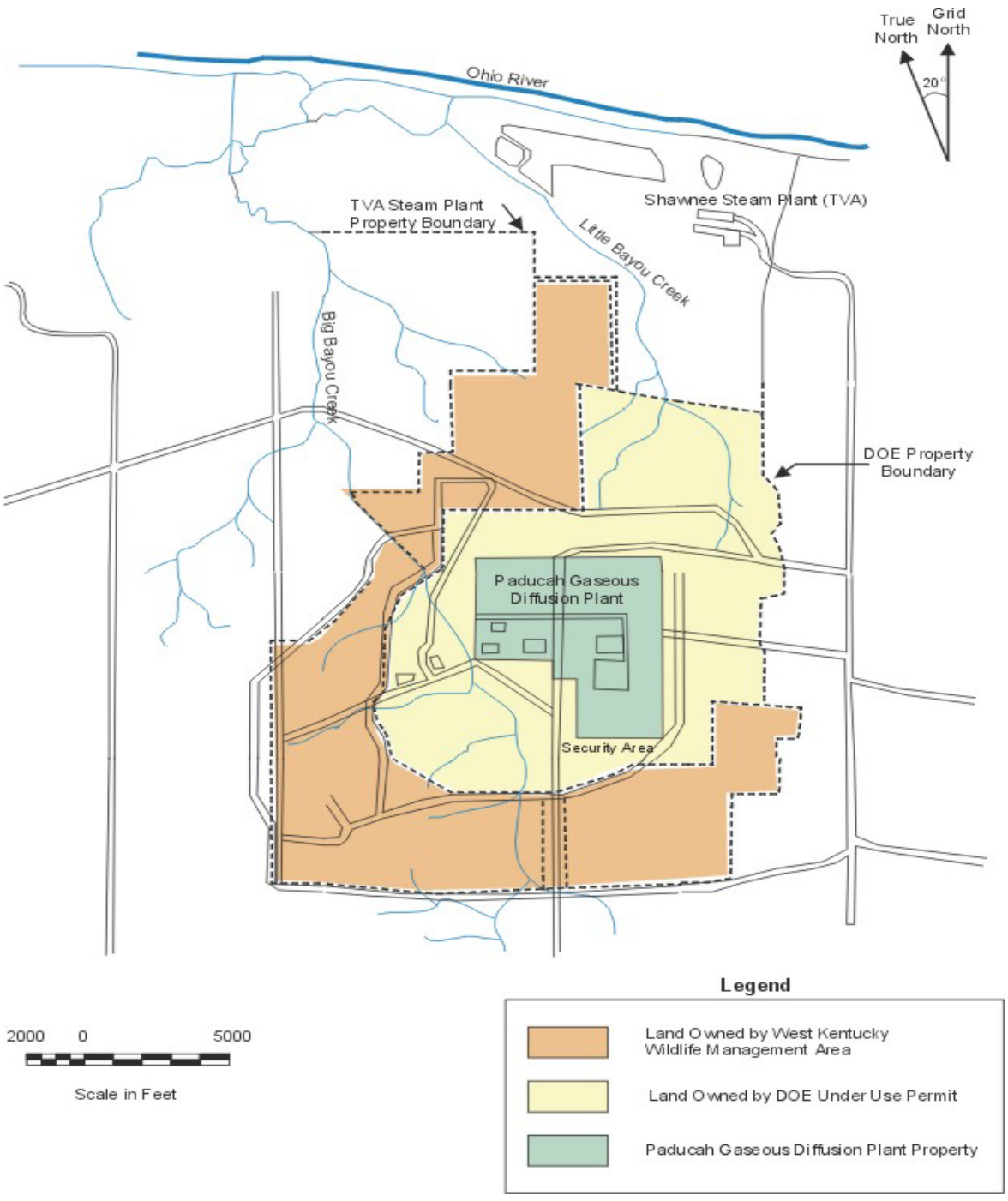

Figure 1.4: Map showing the location of the PGDP and Little Bayou Creek (Clausen et al., 1997).

Climate

The Jackson Purchase area has a mid-continental climate with warm humid summers and moderately cold winters. On average, 40 days of the summer have temperatures over 32.2^{o}C (90^{o}F) and 14 days of the winter have temperatures below freezing. The average monthly temperature ranges from 0.3^{o}C (32.6^{o}F) in January to 26.2^{o}C (79.1^{o}F) in July, with a yearly average of 14.2^{o}C (57.6^{o}F).

Figure 1.5: A view of Little Bayou Creek (looking downstream from site LBC-4) in January 2002.

On average the area receives about 127 cm (50 inches) of liquid precipitation (both as snow and rain) per year. Rainfall occurs mostly in the months from March to July and in November and December, with little precipitation occurring from August to October. Thunderstorms occur sometimes in the summer months. Statistics show that extreme storms, with an average of 16.8 cm (6.6 inches) rainfall in 24 hrs, occur only once in 50 years, while

storms with rainfall of 8.9 cm (3.5 inches) in 24 hrs may occur every two years. About 2% of the annual liquid equivalent precipitation occurs as snow (Figure 1.5), which averages about 33.3 cm (13.1 inches) each year. The general wind direction is south to southwest with an average yearly velocity of 4.4 m/s (14.4 ft/s). The strongest winds blow during the fall and winter months.

1.5 Description of the Contamination Problem

PGDP was established in 1952 to enrich uranium for commercial nuclear power and military defense reactors by the gaseous diffusion process. In this process, UF_6 gas is made to flow through piping fitted with barrier material, which enriches the end product in ^{235}U relative to ^{238}U (Clausen et al., 1992).

TCE was used at PGDP primarily as a degreasing solvent for cleaning. Sources of contamination include burial grounds, test areas and other operational facilities, such as the solid waste management units (SWMUs) 7 and 30, the C-400 cleaning building, the C-720 inactive degreaser, the C-404 burial ground and the C-747 oil landfarm (Fryar, 1997). TCE occurs in ground water (Table 1.1a) both as dissolved phase plumes and dense non-aqueous phase liquid (DNAPL) (Clausen et al., 1992). TCE in ground water was first detected in 1988, downgradient (north) of the site, at concentrations more than 0.005 mg/L, the maximum contaminant level (MCL) of the US Environmental Protection Agency (USEPA) for TCE (Clausen et al., 1992). Technetium (Table 1.1b) was produced in PGDP as a fission by-product through reprocessing of nuclear power reactor tails. Most probably ^{99}Tc was introduced into the aquifer along with leakage of TCE (Clausen et al., 1992) (Table 1.2).

Investigation and monitoring of more than 300 wells has revealed that several large contaminant plumes extend off-site from the plant (CH2M Hill, 1990; CH2M Hill Southeast, 1992; Clausen et al., 1993, 1995; USDOE, 1996). The northwest and northeast plumes (Figure 1.6) are approximately 5 km and 4.3 km in length, respectively (Etienne, 1999). The northwest plume and the offsite ^{99}Tc plume, which overlaps it, have exited PGDP and entered the West Kentucky Wildlife Management Area (WKWMA), where they discharge contaminants into Little Bayou Creek.

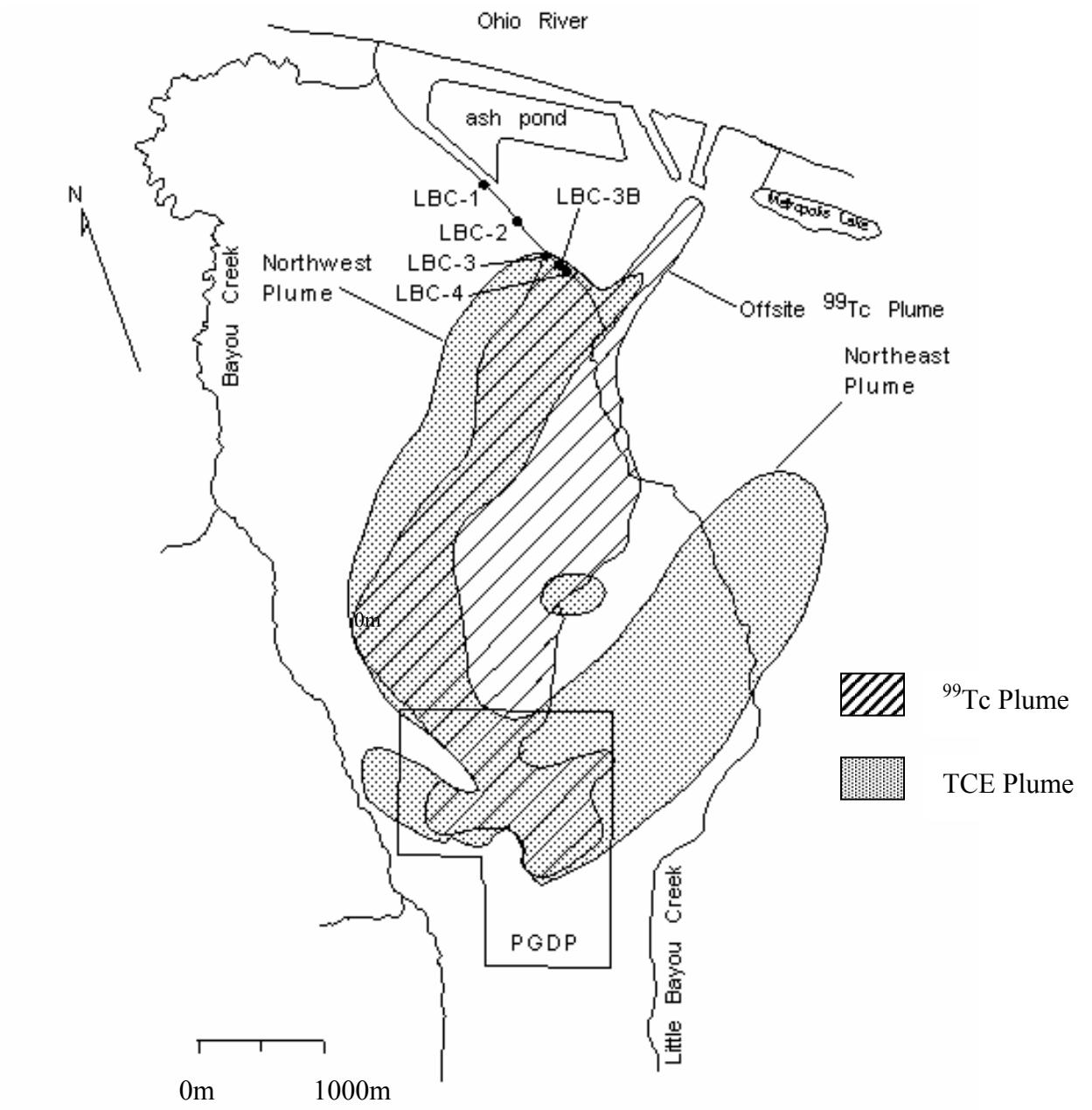

Figure 1.6: Map showing the contaminant plumes and sampling locations (described later) (after Fryar et al., 2000).

Both TCE and ^{99}Tc have been detected in the creek water, adjoining west bank wells, and springs feeding into the creek. In general, TCE concentrations range from 1,100 mg/L at the source to 0.001 mg/L at the distal portion of the plume (Clausen et al., 1995; USDOE,1996). In the

Regional Gravel Aquifer (RGA), the main contaminated aquifer, the maximum concentration of TCE found was 550 mg/L (Clausen et al., 1992).

Table 1.1a: Off-site organic ground water contaminants (after ASTDR, 2001).

Organic contaminants	Number of off-site samples	Number of off-site detects	Off-site maximum concentration in µg/L
Bis(2-ethylhexyl) phthalate	106	13	300
Bromodichloromethane	435	2	16
Carbon tetrachloride	438	3	8
Chloroform	438	6	56
1,1-Dichloroethene	438	2	13
1,2-Dichloroethene[1]	733	4	18
Methylene chloride	142	1	27
Pentachlorophenol	91	1	8[2]
Tetrachloroethylene	438	1	1
Trichloroethylene	5,698	1,090	167,000
Vinyl chloride	438	2	110

Table 1.1b: Off-site radioactive ground water contaminants (after ASTDR, 2001).

Radioactive contaminants	Number of off-site samples	Number of off-site detects	Off-site maximum concentration in pCi/L (Bq/L)	Background range in pCi/L (Bq/L)
Radon 222	386	384	1,855 (68.7)	NA[3]
Technetium 99	~5,000	898	5,804 (215)	<25 (<0.93)
Uranium 234	139	80	24 (0.9)	<2 (<0.07)
Uranium 235	119	3	3(0.1)	<1(<0.04)
Uranium 238	140	120	97(3.60)	<2(<0.07)

Notes

[1] 1,2-Dichloroethene includes data recorded as cis-1,2-dichloroethene and trans-1,2-dichloroethane.

[2] Residential detection limit for pentachlorophenol = 50 μg/l.

[3] Background levels of radon 222 in ground water vary; they are naturally high in some areas

Key: <= less than; Bq/L = becquerels per liter, μg/L = micrograms per liter; NA = not applicable; ND = not detected; NT = not tested; pCi/L = picocuries per liter

Table 1.2: Amount of ^{99}Tc released to environment from PGDP (ASTDR, 2001).

Year	Annual Release (Curies, Ci)	
	Water	Air
1975	6.4	0.8
1976	16	0.1
1977	10	0.1
1978	9.2	0.6

1.6 Chemistry of the Contaminants

Trichloroethene or TCE (C_2HCl_3)

TCE is a synthetic, chlorinated, volatile hydrocarbon (Figure 1.7) used widely since 1940 for dry-cleaning, degreasing operations; as an anesthetic in medicine; and for decaffeinating coffee (Schaumburg, 1990). TCE was classified as a suspected carcinogen, based on laboratory experiments by 1976 in the National Cancer Institute. Eventually it was included in the hazardous substance list of the USEPA in 1976. At present TCE ranks in the 15th position in the hazardous chemicals list of the Agency for Toxic Substances and Disease Registry (ATSDR, 2001 [http://w-chemdb.nies.go.jp/kis-plus/atsdr.htm]).

Chemical structure

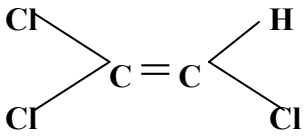

Water solubility: 1100 mg/L

Density: 1.462 g/mL

Viscosity: 0.59 cP

Henry's law constant: 1.18 kPa m^3/mol at 25^o C

Vapor pressure: 8.0 kPa

Octanol-water partitioning coefficient (K_{ow}) (as log_{10}): 2.29

Figure 1.7: Some of the physicochemical properties of TCE (after Sweat, 2000).

TCE is the most frequently reported contaminant at hazardous waste sites (39% of 1179 sites) on the National Priority List (USEPA, 1985; Bourg et al., 1993) and most common chlorinated organic contaminant in ground water systems (Bourg et al., 1993). TCE is also known as trichloroethylene, acetylene trichloride, and ethinyl trichloride. It is a colorless or bluish liquid at room temperature, with an odor similar to chloroform. Minimal and prolonged inhalation of TCE in concentrations greater than 50 ppm may cause adverse effects on human and animal health. The effects include dizziness, headache, impaired reaction time, sleepiness and facial numbness for human beings, and damage of nervous system, kidney, liver, lungs and growth of tumors in animals.

Due to TCE's wide availability and possible harmful effects, the degradation and fate of TCE in ground water have been widely studied. Volatilization is a principal process by which TCE is naturally attenuated. The volatilization rate is controlled by temperature of the system, air and water movement. In the atmosphere, TCE degrades by photo-oxidation with hydroxyl radicals, thereby forming hazardous compounds like phosgene, formyl chloride and dichloroacetyl chloride.

When TCE dissolves in water, an azeotrope with lower boiling point and vapor density than TCE is formed. In subsurface solution, TCE partitions out from water as a dense non-aqueous phase liquid (DNAPL). Various workers (e.g. Schwarzenbach et al., 1993) have noted that TCE can partition hydrophobically by sorption on mineral surfaces or natural organic matter (NOM). In heterogeneous geologic materials, the Freundlich isotherm is most appropriate to describe TCE sorption (Allen-King et al., 1996). The isotherm equation is as follows:

$$C_s = KC_w^n \qquad \text{Equation 1.1}$$

where C_s is the sorbed concentration, C_w is the aqueous concentration, K is an equilibrium constant and n is the measure of isotherm nonlinearity (Schwarzenbach et al., 1993).

Microbial degradation of TCE degradation may be significant, particularly under anaerobic conditions. In the presence of methane and oxygen, TCE can be fortuitously degraded to carbon dioxide (Figure 1.8) by methanotrophic bacteria (Wilson and Wilson, 1985). TCE can also be aerobically degraded by toluene and phenol-oxidizing microorganisms like *Pseudomonas cepacia* (Hopkins and McCarty, 1993; Nelson et al., 1987). Under anaerobic conditions, degradation of TCE is a more general and effective mechanism. Reductive dechlorination can sequentially form DCE (typically cis-1, 2), VC and ethane (Figure 1.9), which may be further reduced to ethane and carbon dioxide by action of various physiographic groups of bacteria including methanogens, Fe-(III)- and sulfate reducers and methylotrophs (Etienne et al., 1999).

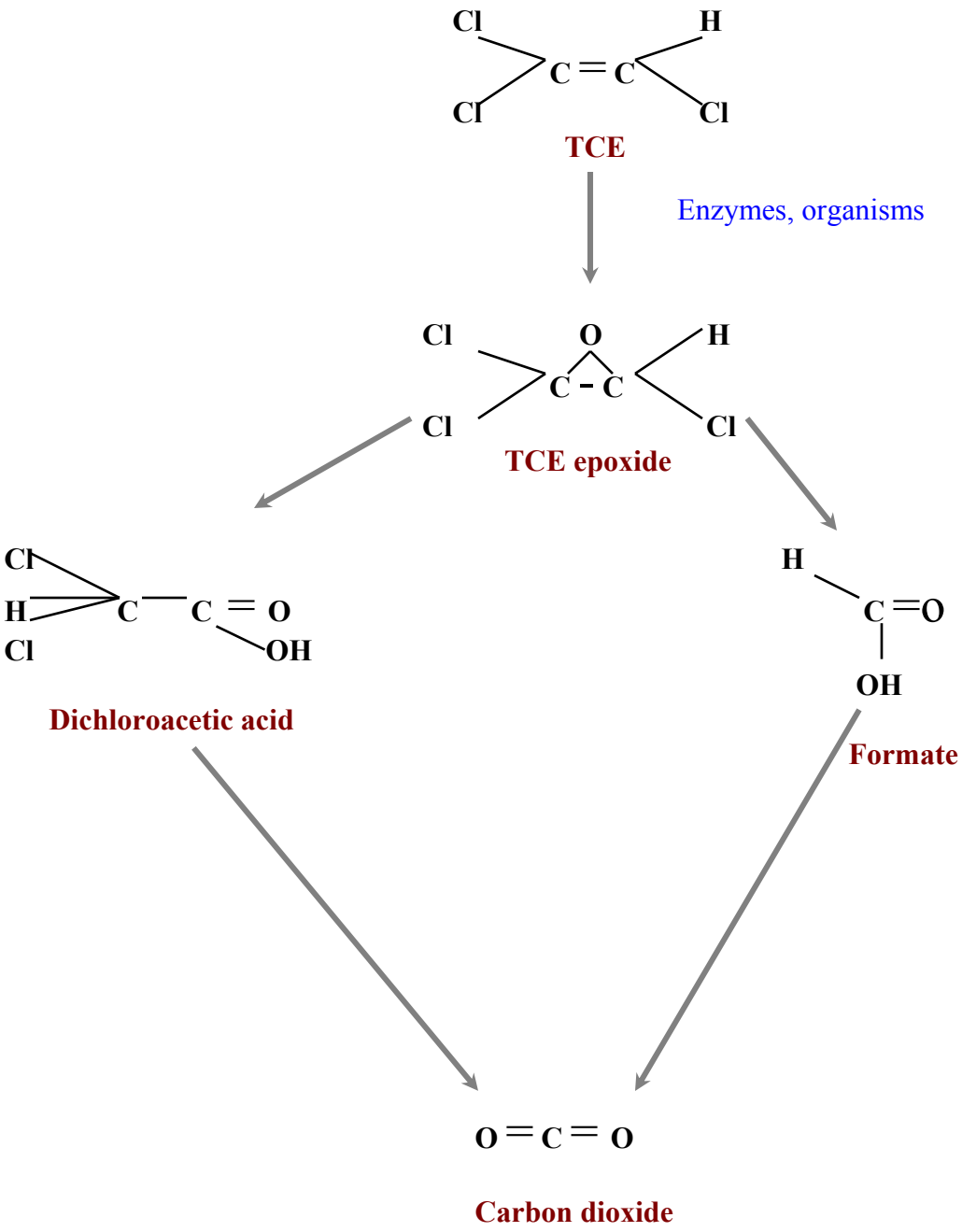

Figure 1.8: Aerobic pathway for TCE transformation (after Etienne, 1999).

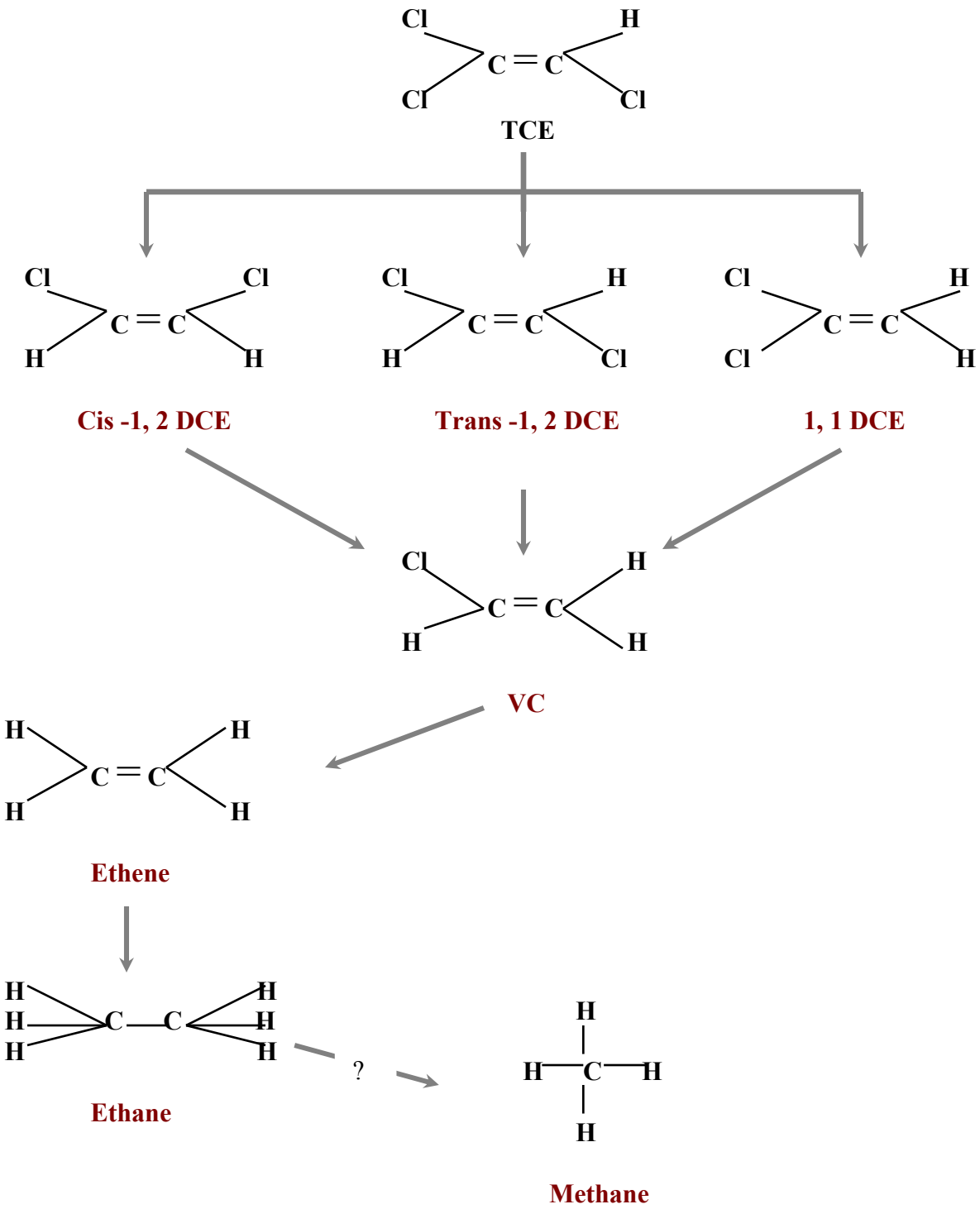

Figure 1.9: Anaerobic pathway of TCE reduction (after Etienne, 1999).

Technetium-99 (^{99}Tc)

Tc is the 43rd element of the periodic table (Group VII, Period 5). It is known to exist in all valence states from +7 to –1, but the most stable are +7, +4, and 0. It has 31 isotopes with mass number 85 to 115, most of which are radioactive. Of these ^{99}Tc is the most commonly encountered isotope. Although it was artificially produced in 1937 by bombardment of molybdenum by atomic particles, ^{99}Tc was not known to occur in the terrestrial environment until 1988, when it was found in trace amounts in molybdenum ore. In the natural state it is highly unstable and by beta particle emission transforms to ruthenium-99 (^{99}Ru). The half-life of the isotope is 2.15×10^5 years (Figure 1.10), and it has a fission yield equivalent to ^{90}Sr or ^{137}Cs, with a specific activity of 1.7×10^{-2} Ci/g. It generally enters the environment associated with effluent liquid resulting from nuclear weapons testing, nuclear power generation, nuclear fuel reprocessing, nuclear waste storage and pharmaceutical use (Wildung et al., 1979). It is most often produced as a by-product of nuclear fission of ^{235}U.

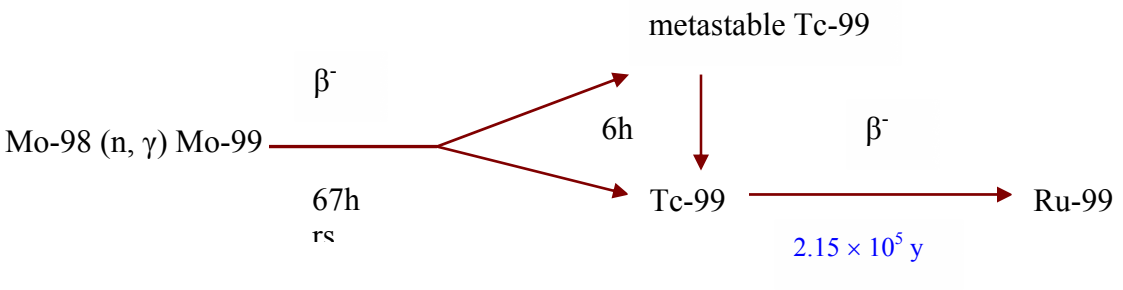

Figure 1.10: Mechanism of ^{99}Tc production by (n, γ) reaction with ^{98}Mo (Till, 1986).

The most stable chemical species of Tc in aqueous solution over a broad range of pH and concentration (1.1×10^{-5} to 0.18 M) is pertechnetate (TcO_4^-) (Wildung et al., 1979). Under oxic conditions the highly mobile Tc(VII) is the dominant species (Figure 1.11), while Tc(IV) is more abundant under anoxic conditions (Winkler et al., 1988). Tc may initially be introduced into the environment as volatile TcF_6, $TcCl_6$, or TcO_3F, each of which readily hydrolyzes to either TcO_4^-, under oxidizing conditions, or to TcO_2 or Tc_2S_7, under reducing conditions. The order of hydrolysis of the Tc oxidation states is IV > II > V and VI > VII (Wildung et al., 1979). TcO_4^-

may be reduced by Zn, HCl, hydrazine, hydroxylamine, ascorbic acid, $SnCl_2$, or dilute H_2SO_4 (Anders, 1960) to $TcO_2 \cdot H_2O$, which is immobile in aqueous systems in the pH range of 3 to 10.

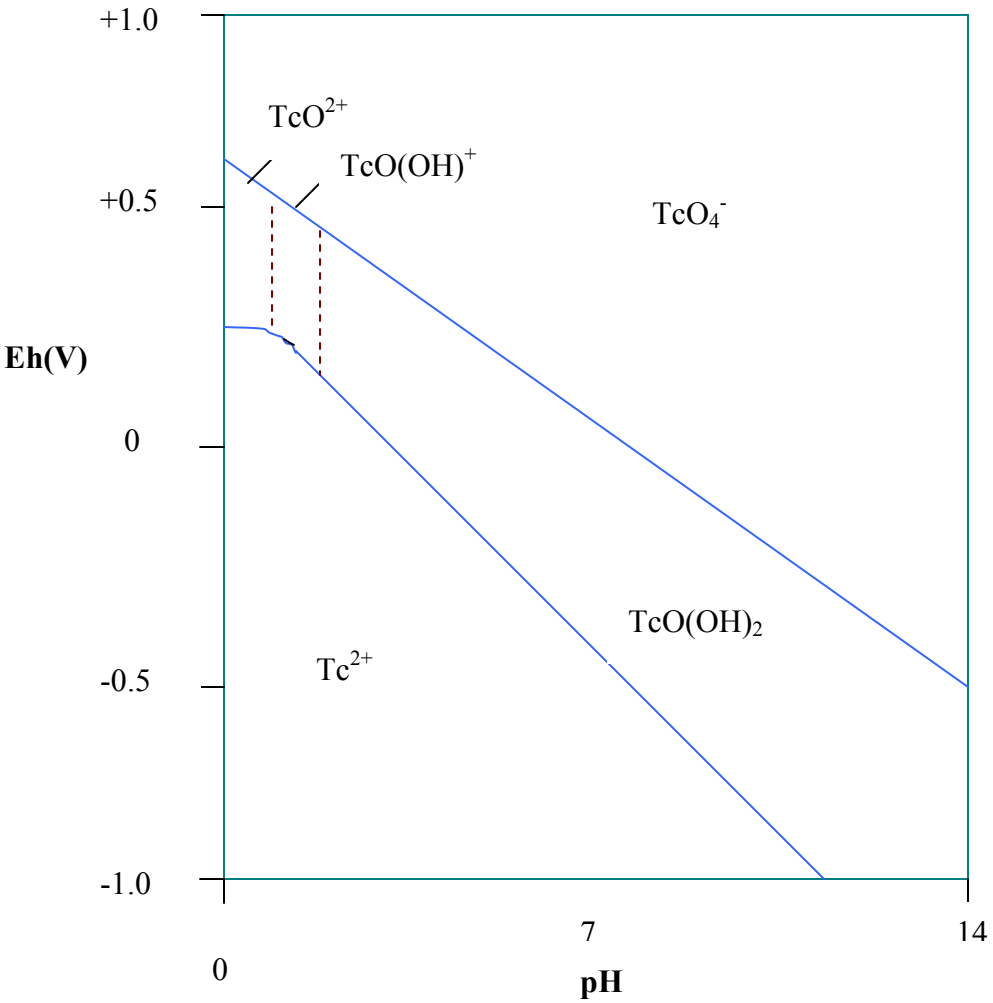

Figure 1.11: Eh-pH-diagram of Tc (after Till, 1986).

^{99}Tc sorption to sediment is directly correlated with the increase in organic carbon content and inversely correlated with decreasing pH. Retention of ^{99}Tc is dependent on the presence of positive charge in the organic compounds (humate and fulvate) and also on the amount of oxic, amorphous Fe-Al fractions (Wildung et al., 1979). Increased microbial activity caused by addition of nutrients to the soil may accelerate sorption (Van Loon et al., 1986; Pignolet et al., 1989).

^{99}Tc bioaccumulates as TcO_4^- in the thyroid, salivary glands, kidneys and gastrointestinal tract of human beings (Atkins, 1970; Till, 1986) and the soluble form accumulates in plants (Wildung et al., 1979). In the human body, ^{99}Tc has a half-life of 2 days before it is ejected by natural body mechanisms (Till, 1986).

^{99}Tc is most probably attenuated by dilution in aqueous systems, sorption to organic carbon-rich sediments, and bioaccumulation in plant and animal tissues (Meyers et al., 1989). ^{99}Tc can also be removed from natural aqueous systems by reduction of TcO_4^- to $TcO_2 \bullet H_2O$. This can be achieved by both abiotic and biotic pathways. Abiotic oxidation of reduced metal oxides and sulfides can be coupled to reduction of TcO_4^- (Daqing and Eriksen). Similarly, the presence of simulatory reducing bacteria like *Geobacter metallireducens* and *Shewanella putrefaciens* can considerably control the speciation of the ^{99}Tc (Lloyd et al., 2000; Kotharu, 2002 [http://umbbd.ahc.umn.edu/tc/tc_map.html]). Because of its very long half-life, the toxicity of ^{99}Tc may remain unchanged for more than 1000 years.

1.7 Regional Geology

Little Bayou Creek flows through the northern tip of the Mississippi Embayment portion of the Gulf Coastal Plain Province. The Mississippi Embayment is a north-south trending trough filled with sediments from the middle portion of North America. The stratigraphic sequence (Figure 1.12 and 1.13) of the region consists of Cretaceous, Tertiary and Quaternary sediments unconformably overlying Paleozoic bedrock (Clausen et al., 1992).

The Paleozoic rocks of the Jackson Purchase area dip northward and eastward toward the Illinois Basin. This general trend is consistent except in areas where there are dip reversals caused by faulting (Schwalb, 1969). The Paleozoic rocks form a part of a large domal structure, the Pascola Arch (Marcher and Stearns, 1962).

The younger sediments of the Mississippi Embayment dip in almost the opposite direction, toward the embayment axis. The Cretaceous and Paleocene deposits along the eastern and northwestern periphery of the outcrop belt are often affected by the northeast-southwest

trending faults, which radiate out from the Reelfoot Lake area of Tennessee. The displacements are generally no more than 30 m (Davis, 1996).

In McCracken County, the youngest bedrock consists of carbonates ranging from Devonian to Mississippian age. These carbonates crop out about 14 km northwest of PGDP in Illinois. The Mississippian-age Fort Payne and Warsaw Formations subcrop beneath the plant. The Fort Payne Formation consists of dark, siliceous, cherty limestone, while the Warsaw is a light-colored fossiliferous limestone (Kolata et al., 1981). A rubble zone with angular to subangular cobbles from the weathering of the Paleozoic bedrock before the deposition of the Mississippi Embayment sediments marks the unconformity between the Paleozoic and younger rocks (Davis et al., 1973; Olive, 1980).

The Tuscaloosa Formation of the Cretaceous era overlies the rubble zone. Though difficult to differentiate from the underlying rubble zone, the Tuscaloosa can be identified by its much more well-rounded, light colored gravels (Clausen et al., 1992).

The Upper Cretaceous McNairy Formation is composed of interlayered clay, silt, sand and lignite layers that dip south to southwest. About 82 m of McNairy sediments overlie the Paleozoic bedrock near the PGDP (Wallin, 1998) (Figure 1.14). The McNairy can be further divided into three stratigraphic subunits. The Levings Member is sandwiched between the upper and lower predominantly sandy units (Sweat, 2000). The sediments of the formation have been identified as fluvial deposits. In particular, the sand layers represent channel deposits, whereas the micaceous clay, silt and lignite layers have been identified as interchannel, bank and backswamp facies deposits.

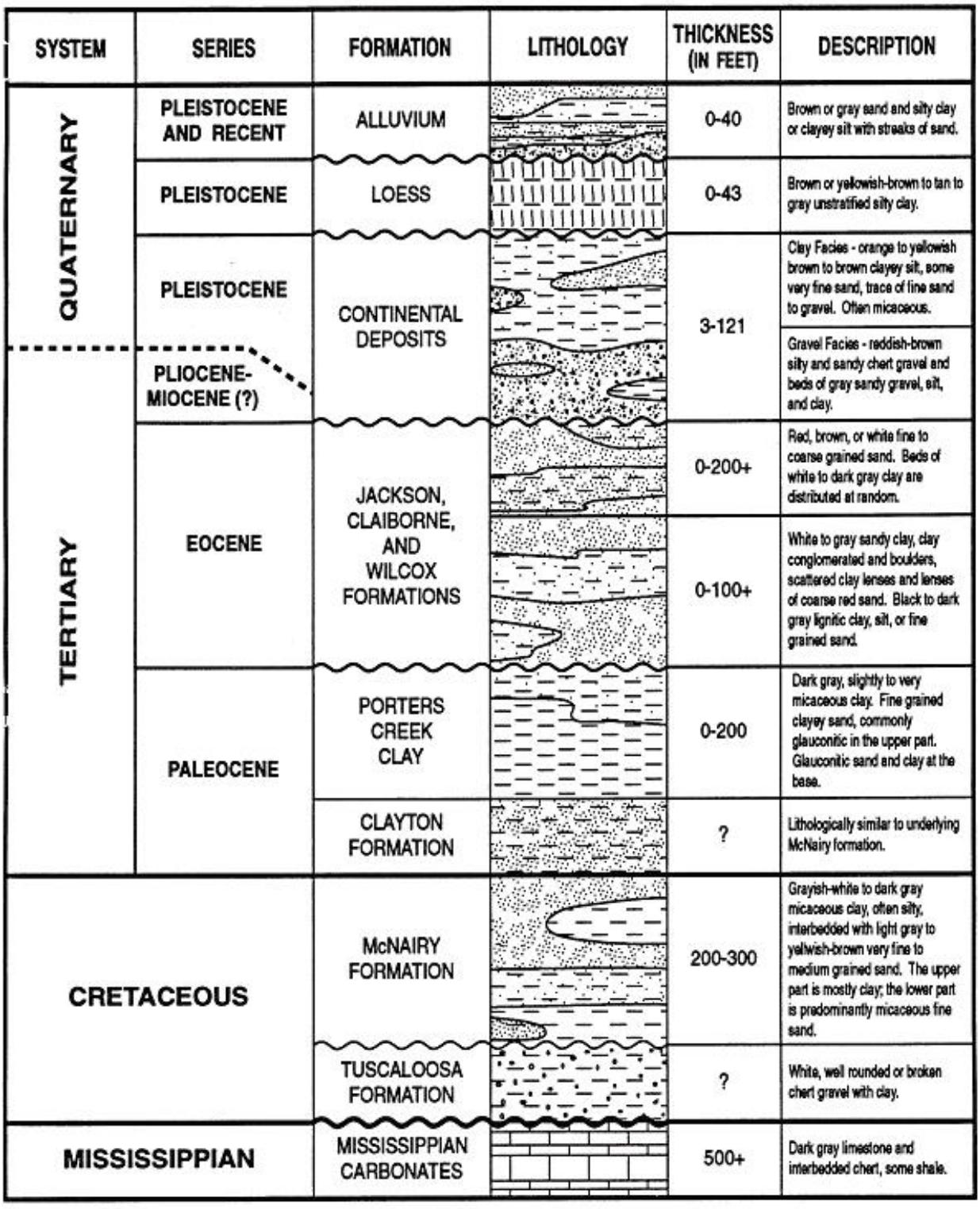

Figure 1.12: Columnar section of the Jackson Purchase Region (Clausen et al., 1992).

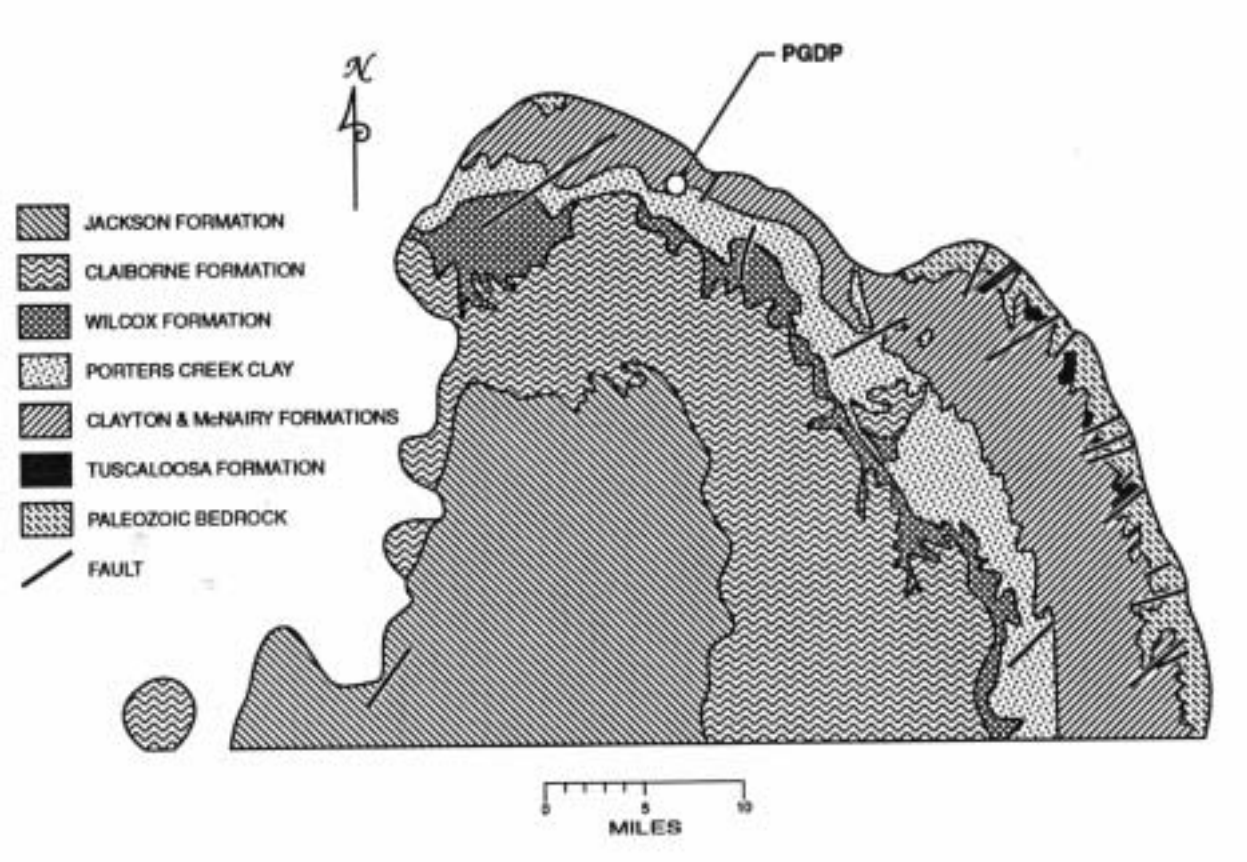

Figure 1.13: Geological map of Jackson Purchase region (Clausen et al., 1992).

The Porters Creek Clay is the first significant Tertiary-age unit in the area. The basal part of the formation is characterized by glauconitic fine-grained sand and clay, which are occasionally fossiliferous. The presence of the glauconite indicates a marine environment of deposition, at least for the lower part of the formation. The contact of the Porters Creek Clay with the overlying Wilcox Formation and the Claiborne group is unconformable in places (Davis, 1996). Exposures are sometimes seen in the stream beds in the vicinity of the PGDP. East-west trending subcrops along buried terraces have also been recorded. The maximum thickness of the Porters Creek documented near the PGDP is 26 m (Clausen et al., 1992).

The Wilcox and Claiborne Groups represent the Eocene deposits of the Jackson Purchase area. They are dominated by fine to very coarse sands with occasional clay. The Wilcox lithology may vary laterally within a few hundred feet. The Wilcox Group in western Kentucky

is subdivided into four formations based on subsurface criteria: the Tallahatta Formation, Sparta Sand, Cook Mountain Formation, and Cockfield Formation from bottom to top, respectively. Overlying the Porters Creek near the extreme southern boundary of the PGDP are the Eocene deposits, which thicken toward the south. The McNairy Formation, Porters Creek Clay and the Wilcox-Claiborne are together termed as the Coastal Plain deposits.

The fining-upward sequence of Pleistocene sediments has been inferred to represent thick valley-fill deposits (Clausen et al., 1992). The Coastal Plain deposits have an erosional contact with the overlying Lower Continental Deposits (LCD), which consist of fluvial deposits of poorly sorted quartz and chert sand and gravel (Olive, 1966; Finch, 1967). There is also a minor gravel deposit of Pliocene age called the Terrace Gravels at about 107 m above mean sea level (amsl). The average thickness of the LCD is about 9 m with a thickness of about 15 m along an east-west trending axis through the PGDP. Due to the relatively high transmissivity, the LCD are also termed the Regional Gravel Aquifer (RGA). The depositional environment of the RGA has been identified as high-energy braided stream and alluvial fan, with a provenance south or southeast of the Jackson Purchase (Davis, 1996). The LCD near the PGDP occurs at a average elevation of 85 m amsl.

The Upper Continental Deposits (UCD) predominantly consist of clay to sand-sized sediments. Occasionally gravel layers with angular to subangular chert grains are also present. Various authors have described the character of the UCD as a mixture of gravel, sand, silt, and clay (Olive, 1966; Finch, 1967); as discontinuous sand lenses enclosed within layers of clay; or as silt with discontinuous gravel beds.

A thin veneer of loess deposits, derived from the Pleistocene glacial deposits of the ancestral Ohio River valley, overlies the UCD. The loess is characterized by eolian yellowish-brown silt and clay with an average thickness of 5 m. A discontinuous layer of Recent alluvium succeeds the loess, thus completing the stratigraphic sequence.

1.8 Regional Hydrogeology

Hydrogeologic characteristics of each of the units as mentioned in the stratigraphic sequence are briefly described as follows (after Carey and Stickney, 2001). Most of them act as potential aquifers.

Mississippian Carbonate Bedrock

This usually yields sufficient water for domestic use and sometimes yields as much as 450 L/min. Ground water exists at depths more than 300 m. Hardness of water ranges from 17 to 238 ppm and TDS from 39 to 273 ppm.

Chert Rubble along the Unconformity

Chert rubble has high yield with an average of 380 L/min, varying with the saturated thickness of the rubble. The water is soft but contains an objectionable amount of iron.

Tuscaloosa Formation

Most wells in the gravel of the Tuscaloosa have yields of about 380 L/day. Yields are low because of the clay matrix and poor sorting. Hardness of water is approximately about 25 to 50 ppm, and dissolved solids range from 50 to 76 ppm.

Clayton and McNairy Formations

These formations yield sufficient water (as much as 3650 L/min), though near the PGDP the McNairy tends to be an aquitard. Hardness of water ranges from 13 to 182 ppm and TDS from 62 to 275 ppm.

Porters Creek Clay

The clay yields very little water from joints and from the intercalated fine sandstone layers. The water is hard and high in iron. The formation is more important as a confining layer.

Claiborne and Wilcox Formations

The formations yield enough water for domestic use, with maximum yield as much as 7500 L/min near areas of the Porters Creek Clay and in areas of perched water. Hardness of water ranges from 7 to 212 ppm, and dissolved solids from 28 to 431 ppm.

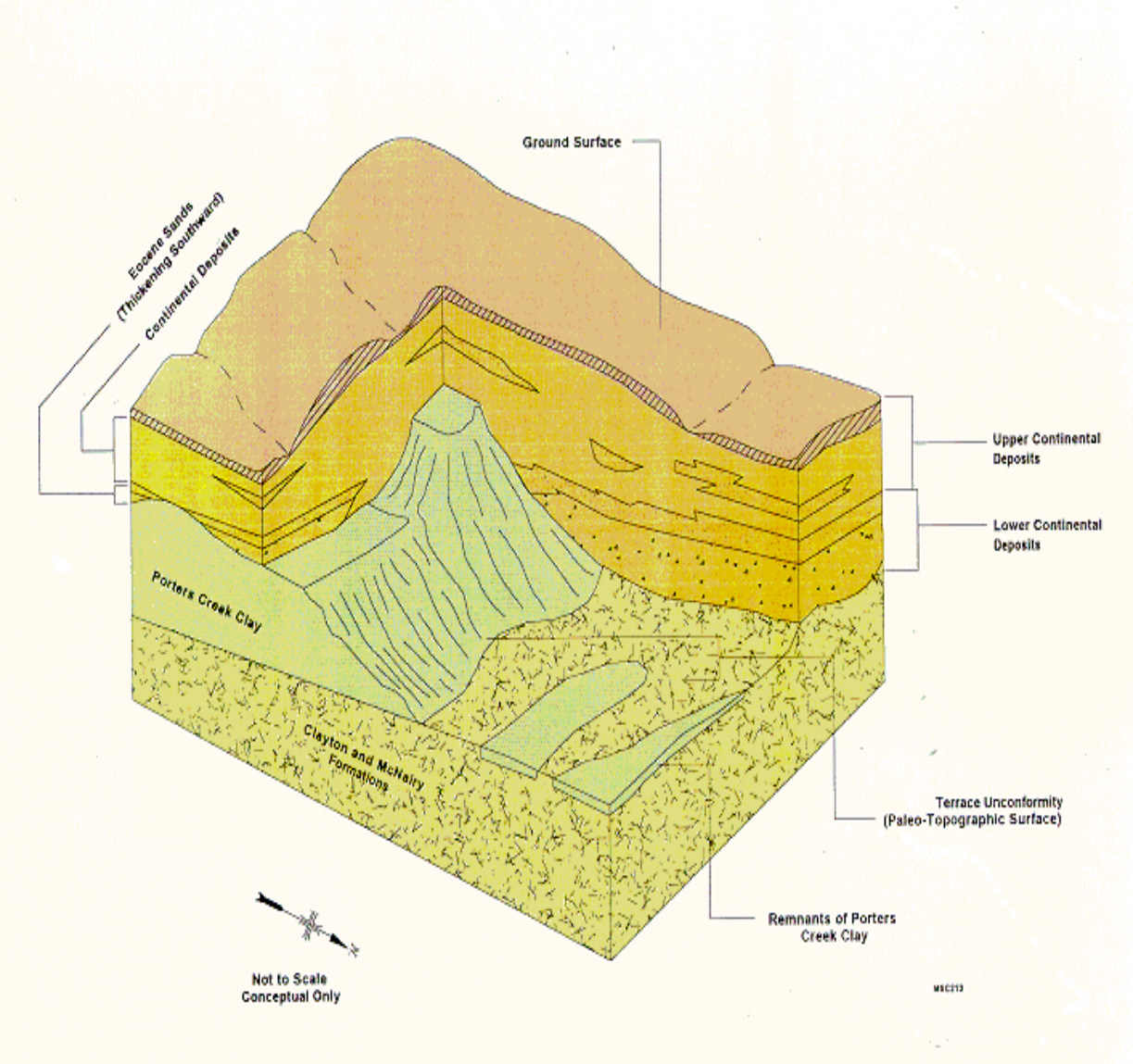

Figure 1.14: Conceptual model of the regional geologic units of the study area (Clausen et al., 1997).

Continental Deposits

These deposits generally yield small quantities of water suitable for household use (most wells in these sediments yield less than 44 L/min), but near Paducah yields can exceed 4400 L/min. Water ranges in hardness from 8 to 724 ppm and in TDS from 43 to 782 ppm.

Loess and Alluvium

The loess does generally not act as an aquifer, but does yield small amounts of water to a few wells. When saturated by rainfall, it transmits water to underlying aquifers. The alluvium yields sufficient amount of water (more than 2200 L/day) to drilled wells in the Ohio River valley. Water ranges in hardness from 12 to 664 ppm and in TDS from 53 to 1220 ppm.

1.9 Site Hydrogeology

Clausen et al. (1992) delineated five distinct flow systems at the PGDP: the Upper Continental Recharge System (UCRS), the Regional Gravel Aquifer (RGA), the Terrace Gravels, the McNairy Formation and the Mississippian bedrock. Earlier studies showed that topographically controlled recharge and discharge occur throughout the area constituting the flow system. The ground water in the vicinity of the PGDP flows northward to the Ohio River, which is the base level of all the local systems (Clausen et al., 1992). Brief hydrostratigraphic descriptions of the major lithostratigraphic units are as follows.

The Continental Deposits at and near Paducah have been divided into five hydrogeological units (HU) (Clausen et al., 1992). Of these, HU-1 denotes the surface loess, HU-2 is the UCRS, HU-3 is the confining layers of silt and clay above the RGA, HU-4 is the sandy cap layers of the RGA, and HU-5 is the RGA. Near Paducah, the McNairy is predominantly clay along with a lesser amount of very fine micaceous sand (Davis, 1996).

Studies indicate that a ground water mound exists in the northwestern part of the PGDP. This is probably a manifestation of higher than normal recharge due to trenching, excavation, and the presence of unlined lagoons near the northern boundary of the plant (Clausen et al., 1992). Similarly, a water table depression probably exists in the center of the plant, caused by thinning of the underlying HU-3 and thickening of the adjoining HU-2 (Clausen et al., 1992).

This results in a high discharge rate to the HU-5 or RGA near the center of the plant, thus turning HU-2 or UCRS into an effective recharge system. The flow is predominantly vertical within the Upper Continental Deposits (UCD) or HU-2 (UCRS) of Clausen et al. (1992). A layer of the UCRS that acts as an aquifer occurs at an elevation of about 107 m amsl.

The HU-5 or RGA dominates the local flow system (Clausen et al., 1992). The lateral gradient within the RGA is very low (on the order of 10^{-4}) (Table 1.3). The ground water flow tends mostly north-northeastward toward the Ohio River (Figure 1.15) with an average hydraulic gradient of 0.0006 (Clausen et al., 1995). The RGA behaves mostly as a leaky or semi-confined aquifer. An increased gradient occurs in the discharge zone near the Ohio River, along with a gradient shift toward the surface, resulting in upward ground water flow. Flooding of the Ohio River can cause gradient reversals (Fryar et al., 2000). Also, the flow in the RGA may be affected by the east–west trending high transmissivity paleochannel beneath the PGDP (Clausen et al., 1992) and by northeast-southwest trending faults (Langston et al., 1998). Some vertical gradient reversal can also occur near the hinge line of the system (Clausen et al., 1992). The RGA gets most of its recharge either from the UCRS or the Terrace Gravels south of the plant. Some exchange of ground water takes place between the McNairy Formation and the RGA in the vicinity of the PGDP (Davis, 1996). Ground water near the study site has a near neutral pH (range from 5.34 to 7.86 for 199 of 205 measurements) and Eh in the range of 113 to 680 mV (Fryar, 1997), indicating generally oxidizing conditions.

The McNairy Formation, which lies beneath the HU-5 or the RGA, is the other important hydrogeologic unit in the area besides the RGA. Among the subunits of the McNairy, the upper sandy member and the Levings Member have been identified to be a single hydrologic subunit. The hydraulic conductivity of this subunit ranges from about 6.3×10^{-6} cm/s near the top to 1.62×10^{-7} cm/s near the base, with an anisotropy ratio (K_x/K_z) of 39:1 (Davis, 1996). The entire thickness of the McNairy has a hydraulic gradient of about 0.03 and is believed to be hydraulically connected to the underlying rocks (Davis, 1996). The McNairy Formation is recharged through outcrops near Kentucky Lake, southeast of the PGDP, as well as from the RGA. The water in the formation moves north-northwest to discharge into the Ohio River (Sweat, 2000).

Table 1.3: Hydraulic conductivity of each lithostratigraphic unit in the study area (Clausen et al., 1992).

Unit	Range of hydraulic conductivity (cm/s)
Loess	10^{-7} to 10^{-4}
Upper Continental Deposits (clay)	10^{-8} to 10^{-3}
Upper Continental Deposits (sand)	10^{-5} to 10^{-2}
Regional Gravel Aquifer	10^{-4} to 1
Porters Creek Clay	10^{-9} to 10^{-7}
McNairy Formation	$<10^{-6}$ to 10^{-3}

1.10 Ground Water-Stream Water Interactions

Streams and ground water interact in three fundamental ways. Streams gain water from inflow of ground water through the stream bed (gaining or influent stream), they lose water to ground water by outflow through the stream bed (losing or effluent stream), or they do both, gaining in some reaches and losing in other reaches (Winter et al., 1998). In many cases the losing and gaining conditions may vary within a short time as well as seasonally. This is particularly true after a heavy shower causes a rise in stream stage and temporary flow into the banks. For a gaining reach, the altitude of the water table in the vicinity should be higher than the stream water surface, while the converse applies for a losing reach.

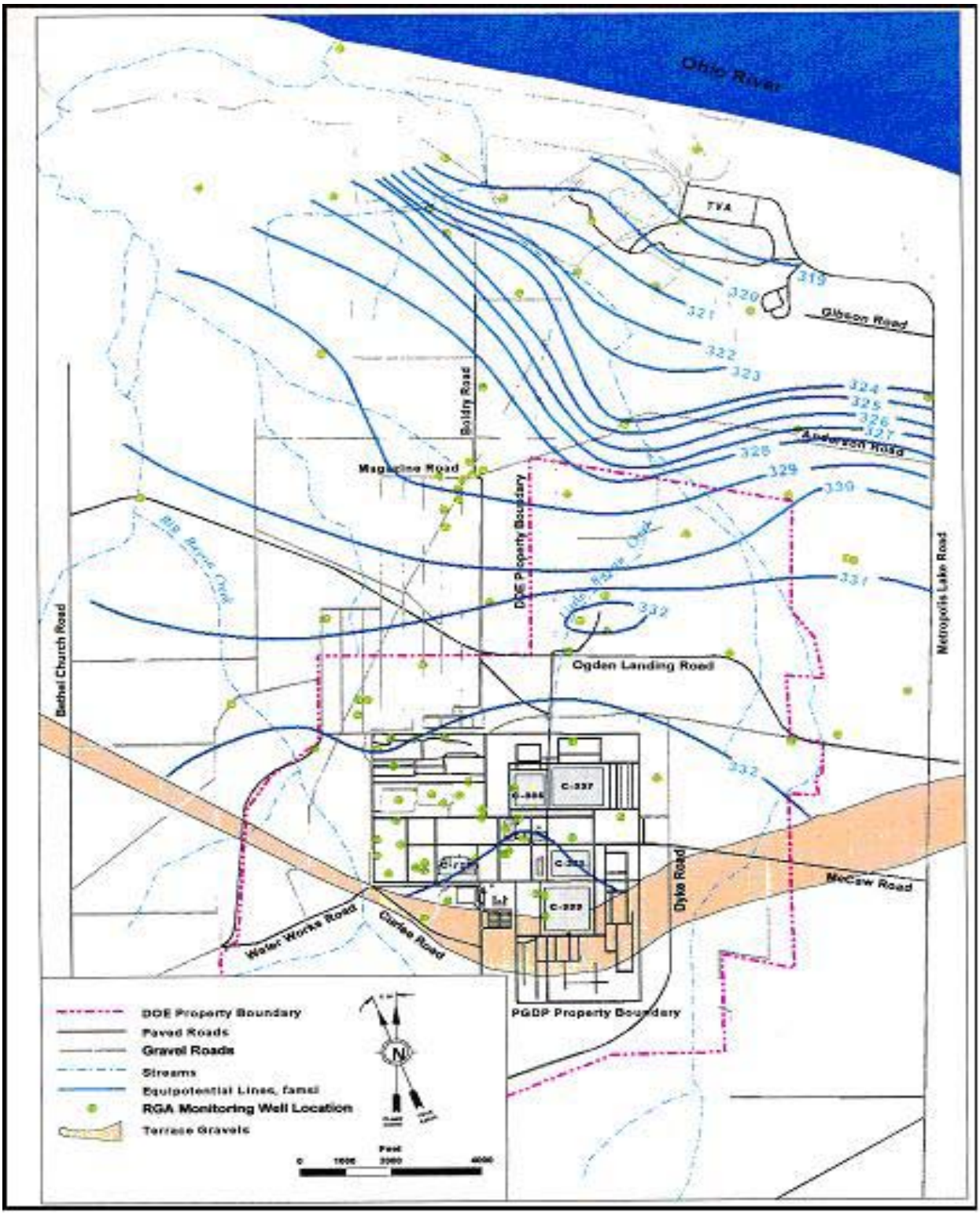

Figure 1.15: Potentiometric surface map of the RGA in the PGDP area in May 1997 (Clausen et al., 1997).

In an alluvial geomorphic setting, the baseflow component of the ground water flux is perpendicular to the stream (toward or away from the stream depending on stream stage). The underflow moves parallel to the stream flow direction. Underflow dominance is a common feature in the tributaries of alluvial river systems (Larkin and Sharp, 1992).

Previous studies have established that both gaining and losing reaches are present in the study area. Both Bayou and Little Bayou Creeks tend to gain flow where they intersect the RGA. Local storms, river floods and seasonal dry periods sometimes cause reversals in the hydraulic gradient (Fryar et al., 2000). A losing or no-net-discharge condition mostly exists in Bayou Creek, as indicated by a downward or lateral hydraulic gradient (Wallin, 1998). In some locations, the presence of an upward hydraulic gradient indicates a local confined condition rather than a gaining reach.

In Little Bayou Creek, the transition from losing to gaining conditions occurs in the Ohio River flood plain. The creek is fed primarily by runoff or plant discharge from outfall 10 in its upper reaches and the flow does not significantly increase until about 3.7 km above the stream mouth. Below this point it receives extensive ground water discharge from the RGA (Evaldi and McClain, 1989; Fryar et al., 2000). Ground water discharge is indicated by an upward hydraulic gradient and higher seepage flux and the presence of small springs and sand boils. Seepage to the stream from an ash pond at the Tennessee Valley Authority's Shawnee Plant has also been established by detection of boron in stream water (Fryar et al., 2000). The presence of riffles and pools probably leads to advection of the stream water through the bed at some locations (White et al., 1987).

Chapter 2
Methods of Study

One of the main objectives of the present study is to quantify the discharge of the stream for each season and to relate the nature and degree of attenuation of the studied contaminants to discharge. Therefore, surface flow was gaged and flow rates were calculated from tracer injection. Moreover, water samples were collected for analyses of TCE and ^{99}Tc in a commercial laboratory. Field work was done in January, June, August, and October 2002 and January 2003 in order to examine seasonal variability in the nature and rate of attenuation. The monitoring in January 2003 was undertaken in order to examine the reproducibility of the results for at least one season. For each sampling round, the field method and laboratory analyses were similar except in cases where techniques evolved with practice.

The total length of the study reach is 1075 m (from LBC-1 to LBC-4) (Table 2.1). The tracer tests were done along 290-m segment from 10 m downstream of LBC-4 to LBC-3B and –3 (Figure 1.6). The bed morphology includes pools and riffles, which are common throughout the stream, but appears to lack sand boils or springs, which may induce error in the measurement of tracer concentrations. Also, this stretch of the stream is relatively linear, which minimized the possibility of the retention of the tracers in stagnant zones away from the main channel. For flow measurement and contaminant sampling, two other downstream locations (LBC-1 and-2) were included in the study for comparison with the monitoring studies of Fryar et al. (2000) and LaSage and Fryar (2000). The study locations are shown in Figure 1.6.

Table 2.1: The distance for each location relative to the farthest downstream site (LBC-1).

Location number	Distance (in meters)
LBC-1	0
LBC-2	410
LBC-3	775
LBC-3B	1016
LBC-4	1075

2.1 Contaminant Sampling

Samples were collected at each of the five study locations for TCE and ^{99}Tc (Figure 2.4). Amber glass vials (40 mL) were used for sampling TCE. Water samples were taken by dipping the vials completely in the stream water. The vials were filled to the rim and then 2 to 5 drops of HCl (6N) were added as a preservative. Water was then added to give a positive meniscus, after which the vials were capped with care to prevent the presence of any headspace. For a properly taken sample, the septum of the vial slightly bulges out. The ^{99}Tc samples were taken simultaneously with the TCE samples in 1-L high density polyethylene (HDPE) bottles to which 10 mL of HNO_3 (6N) were added as a preservative. After sampling, the vials were chilled and the samples were shipped to Severn Trent Laboratories (STL, Earth City, Missouri). At STL, TCE and other volatile organic compounds were analyzed by gas chromatograph-mass spectrometer according to USEPA method SW846/8260B (USEPA, 1986), while ^{99}Tc was analyzed by liquid scintillation counter. Field blanks with distilled and/or de-ionized water and replicate samples were taken for quality control.

2.2 Flow Measurements

Principles and Background: Stream discharge may be defined as the volume of water flowing through an area per unit time and is commonly expressed as cubic feet per second (cfs) or cubic meters per second (m^3/s). In order to minimize the variability in flow induced by runoff, gaging occurred under baseflow conditions, which for this study were considered to occur at least three days after rainfall and were marked by lack of visible turbidity.

Field Methodology: Discharge was measured by the cross-section method, which involved stretching a measuring tape across the stream perpendicular to the direction of flow. Each measuring location was chosen in such a way that the stream reach in the immediate vicinity was almost linear and the stream bed was relatively uniform. Measurement of depth and flow velocity of the vertical section across the stream channel at multiple points permitted calculation of the stream discharge at that location. The equation used for discharge measurement is

$$Q = \Sigma(a \times v) \qquad \text{Equation 2.1}$$

where

Q = discharge

a = area of each vertical cross section of the stream at that location

v = mean velocity of flow normal to the cross sectional area

Flow velocity was measured by the six-tenths method of Rantz (1982). This involved selection of gaging points along the tape (figure 2.5) so that each measured section ideally contained a maximum of 5% of total discharge. Hence the distances between each measuring point ranged from 0.152 m (0.5 ft) to 0.610 m (2 ft), depending on the nature of flow in that section based on visual estimation. The velocity for each vertical section is taken as the mean velocity. An electro-magnetic velocity sensor manufactured by Marsh-McBirney was set with a calibrated top-setting rod at about 60% of the total depth from the surface of the water. The velocity measurement in this method did not incorporate the flow in the hyporheic (ground water/stream mixing) zone or uncertainties associated with shallow depth, an uneven streambed and non-perpendicular flow. However, gaging provides a reasonable lower bound on discharge estimates for reaches of the creek that are relatively straight and unobstructed.

The total (surface and hyporheic) discharge of the creek below the injection point of the tracers can be calculated using the following empirical equation (Kilpatrick and Cobb, 1985):

$$Q = (5.89 \times 10^{-7}) \times \frac{S_G V_1 C}{A_C} \qquad \text{Equation 2.2}$$

where

Q = discharge below injection point (ft^3/s)

S_G = specific gravity of the injected solution

V_1 = volume (ml) of concentrated tracer solution injected into the stream

C = concentration (μg/l) of tracer solution injected

A_C = area under the time-concentration curve

2.3 Tracer Tests

In order to account for hyporheic-zone flow and monitor natural attenuation of TCE and ^{99}Tc, five seasonal tracer tests were conducted. In total, four tracers were injected into the stream 10 m downstream of LBC-4 (Figure 2.3) and were sampled at specified time intervals at LBC-3B and-3. The tracers injected are sodium bromide (NaBr), sodium nitrate ($NaNO_3$), rhodamine WT dye, and propane (C_3H_8). Specified amounts of each of the first three tracers were dissolved in 20 L of stream water in each of two HDPE carboys. The carboys were then shaken well and were dumped simultaneously into the stream as a slug at the beginning of each experiment. The propane gas was injected by constant bubbling into the stream from tanks through a regulator and diffuser. Both the slug tracers and the propane were injected across most of the width of the stream to facilitate transverse mixing.

To identify the distance of homogeneous mixing of the tracers the following equation was used (Kilpatrick and Wilson, 1989):

$$L_0 = 0.1 \times \frac{v \times B^2}{E_z} \qquad \text{Equation 2.3}$$

where

L_0 = distance of the stream from the tracer injection point required for optimum mixing

v = mean stream velocity

B = average stream width

E_z = lateral mixing coefficient

The value of v for Little Bayou Creek is about 0.04 m^3/s, B is 6.4 m and E_z is about 0.004 to 0.005 m^2/s from published values (Kilpatrick and Wilson, 1989). Hence the value of L_0 is in the range of 33 to 41 m.

Stream water samples for all the tracers were collected from the interval of the stream with highest velocity, as gaged at LBC-3B and LBC-3 (Figure 2.6). The sample containers (vials and bottles) were oriented downstream and fully immersed in the water for filling. One set of samples was taken before the visible dye cloud arrived at LBC-3B and LBC-3, in order to

measure the background concentrations of the tracers in the stream. Samples were collected at each location from the arrival to the departure of the cloud, with the time intervals between the samples increasing over time to account for tailing of the slug. Generally, the time interval varied from 3 to 5 minutes during the initial phases and 7 to 15 minutes during the later phases, depending on the stream velocity. All the samples thus collected were chilled and stored in the dark after departure from the field site until they were analyzed. Nitrate samples were frozen to inhibit denitrification during storage (Avanzino and Kennedy, 1993). The principles behind using each of these tracers, their sampling processes and analysis procedures are discussed below.

Sodium Bromide

NaBr in aqueous solution dissociates into Na^+ and Br^-. For the present study, the Br^- was used as a conservative tracer to estimate both the surface and hyporheic flow for comparison with the surface-flow values obtained from stream gaging. The assumption of conservative behavior, which will be examined subsequently, means that Br^- concentrations would be affected only by in-stream dilution. Therefore, in areas where there is hyporheic flow, the difference between the values obtained from the flow meter and tracer dilution would represent an estimate of underflow. This would also give an estimation of the attenuation of ^{99}Tc by dilution, as this radionuclide is conservative under aerobic conditions. However, studies in other Coastal Plain sediments (Boggs et al., 1992; Seaman et al., 1995) have found that Br^- may sorb onto variably charged clay minerals. Such sorption occurs at acidic pH values and depends on the ionic strength and the concentration of the predominant cation. The background concentration of Br^- in Little Bayou Creek (less than 1 mg/L) (A.E. Fryar, Department of Geological Sciences, University of Kentucky, unpublished data) is comparable to the detection limit.

The mass of the salt added was selected based on stream discharge. Generally, in the winter months, the discharge rate is lower than the rest of the year, so 1 kg of NaBr was added in January 2002 and 2003, while 2 kg of NaBr were added in June. The samples were collected in 125 mL HDPE bottles without any headspace restriction. Br^- was analyzed by ion chromatography (DX-500 ion chromatograph) at the Kentucky Geological Survey and the Department of Forestry, University of Kentucky. The detection limit was 0.1 mg/L.

Sodium Nitrate

Sodium nitrate dissociates into Na^+ and NO_3^-. The NO_3^- ion was used as an indicator of the redox condition of the stream system. A decrease in the mass of the nitrate from the injection point to the sampling locations, or delayed breakthrough of nitrate relative to the conservative tracers, would suggest reduction of NO_3^- and thus of ^{99}Tc. As the surface water is sufficiently oxic (A.E. Fryar, Department of Geological Sciences, University of Kentucky, unpublished data), any such reduction would be taking place in the hyporheic zone. As discussed earlier, under oxic aqueous conditions, the highly mobile pertechnetate ion (TcO_4^-) is the dominant Tc species. Under reducing conditions, the TcO_4^- will be transformed into much less mobile $TcO_2 \cdot H_2O$. A decrease in nitrate should indicate the occurrence of anoxic conditions. From June 2002 onward, 2 kg of $NaNO_3$ were added as a tracer in stream water. The sample collection procedure was the same as that of bromide. The background concentration was less than 1 mg/L (A.E. Fryar, Department of Geological Sciences, University of Kentucky, unpublished data). NO_3^- was analyzed by auto-analyzer in the Department of Forestry and by ion chromatography [DX-500 ion chromatograph] at the Kentucky Geological Survey.

Rhodamine WT

Rhodamine WT (5 to 20% solution) dye was used both as a visual tracer to delineate the tracer plume and as a quantitative tracer. Although rhodamine WT has also been assumed to be conservative in stream tracing studies (Kilpatrick and Cobb, 1985), the dye consists of a mixture of two isomers (Figure 2.1), one of which (the meta isomer) may hydrophobically sorb to sediment (Vasudevan et al., 2001). Therefore, the breakthrough curves of the dye were compared with those of Br^- to assess TCE sorption to the stream sediments. Dye samples were collected in 40-mL amber glass vials to minimize photo-degradation of the dye. Rhodamine WT concentrations were analyzed by fluorometry in the laboratory of the Kentucky Geological Survey. About 5 mL of each sample were introduced in cuvettes into the fluorometer (Varian Cary Eclipse fluorescence spectrophotometer), which detected the dye concentration automatically, based on a calibration curve spanning various concentrations (range 1 μg/L to 2000 μg/L).

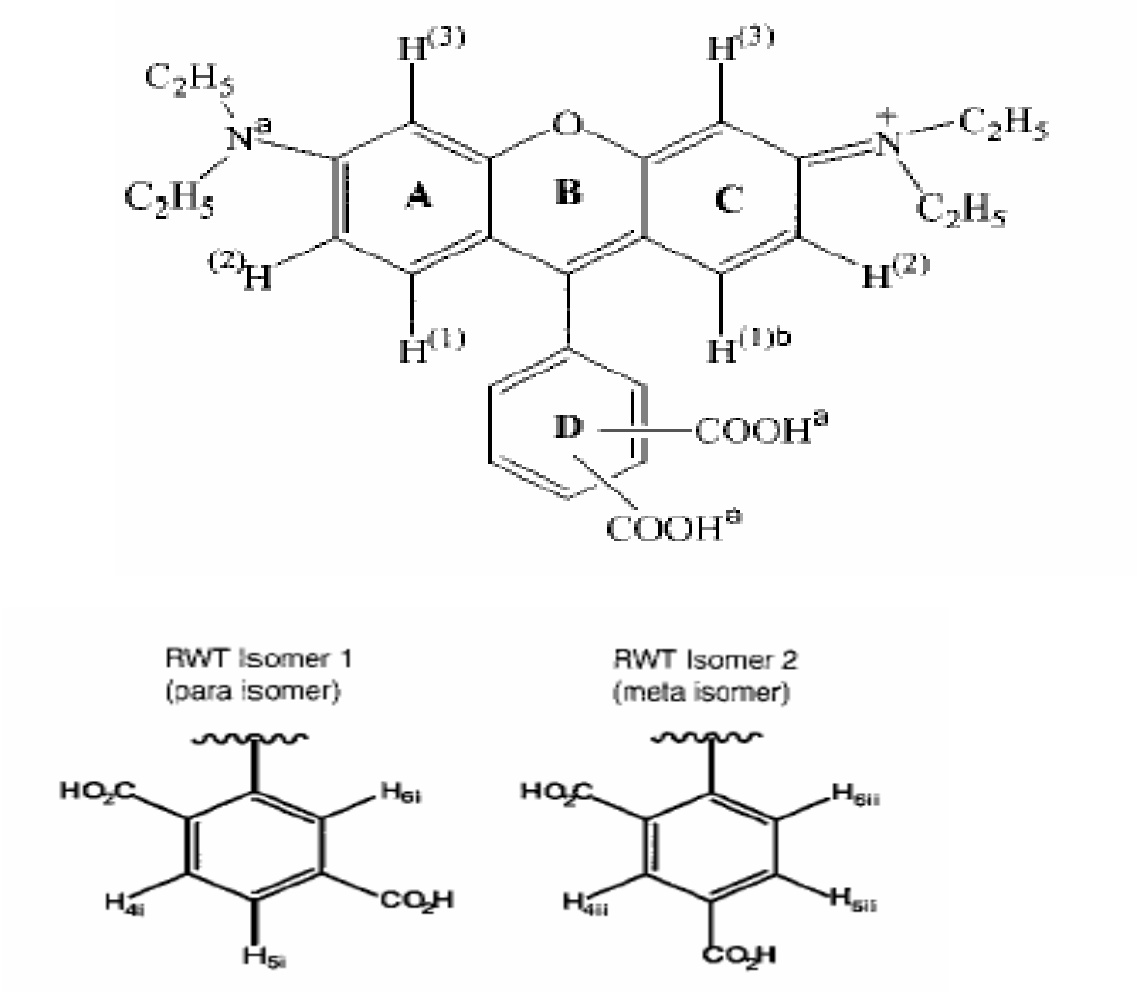

Figure 2.1: Structure of Rhodamine WT and its isomers corresponding to molecular mass 487Da (Vasudevan et al., 2001).

Propane

Propane (C_3H_8) was used as a non-conservative tracer to simulate the attenuation of TCE by in-stream volatilization. The volatilization coefficient of the propane was compared with a standard ratio to estimate the actual volatilization rate of TCE. The standard volatilization ratio, which is independent of stream turbulence, is TCE/propane = 0.79 $^{+}$/- 0.21 (Smith et al., 1980).

Propane was bubbled into the stream at LBC-4 from a tank attached to a regulator; delivery pressure was maintained at ~ 100 kPa. The gas was made to bubble out through a diffuser, 0.97 m long, made of 0.4-cm (nominal) PVC pipe studded with six porous stainless

steel frits (diameter 2.29 cm) placed at 10.16-cm intervals. The diffuser was anchored to the stream bed and covered with a plastic tarpaulin to inhibit degassing from the stream surface. Samples of propane dissolved in stream water were collected in 40-mL amber glass vials without headspace. The propane samples had a holding time of 9 days. Propane concentrations in the collected stream water samples were analyzed by gas chromatograph-flame ionization detector (Shimadzu GC-14A with Chromatopac C-R5A) in the Department of Agronomy, University of Kentucky. Before analysis, 10 mL of headspace were created in each of the vials by drawing water through the septum with a syringe while keeping the vials airtight. After creating the headspace, the samples were left to equilibrate at room temperature for 6 to 10 hours. Subsequently, the vials were shaken for about 1 minute and then 50 μL of air were withdrawn from each of the vials and analyzed for the concentration of propane that partitioned into the headspace (C_g). Calibration curves for the GC-FID were produced from the analysis of standards with known volume of propane. These included 500 μL and 100 μL of 15.7 and 991 ppm propane standards (Supelco Scotty® II). Using Henry's Law, the concentration of propane that partitioned into the water in the vial (C_w) was calculated as:

$$C_W = \frac{C_g}{K_H} \qquad \text{Equation 2.4}$$

where K_H is the Henry's law constant for propane. Given the volume of water remaining in the vial (V_w) and the mass of the gas (M_g) in the headspace, the initial total concentration of propane in stream water (C_i) can be calculated as:

$$C_i = C_w + \frac{M_g}{V_w} \qquad \text{Equation 2.5}$$

or

$$C_i = C_w + C_g \qquad \text{Equation 2.6}$$

The concentrations of propane thus found from the analytical measurements were used in the OTIS-P model (discussed later) to find the volatilization coefficient between the sampling points LBC-3B and -3. The standard conversion ratio of Smith et al. (1980) was then used with first-order decay (volatilization) coefficient values from the simulations in order to calculate the volatilization rate of TCE.

The decay or volatilization coefficient (k) and volatilization rate (R) of TCE were also calculated from the first-order decay equation:

$$k = -\frac{1}{t} ln(C_f / C_i) \qquad \text{Equation 2.7}$$

and

$$R = C_i \times k \qquad \text{Equation 2.8}$$

where

k = first-order decay coefficient

t = travel time between the two sampling locations

C_i = concentration of TCE at the upstream sampling location

C_f = concentration of TCE at the downstream sampling location

The two values for the volatilization coefficient were compared to examine the assumption that volatilization of TCE in Little Bayou Creek is a first-order mass-loss process.

2.4 Travel Time, Tracer Mass Recovery, and Contaminant Flux

The travel times between the injection location and the two sampling locations for each of the conservative tracers and monitored periods were calculated as follows. The x-coordinate (time) values of the centroids (centers of mass) for the areas under the observed time-concentration flux curves at LBC-3B and LBC-3 were compared (see Figure 2.2 for an example). The area under the curve was calculated using the trapezoidal rule:

$$A_C = \sum_{i=1}^{n} C_t \times \Delta t \qquad \text{Equation 2.9}$$

where

A_C = observed area under the time-concentration curve of the tracer

C_i = observed concentration at time t

$C_t = \{C_i + C_{(i-1)}\}/2$

$\Delta t = t_i - t_{(i-1)}$

and n is the number of observations.

The centroid was calculated by using MATLAB® Version 6.1 (Mathworks, Inc.). Sample codes are enclosed (Appendix B).

The recovered mass percentages (M_R) for the solute tracers (bromide, nitrate and rhodamine WT) at each of the sampling sites (LBC-3B and -3) in each season were calculated by the following equation:

$$M_R = \frac{A_C \times Q}{M_a} \times 100 \qquad \text{Equation 2.10}$$

where

Q = volumetric surface discharge rate

M_a = mass of the tracer of interest added to the stream

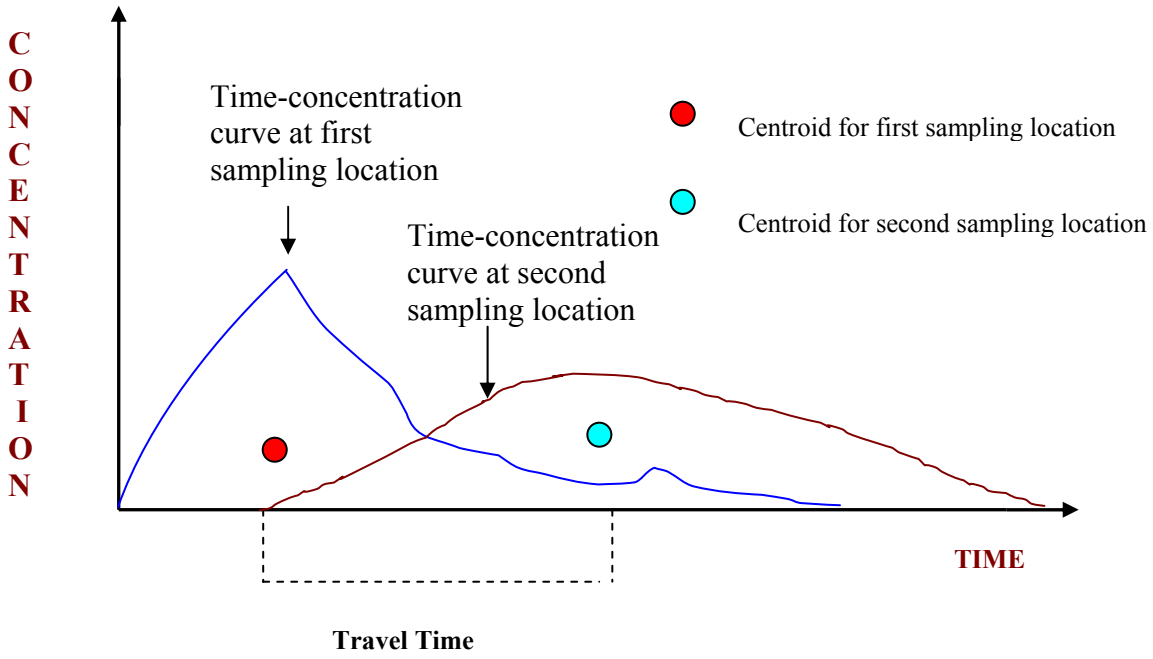

Figure 2.2: Schematic representation of travel time calculation.

The fluxes (F) of TCE and ^{99}Tc between LBC-4 and -3B and between LBC-3B and -3 for each monitored periods were calculated by the following equation:

$$F = C_d Q_d - C_u Q_u \qquad \text{Equation 2.11}$$

where

C = contaminant concentration

d = downstream monitoring location

u = upstream monitoring location

2.5 Modeling

For each season, transport and fate were modeled using the One Dimensional Transport with Inflow and Storage (OTIS) code of Runkel (1998). The original version of OTIS was developed by Runkel and Broshears (1991) from a transient storage model presented by Bencala and Walters (1983). Transient storage implies temporary detainment of solutes in small eddies and stagnant zones, where water is stationary in comparison to the relatively fast moving water near the center of the stream channel (Runkel, 1998). In OTIS, the mass balance equations have been defined for two conceptual zones: the main channel and the transient storage zone. The main channel is defined as the portion of the stream where advection and dispersion dominate all other transport mechanisms.

The primary assumption for OTIS is that the transport takes place in one dimension, i.e., the concentration varies only in longitudinal direction and not along width or depth (Runkel, 1998). The other model assumptions are (after Runkel [1998]):

Main Channel

• The physical processes affecting solute concentrations include advection, dispersion, lateral inflow, lateral outflow, and transient storage.

• The chemical reactions affecting solute concentrations include sorption to the streambed and first-order decay.

• All model parameters describing physical processes and chemical reactions may be spatially variable (in 1-D).

• Model parameters describing advection and lateral inflow may be temporally variable. These parameters include the volumetric flow rate, main channel cross-sectional area, lateral inflow rate, and the solute concentration associated with lateral inflow. All other model parameters are temporally constant.

Storage Zone

• Advection, dispersion, lateral inflow, and lateral outflow do not occur in the storage zone. Transient storage is the only physical process affecting solute concentrations.
• The chemical reactions affecting solute concentrations include sorption and first-order decay.
• All model parameters describing transient storage and chemical reactions may be spatially variable (in 1-D).
• All model parameters describing transient storage and chemical reactions are temporally constant.

The mathematical conceptualization of the physical processes considered in the model gives rise to a coupled set of differential equations for the main channel and storage zone for conservative tracers (Runkel and Broshears, 1991):

$$\frac{\partial C_s}{\partial t} = -\frac{Q\partial C}{A\partial x} + (\frac{1\partial}{A\partial x} \times \frac{AD \times \partial x}{\partial x}) + \frac{q_{LIN}}{A}(C_L - C) + \alpha(C_S - C) \qquad \text{Equation 2.12}$$

$$\frac{dC_s}{dt} = \alpha \frac{A}{A_S}(C_S - C) \qquad \text{Equation 2.13}$$

where

A = main channel cross-sectional area
A_S = storage zone cross-sectional area
C = main channel solute concentration
C_L = lateral inflow solute concentration
C_S = storage zone solute concentration
D = dispersion coefficient
q_{LIN} = lateral inflow rate

x = distance

α = storage zone exchange coefficient

For nonconservative tracers the above equations are modified for kinetic sorption and first-order decay:

$$\frac{\partial C}{\partial t} = L(C) + \rho\lambda^1(C_{sed} - K_d C) - \lambda C \qquad \text{Equation 2.14}$$

$$\frac{dC_s}{dt} = S(C_s) + \lambda^1{}_s(C^1{}_s - C_s) - \lambda_s C_s \qquad \text{Equation 2.15}$$

where

$C^1{}_S$ = background storage zone solute concentration

C_{sed} = sorbate concentration on the streambed sediment

K_d = distribution coefficient

λ = main channel first-order decay coefficient

λ_S = storage zone first-order decay coefficient

λ^1 = main channel sorption rate coefficient

$\lambda^1{}_S$ = storage zone sorption rate coefficient

ρ = mass of accessible sediment/volume water

L(C) = physical processes in the main channel } right hand side of the above equations

$S(C_S)$ = physical processes in the storage zone

The OTIS-P model, based on the mathematical framework of OTIS, works with the nonlinear least square (NLS) algorithms of STARPAC (Donaldson and Tryon, 1990). OTIS-P thus provides an automated means of estimating the optimum values of model parameters. The model allows estimation of 10 parameters: dispersion coefficient (DISP), main channel cross-sectional area (AREA), storage zone cross-sectional area (AREA2), storage zone exchange coefficient (ALPHA), main channel first-order decay coefficient (LAMBDA), storage zone first-order decay coefficient (LAMBDA2), main channel sorption coefficient (LAMHAT), storage zone sorption coefficient (LAMHAT2), mass of accessible sediment (RHO), and distribution coefficient (KD).

OTIS-P was applied to estimate values of parameters for the reach extending from LBC-3B to LBC-3. The NLS algorithms helped to identify the optimum sets of parameters by convergence method through sensitivity analysis. According to the model requirement, the observed concentrations of each solute at the first sampling point (LBC-3B) were taken as the upstream boundary condition. In the parameter input file, the number of the boundary condition (NBOUND) was kept equal to the number of observations at LBC-3B and the boundary condition option (IBOUND) was set to 3. The downstream boundary was taken at a distance of 100 m beyond the last sampling point (LBC-3) so that the boundary condition would not interfere with the simulation. For each of the slug tracer solutes, three parameters were estimated (IFIXED = 0 in the STARPAC input file): DISP, AREA, and AREA2 with varying values for ALPHA. For conservative solutes, the other parameters were kept constant (IFIXED = 1). The observed concentrations at LBC-3 were entered into the data input file. Sample parameter input file, data input file and STARPAC input files are enclosed in Appendix C.

Once the parameters were estimated, the values were transferred to OTIS for forward simulation of the transport of each solute along the reach from LBC-3B to LBC-3. Plots of observed and simulated concentrations were visually compared.

For the nonconservative tracer propane, OTIS-P was also used to estimate the parameters (DISP, AREA and LAMBDA) for transport under steady flow with IBOUND = 3 for continuous injection. The upstream boundary condition was specified by the observed values at LBC- 3B. Volatilization of propane was considered as a first-order decay process (IDECAY=1 in parameter input file). Initial values were taken from Genereux and Hemond (1992) for the main channel first-order decay coefficient (LAMBDA) and storage zone first-order decay coefficient (LAMBDA2). As in the case of the conservative tracers, the estimated values were used in OTIS for forward simulations, and ultimately the modeled values were compared with the observed values.

Figure 2.3:Tracer test in January 2002. The tracer plume produced by the slug injection caused the red coloration of the stream. The two carboys for slug injection and the propane tanks are visible at the injection point in the foreground. Looking downstream (north) from LBC-4.

Figure 2.4: Dr. Alan Fryar collecting the VOC samples at LBC–1, October 2002.

Figure 2.5: The author gaging the stream at LBC–3, October 2002.

Figure 2.6: Gaye Brewer collecting samples at LBC–3 during the tracer test in October 2002.

Chapter 3
Results

3.1 January 2002

The stream was gaged and sampled for contaminants on January 17. Discharge (Table 3.1; Figure 3.1) ranged from 0.03 m^3/s to 0.05 m^3/s, with the highest value at LBC-2. ^{99}Tc concentrations ranged from 21.9 to 28.6 pCi/L, with highest values at LBC-3 and lowest values at LBC-4. Except the peak concentration, the values were almost similar in all of the sampling locations (Table 3.2; Figure 3.2). TCE values decreased downstream from 18 μg/L at LBC-4 to 8.2 μg/L at LBC-1 (Table 3.3; Figure 3.3). Identical concentrations were found at LBC-4 and –3B.

The tracer test started at 9:25 A.M., January 18. Mass of tracers added and their concentrations are listed in Table 3.4. Monitoring was discontinued after 115 minutes at LBC-3B and after 208 minutes at LBC-3. Propane injection was discontinued after 208 minutes. The air temperature was 3.4^oC and stream temperature was 5.3^oC (Figure 3.4).

The plot of bromide concentration with time (Figure 3.5) shows that concentration peaked at 28 minutes at LBC-3B and 98 minutes at LBC-3 after starting the experiment. The peak concentration was 12.3 mg/L at LBC-3B and 8 mg/L at LBC-3. The time-concentration plot for LBC-3B is much more symmetrical than that for LBC-3. The asymmetry of the plot for LBC-3 indicates longer tailing of the solute. A secondary peak (1.3 mg/L) is observed for the plot of LBC-3B at 78 minutes. The center of mass (centroid) is at 35.74 minutes for LBC-3B and 112.40 minutes for LBC-3. Hence the travel time of bromide center of mass from LBC-3B to -3 was 76.93 minutes.

Table 3.1: Surface discharge values (in m^3/s) at the study locations.

LBC	Distance (m)	January 2002	June	August	October	January 2003
1	0	0.034	0.088	0.032	0.034	0.12
2	410	0.049	0.067	0.033	0.036	0.055
3	775	0.032	0.059	0.036	0.032	0.065
3B	1016	0.029	0.058	0.035	0.038	0.066
4	1075	0.031	0.059	0.034	0.028	0.065

Table 3.2: ^{99}Tc concentrations (in pCi/L) at the study locations.

LBC	Distance (m)	January 2002	June	August	October	January 2003
1	0	23.7	73.4	42.1	20.9	22.6
2	410	24.5	70.1	44.6	32.7	25.4
3	775	28.6	74.8	44.5	21.9	26.2
3B	1016	23.3	70.3	44.6	18.3	25
4	1075	21.9	82.9	51.9	23.6	100.4

Table 3.3: TCE concentrations (in μg/L) at the study locations.

LBC	Distance (m)	January 2002	June	August	October	January 2003
1	0	8.2	23	11	5.4	7.8
2	410	12	37	23	10	11
3	775	16	46	28	13	13
3B	1016	18	57	33	17	15
4	1075	18	59	37	18	15

Table 3.4: Details of the tracers used in the present study.

Seasons	Tracer name	Mass added	Concentration	Background concentration
January 2002	Sodium bromide	1 kg	19415 mg/L	0.2 mg/L at LBC-3B 0.2 mg/L at LBC-3
	Rhodamine WT 20%	600 g	3000 mg/L	NIL
	Propane	Continuous injection at ~100 kPa pressure		
June	Sodium bromide	2 kg	38830 mg/L	0.5 mg/L at LBC-3B 0.3 mg/L at LBC-3
	Sodium nitrate	2 kg	36470 mg/L	1.1 mg/L at LBC-3B 1.1 mg/L at LBC-3
	Rhodamine WT 5%	515 g	2550 mg/L	NIL
	Propane	Continuous injection at ~100 kPa pressure		
August	Sodium nitrate	2 kg	36470 mg/L	0.93 mg/L at LBC-3B 0.78 mg/L at LBC-3
	Rhodamine WT 5%	412 g	2040 mg/L	NIL
	Propane	Continuous injection at ~100 kPa pressure		
October	Sodium nitrate	2 kg	36470 mg/L	0.75 mg/L at LBC-3B 0.61 mg/L at LBC-3
	Rhodamine WT 5%	412 g	2040 mg/L	NIL
	Propane	Continuous injection at ~100 kPa pressure		
January 2003	Sodium nitrate	2 kg	36470 mg/L	0.72 mg/L at LBC-3B 0.84 mg/L at LBC-3
	Rhodamine WT 5%	412 g	2040 mg/L	NIL
	Propane	Continuous injection at ~100 kPa pressure		

The rhodamine WT concentration (Figure 3.6) peaked 28 minutes at LBC-3B and 98 minutes at LBC-3 after starting the experiment. The peak concentration was 2.04 mg/L at LBC-3B and 1.71 mg/L at LBC-3. Like the bromide concentration curves, the rhodamine plot for

LBC-3B is relatively symmetrical, while the plot for LBC-3 shows much more prominent tailing. A secondary peak (0.52 mg/L) is also observed for the plot of LBC-3B at 53 minutes. The center of mass (centroid) is at 37.43 minutes for LBC-3B and 113.36 minutes for -3. Hence the travel time of the rhodamine WT from LBC-3B to LBC-3 was 75.93 minutes.

The comparison between the normalized (C/C_o) time-concentration plots (Figure 3.7) shows that the curves for bromide and rhodamine WT at LBC-3B are almost superimposed, although the secondary peak for bromide appeared 25 minutes later than that of rhodamine WT. The plots of the tracers for LBC-3 are also similar to each other, but the area under the time-concentration curve for bromide was less than that of rhodamine WT.

The time-concentration plot of the continuously injected non-conservative tracer, propane (Figure 3.8), is different from that of the other tracers. The noisy nature of the plot can be attributed to the highly volatile nature of the propane and its potential sensitivity to factors such as changes in delivery pressure and air temperature as well as possible analytical error. The propane concentration approached a plateau at 1.2×10^{-4} moles/L after 38 minutes for LBC-3B and 1.0×10^{-4} moles/L after 133 minutes for LBC-3.

Portions of the tracer cloud were found to get caught in stagnation zones for all of the monitored periods (Figure 3.9). These portions moved downstream more slowly than the main cloud and were reflected as secondary peaks in the time-concentration plots for the slug tracers.

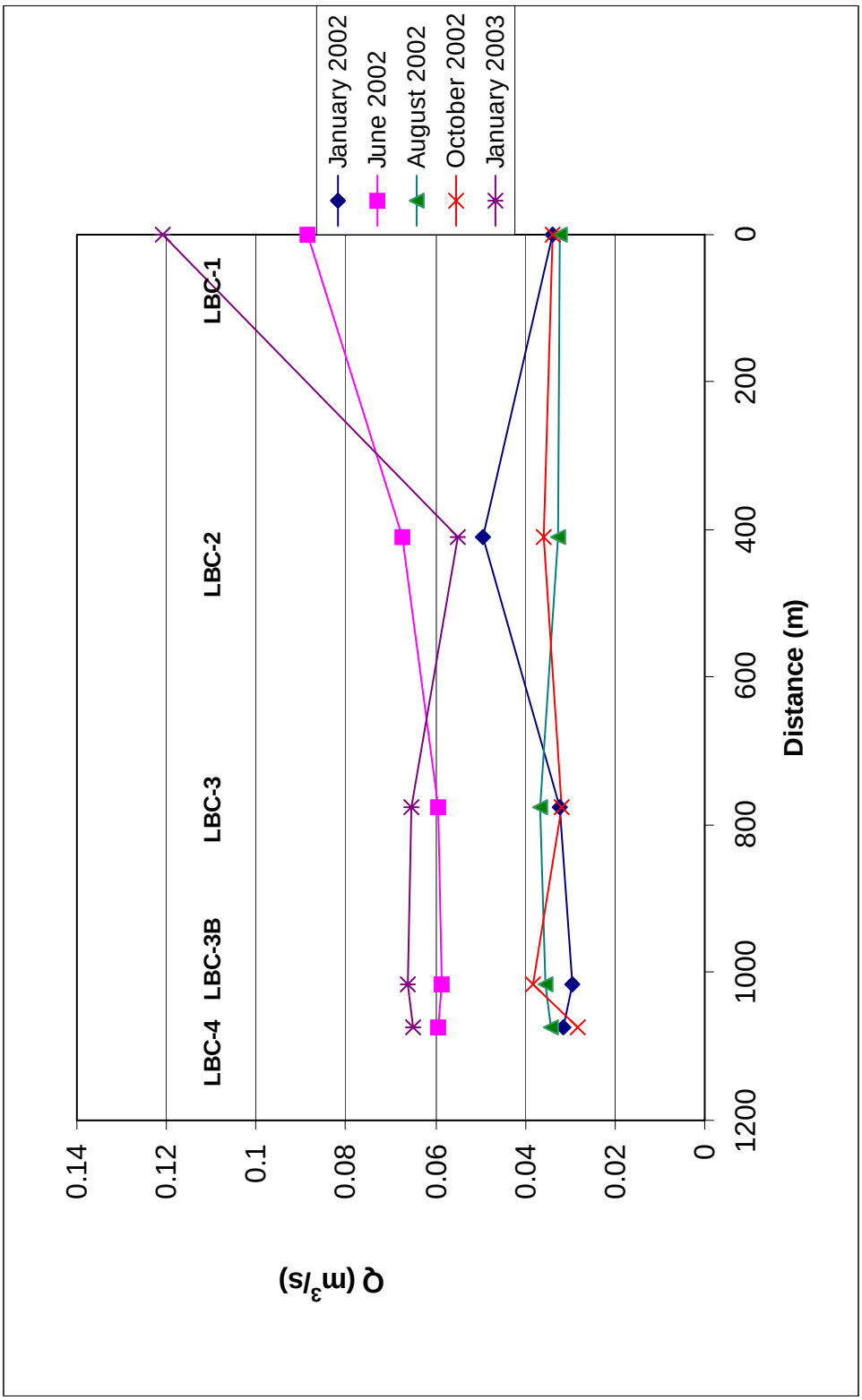

Figure 3.1: Surface discharge values at the five study locations.

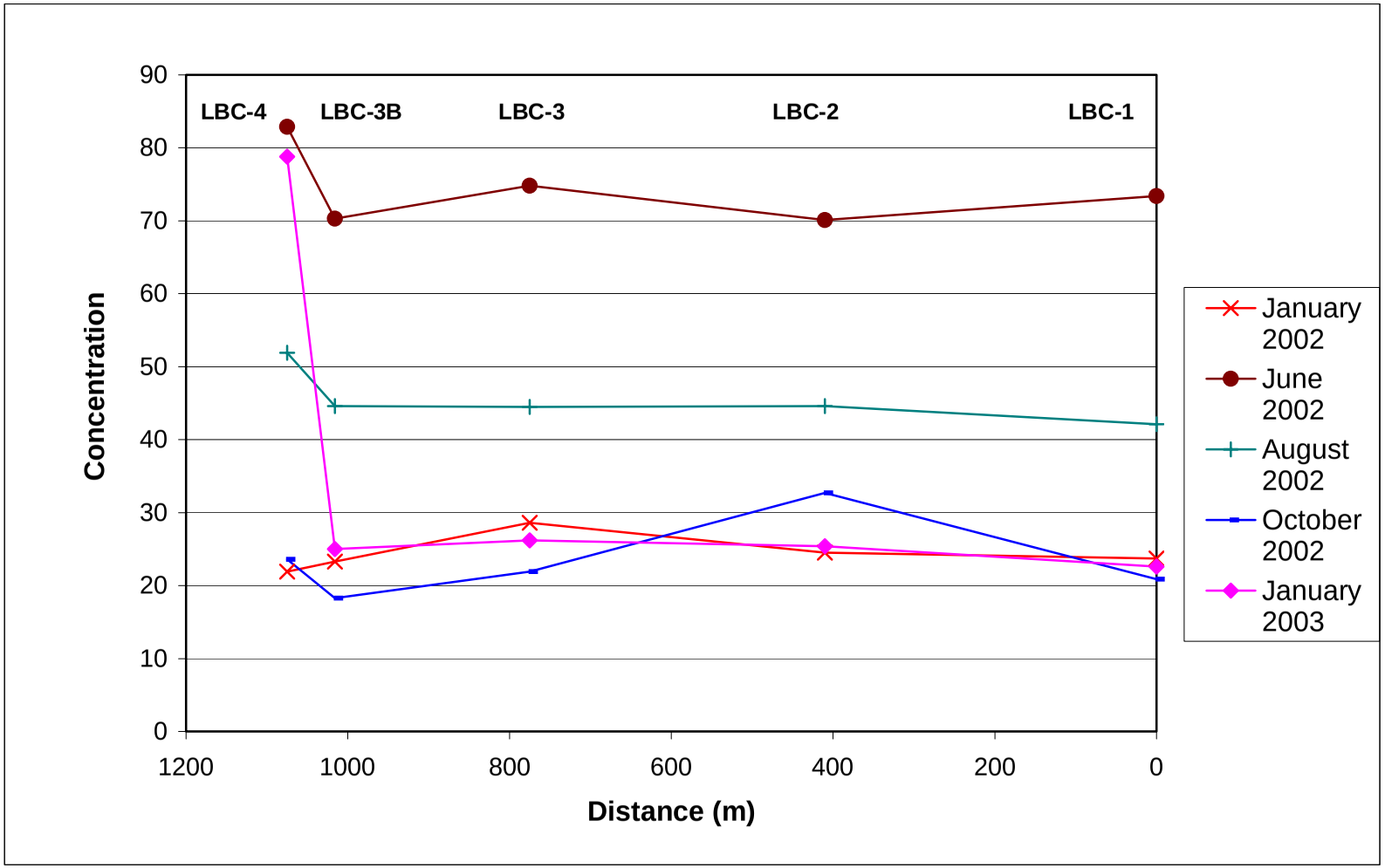

Figure 3.2: ^{99}Tc concentration (pCi/L) at the sampling locations.

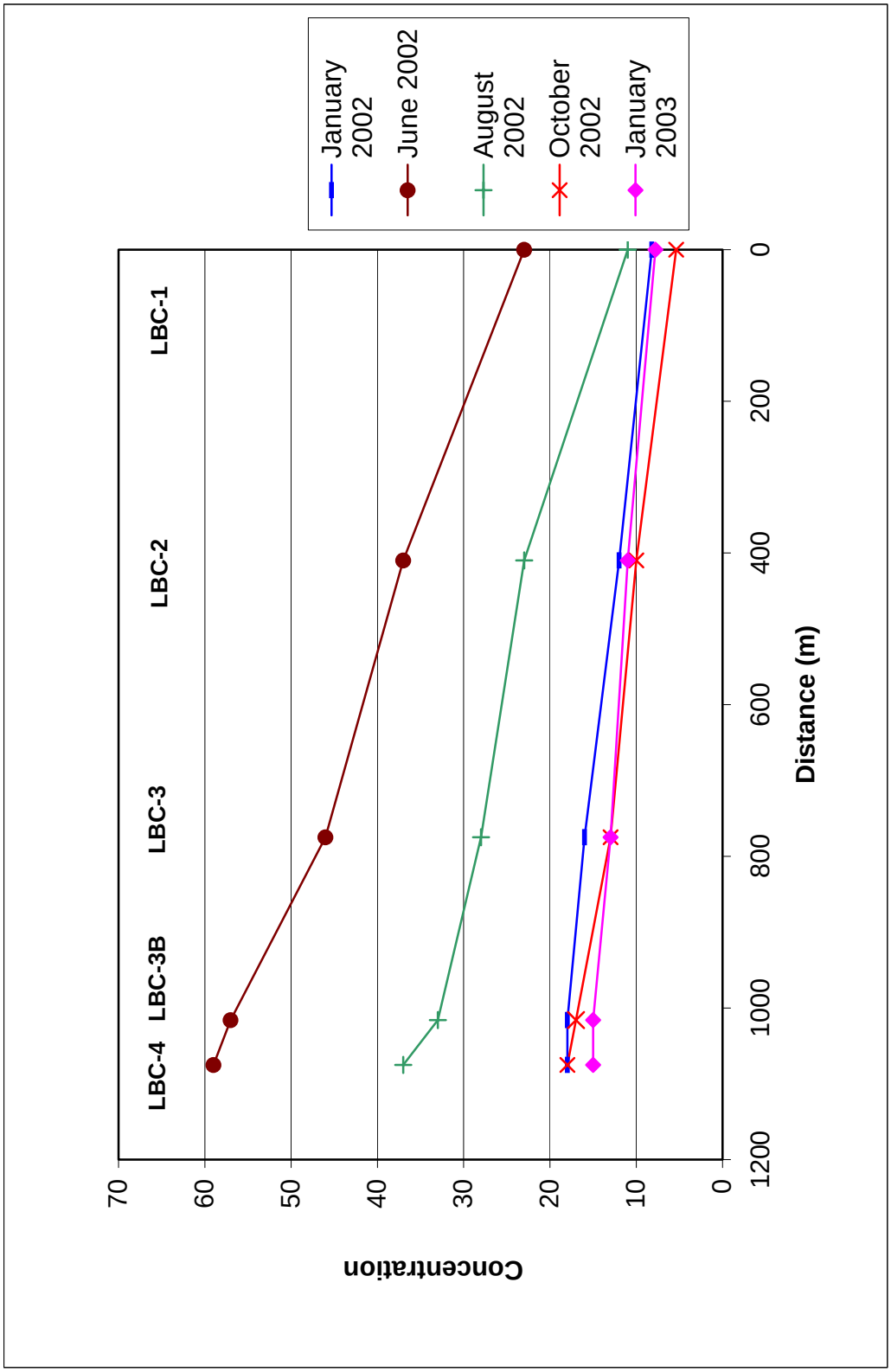

Figure 3.3: TCE concentrations (µg/L) at the sampling locations.

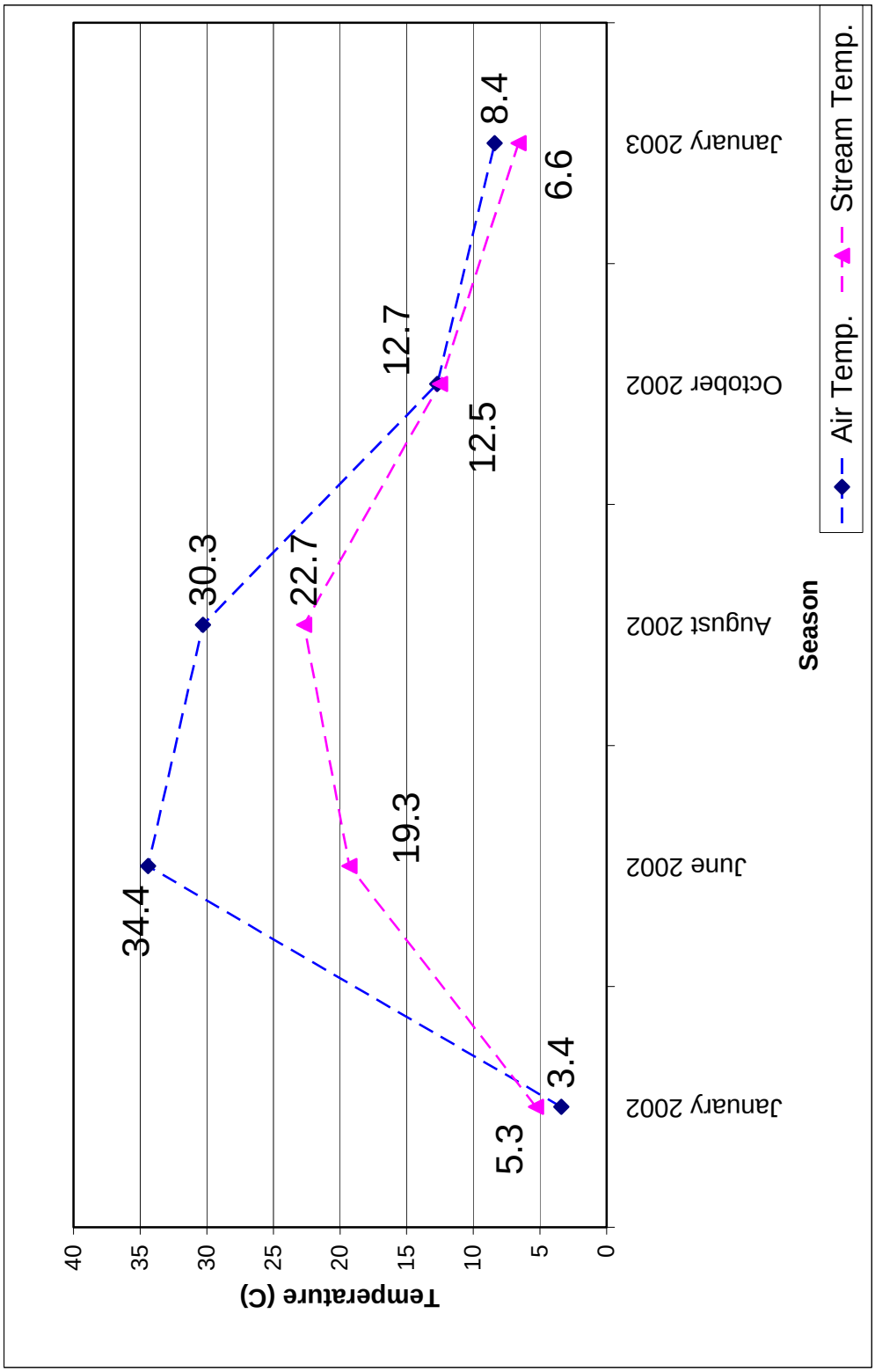

Figure 3.4: Temperature at the injection point during tracer tests.

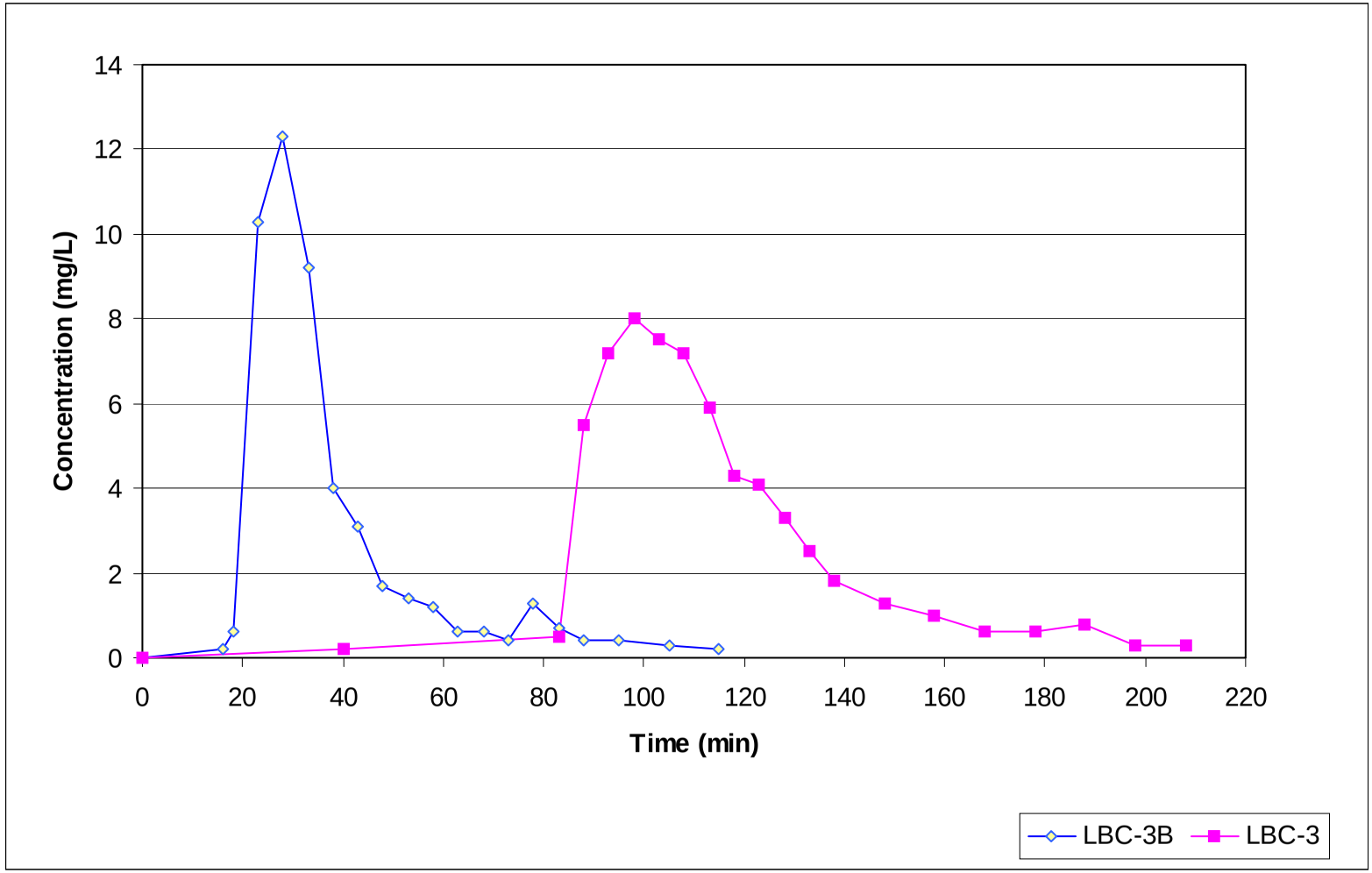

Figure 3.5: Time-concentration plot for bromide at LBC- 3B and -3, January 2002.

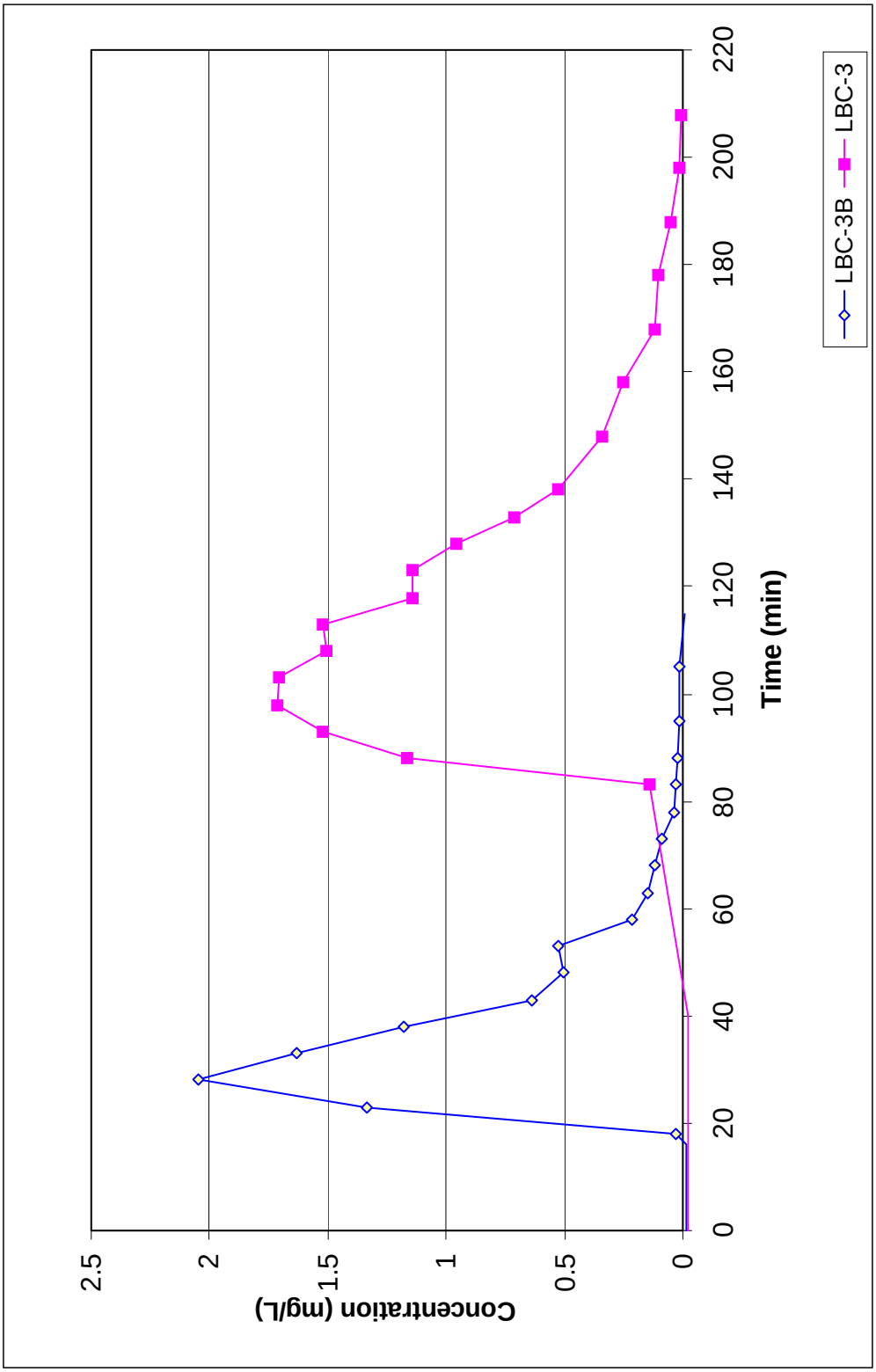

Figure 3.6: Time-concentration plot for rhodamine WT at LBC-3B and -3, January 2002.

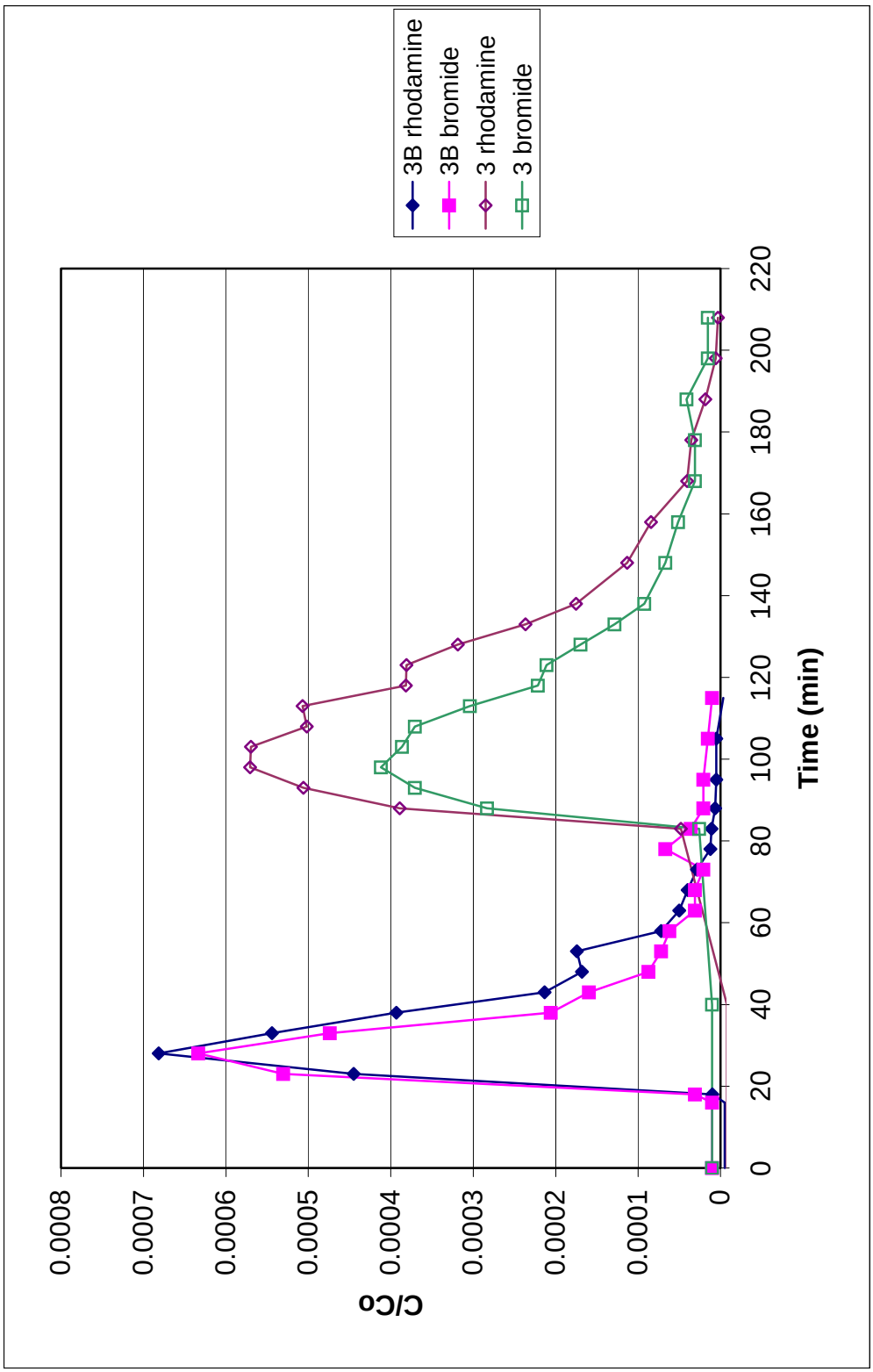

Figure 3.7: Time-normalized concentration plot for bromide and rhodamine WT at LBC-3B and -3, January 2002.

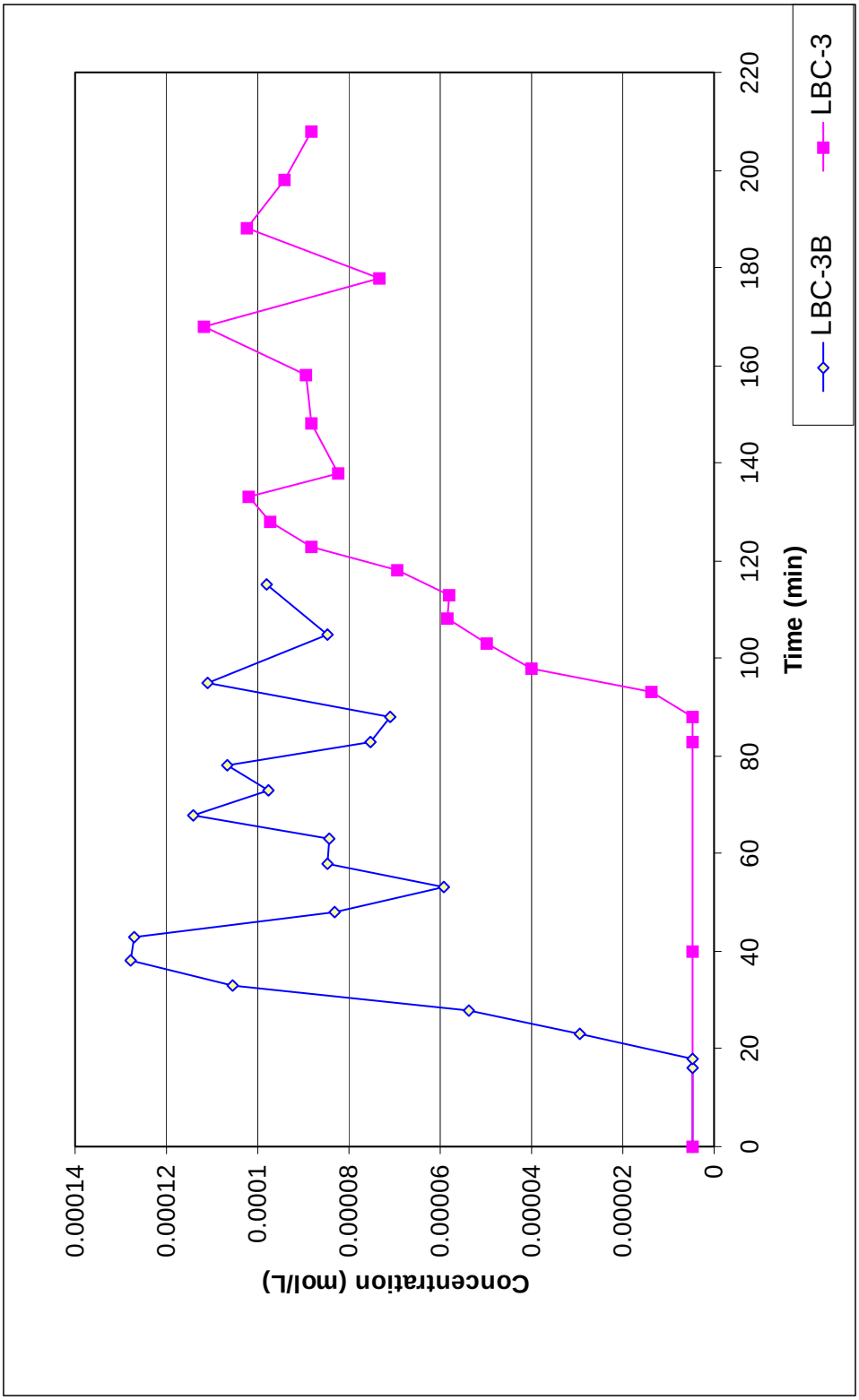

Figure 3.8: Time-concentration plot for propane at LBC-3B and -3, January 2002.

Figure 3.9: In-stream transient storage of part of the tracer cloud in a stagnation zone, January 2003

3.2 June 2002

The stream discharge measured on June 5 was much higher than that in any of the other monitored periods except January 2003. The discharge rate ranged from 0.059 m^3/s at LBC-3B to 0.089 m^3/s at LBC-1 to and tended to increase downstream (Table 3.1; Figure 3.1). The ^{99}Tc concentrations varied over a small range at all the sampled locations except at LBC-4. The values ranged from 73.4 to 82.9 pCi/L (Table 3.2; Figure 3.2). Concentrations of TCE in June ranged from 59 μg/L at LBC-4 to 23 μg/L at LBC-1 (Table 3.3; Figure 3.3). The concentrations decreased downstream with a gradient steeper than during any other monitored periods (Figure 3.3). Characteristically, the concentrations of both TCE and ^{99}Tc in June were found to be highest among all the monitored periods and the highest concentrations were about three times higherthan the corresponding values observed in January 2002.

The tracer test was started at 9:31 AM on June 6. Sampling of tracers in the stream water was discontinued after 70 minutes at LBC-3B and after 155 minutes at LBC-3. The air and stream temperatures at the injection location were 34.4°C and 19.3°C, respectively (Figure 3.4).

As noted in Table 3.4, the mass of sodium bromide was doubled from the amount in January owing to the increased discharge. An equivalent mass of sodium nitrate was also added. The time-concentration plot of bromide (Figure 3.10) shows that the concentration peaked 15 minutes at LBC-3B and 53 minutes at LBC-3 after the injection of the tracers in the stream. The peak concentrations observed were more than twice than those observed in the previous run. The values reached 30.9 mg/L at LBC-3B and 14.89 mg/L at LBC-3. In spite of the asymmetry in the plot due to the tailing effect, the curves at both locations are much more symmetrical than those of January. As for January, the curve at LBC-3B was much steeper than at LBC-3. The secondary peak (3.89 mg/L) in the curve of LBC-3B was observed after 49 minutes. A secondary peak was not evident in the curve of LBC-3. The centroid of the bromide plot was at 20.39 minutes for LBC-3B and at 60.94 minutes for LBC-3. Thus the travel time for the bromide center of mass between the sampling locations was 40.54 minutes.

The nitrate (NO_3^--N) concentration (Figure 3.11) peaked 15 minutes at LBC-3B and 53 minutes at LBC-3 after starting the experiment. The relative difference between the peak

concentrations at LBC-3B and -3 is much less conspicuous in the case of nitrate than that of bromide or rhodamine WT. The highest concentrations were 4.83 mg/L at LBC-3B and 4.29 mg/L at LBC-3. Similar to the bromide concentration curve, the nitrate concentration curve for LBC-3B is relatively steep, while the plot for the LBC-3 shows more prominent tailing. Instead of a secondary peak, a sink (1.18 mg/L) was observed in LBC-3B curve for nitrate, 28 minutes after tracer injection. The centroid is at 23.72 minutes for LBC-3B and 60.06 minutes for LBC-3. Hence the mean travel time of nitrate from LBC-3B to LBC-3 was 36.34 minutes.

The peak concentration of rhodamine WT (Figure 3.12) was almost half that observed in January. The concentrations peaked at 1.07 mg/L at 15 minutes after tracer injection at LBC-3B and at 0.49 mg/L at 58 minutes at LBC-3. As for bromide, the relative difference between the peaks at LBC-3B and -3 is quite prominent, but both the curves were much more symmetric than the other two solute tracers (bromide and nitrate) or than the rhodamine WT curves observed in January. The tailing for the LBC-3 curve was characteristically quite short. A subdued, inconspicuous secondary peak (0.034 mg/L) was observed after 46 minutes. The centroid at LBC-3B was after 19.18 minutes and at LBC-3 was after 60.63 minutes. The travel time from LBC-3B to 3 was 31.45 minutes.

The visual comparison of superimposed normalized (C/C_o) time-concentration plots (Figure 3.13) shows that at LBC-3B, the peaks of the three tracers mentioned above are almost co-linear. The areas under the curves are in the order of bromide > rhodamine WT > nitrate. The secondary peak of bromide formed 3 minutes after rhodamine, while no such peak was observed in the nitrate plot.

Due to the greater widths of the plots at LBC-3, it is difficult to identify the relative positions of the peak concentrations, but qualitative inspection shows that bromide peaked minutes before rhodamine WT. The tailing of the curves for bromide and nitrate at LBC-3 is quite conspicuous in comparison to rhodamine WT. The order of area under the curve for the tracers is not changed from that of LBC-3B.

The time-concentration plot for propane (Figure 3.14) was much less noisy than that observed in January 2002. Concentration plateaus were reached at about 6.9×10^{-5} moles/L after 20 minutes for LBC-3B and 6.6×10^{-5} moles/L after 67 minutes for LBC-3. Interestingly, the concentrations seem to increase again after 64 minutes at LBC-3B and 145 minutes at LBC-3, probably due to change in tank delivery pressure.

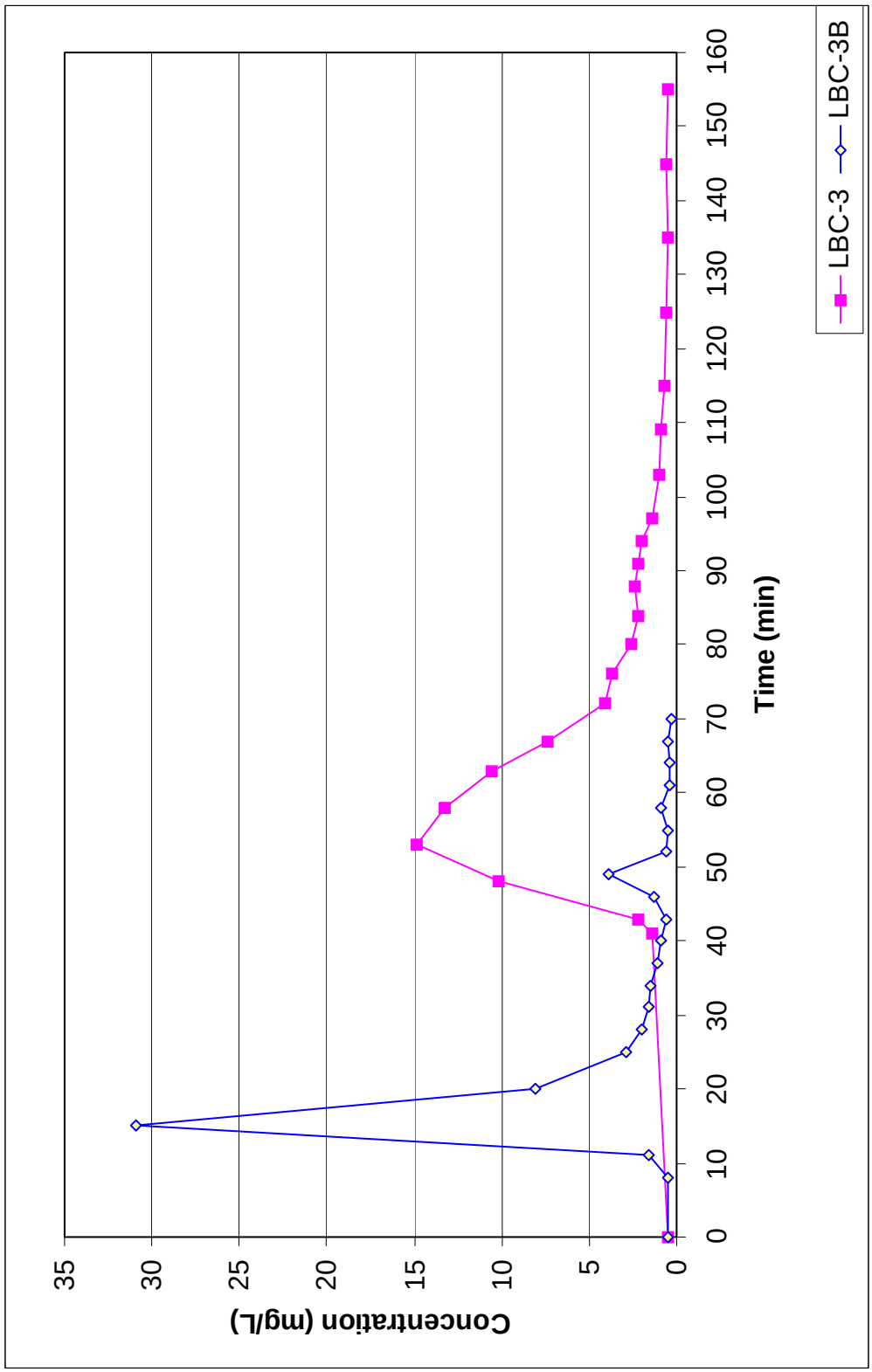

Figure 3.10: Time-concentration plot for bromide at LBC-3B and -3, June 2002.

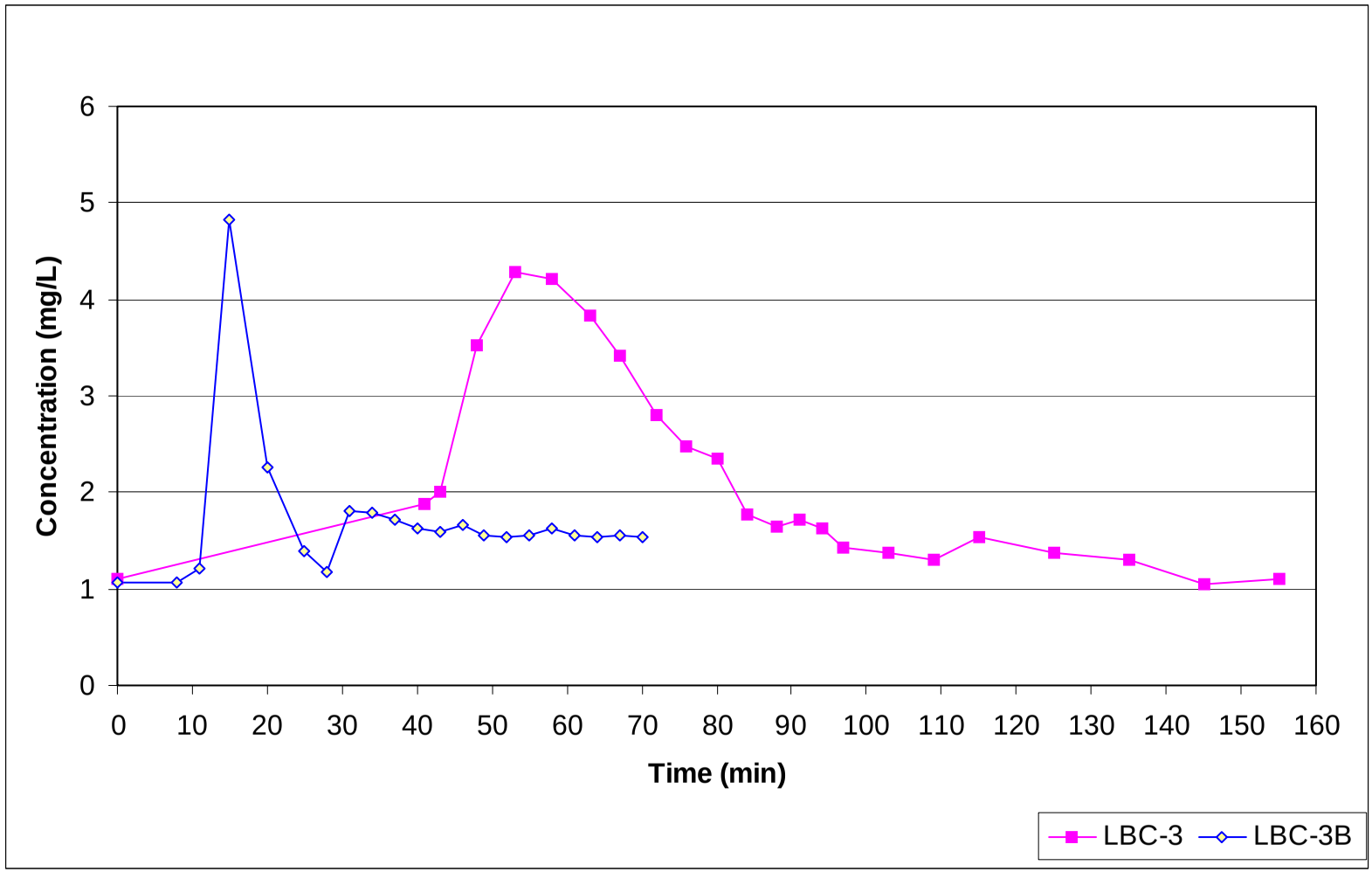

Figure 3.11: Time-concentration plot for nitrate (NO_3^--N) at LBC-3B and -3, June 2002.

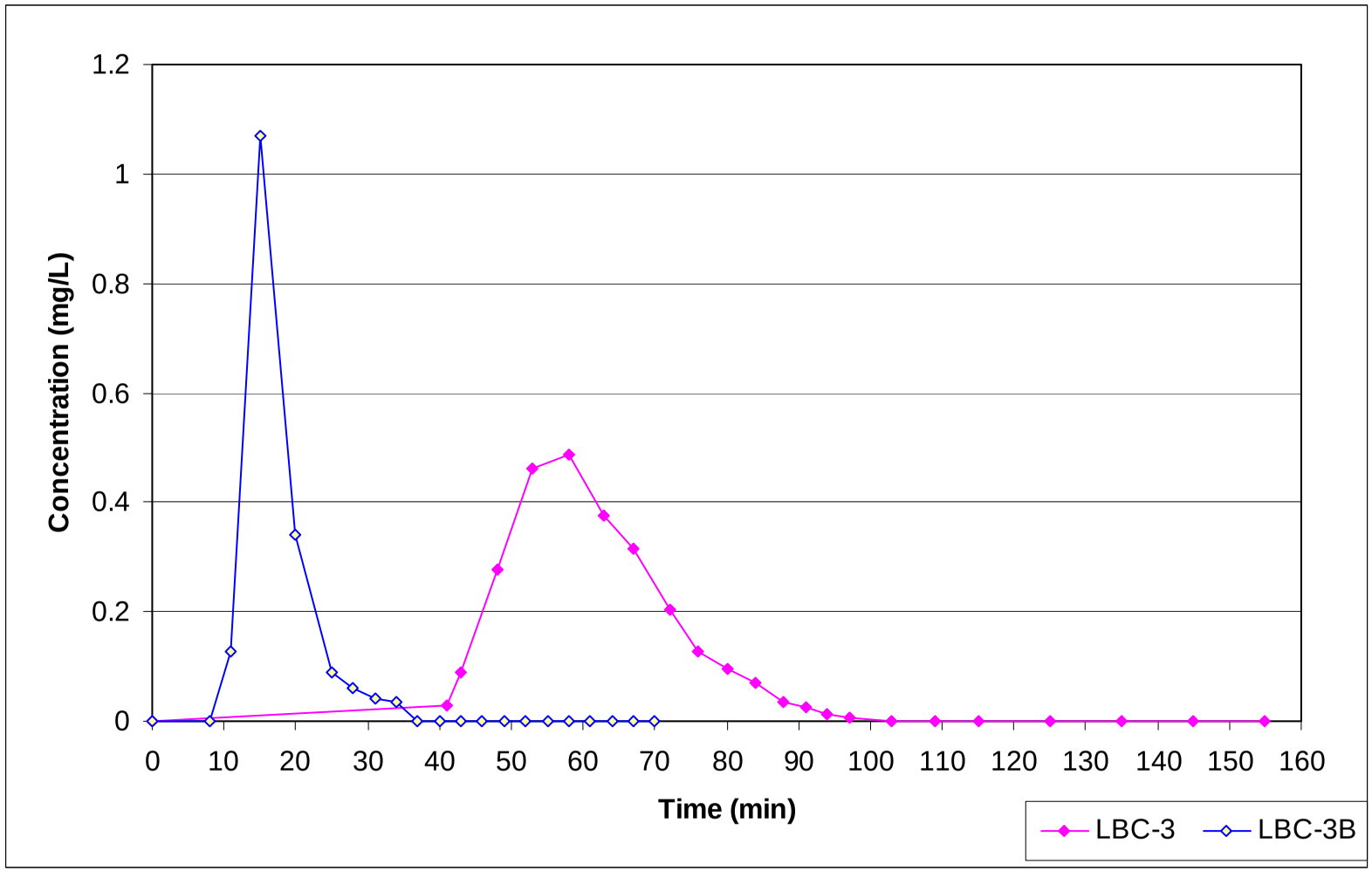

Figure 3.12: Time-concentration plot for rhodamine WT at LBC- 3B and -3, June 2002.

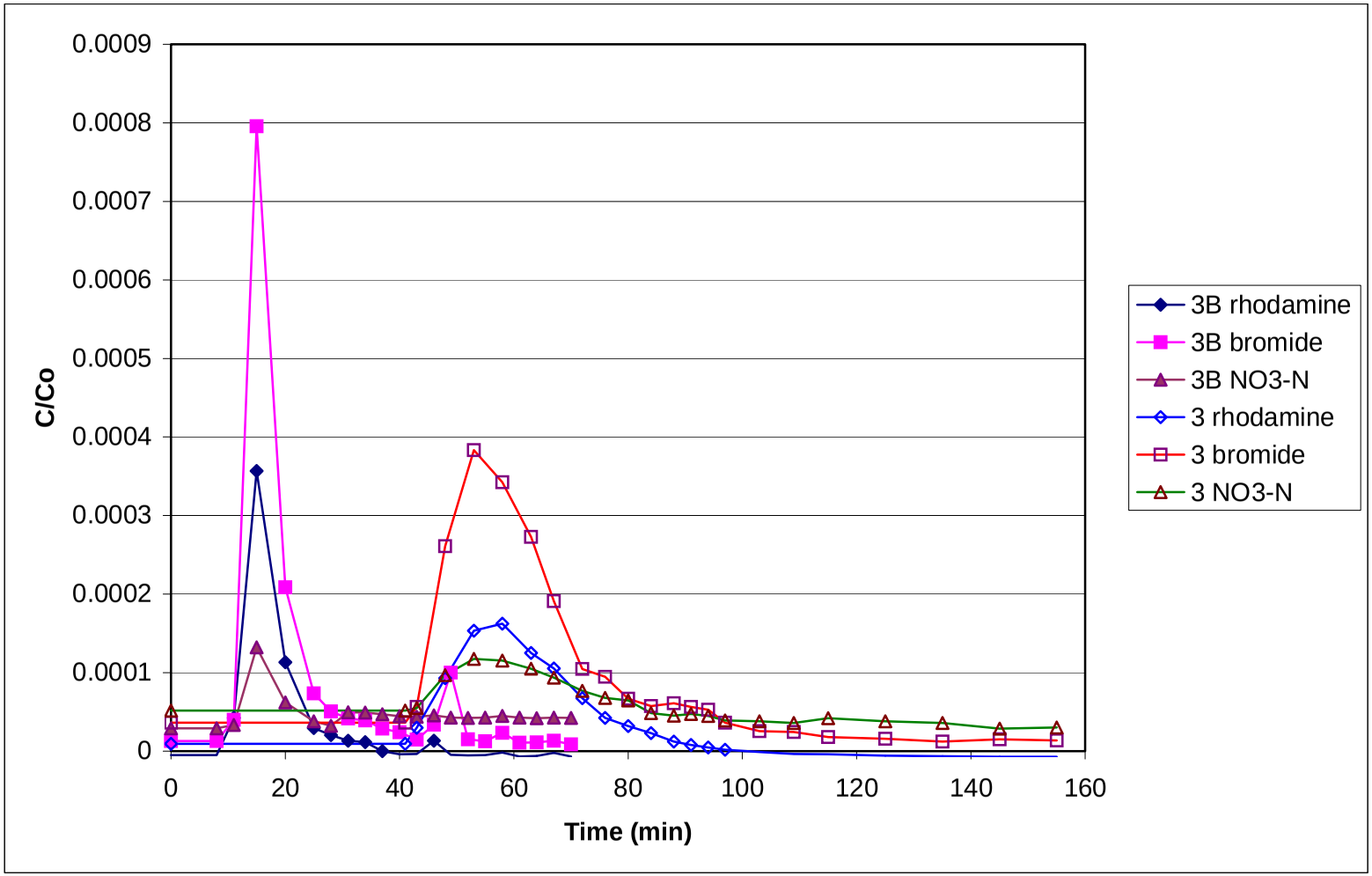

Figure 3.13: Time-normalized concentration plot for bromide, nitrate and rhodamine WT at LBC-3B and -3, June 2002.

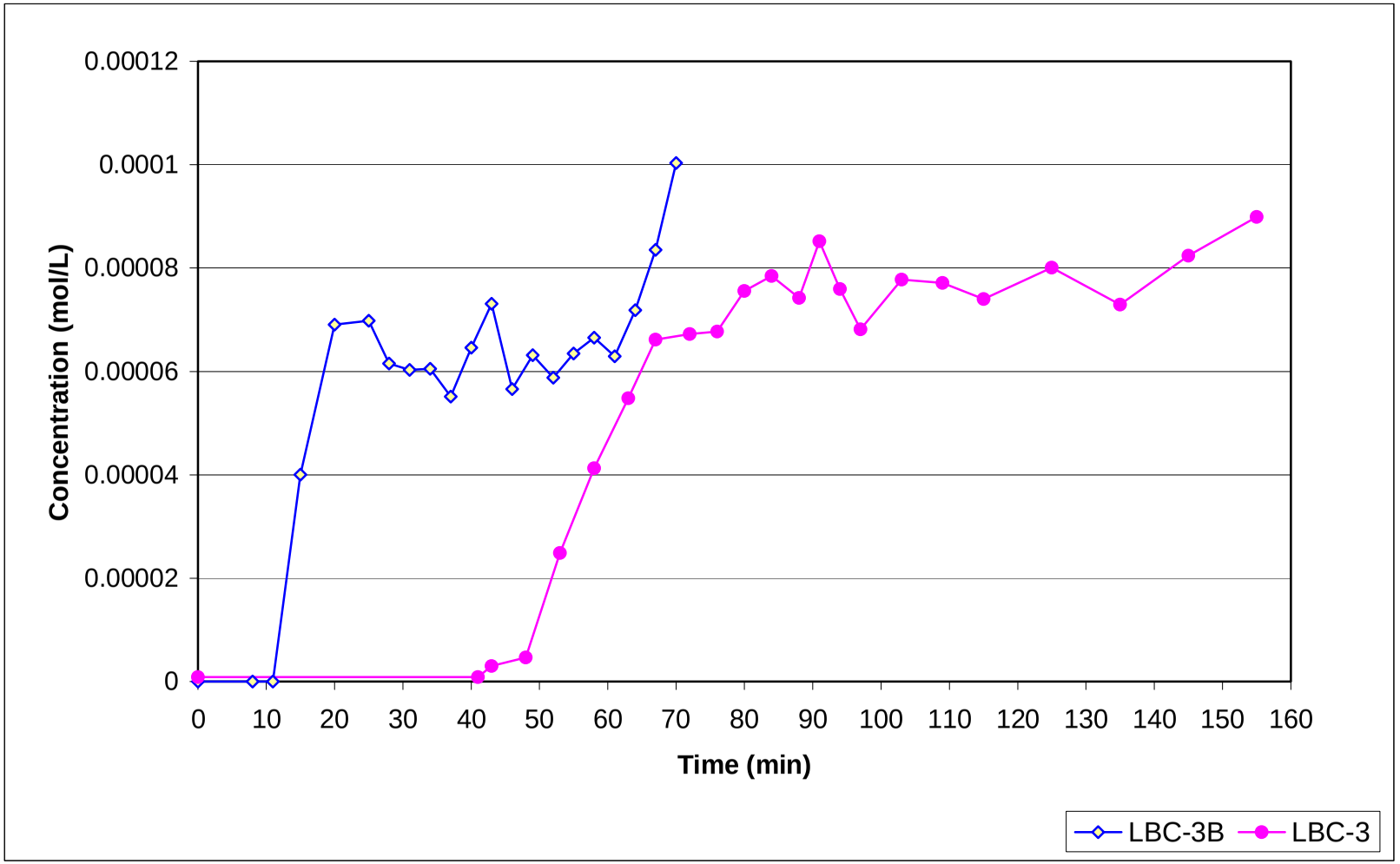

Figure 3.14: Time-concentration plot for propane at LBC-3B and -3, June 2002.

3.3 August 2002

Unlike the previous monitoring periods, the stream was gaged on the day of the experiment just before tracer injection. The surface water discharge value ranged from 0.032 m^3/s to 0.037 m^3/s (Table 3.1; Figure 3.1). The highest discharge was at LBC-3. The ^{99}Tc and TCE concentrations which were measure on samples collected on August 12 were intermediate between June and the other monitored periods. The ^{99}Tc was highest at LBC-4 (51.9 pCi/L) and lowest at LBC-1 (42.3 pCi/L) (Table 3.2; Figure 3.2). The concentrations at LBC-3B, -3 and –2 were almost identical. On the other hand, the TCE concentrations (Table 3.3; Figure 3.3) gradually declined from LBC-4 (37 μg/L) to LBC-1 (11 μg/L).

The third tracer test was started at 11:30 A.M. August 24. The monitoring of stream water continued for 127 minutes at LBC-3B and for 179 minutes at LBC-3 after the injection of the tracers into the creek. The ambient air temperature at the injection location was 30.3°C and stream temperature was 22.7°C (Figure 3.4). Due to the similar behavior of bromide and rhodamine WT in the previous tests, bromide was not used in this test. Instead, rhodamine WT was considered both as a conservative and visual tracer. Nitrate was used to understand the redox condition of the stream.

Figure 3.15 shows that the NO_3^--N concentration peaked 30 minutes at LBC-3B and 93 minutes at LBC-3 after the injection of the tracers into the stream. The peak concentrations (5.69 mg/L at LBC-3B and 3.13 mg/L at LBC-3) were slightly greater than those observed in the previous run. The curves at both the sampling locations were asymmetrical with prominent tails. Like the previous instance, the curve at LBC-3B is much more steep and the peak concentration was almost twice that of LBC-3. A very conspicuous secondary peak in the curve of LBC-3B occurred after 72 minutes. The concentration of this secondary peak (3.68 mg/L) was greater than the highest concentration at LBC-3. No such secondary peak was found for LBC-3. The centroid of the plot was at 53.08 minutes for LBC-3B and 117.44 minutes for LBC-3. Therefore, the travel time for the nitrate center of mass between the sampling locations was 64.36 minutes.

The rhodamine WT concentration (Figure 3.16) peaked at 33 minutes at LBC-3B and 99 minutes at LBC-3 after starting the experiment. The peak concentrations, 0.86 mg/L at LBC-3B

and 0.40 mg/L at LBC-3, were less than the values observed in the previous two experiments. Like the nitrate concentration curves, the rhodamine WT plots for both LBC-3B and -3 are very asymmetrical with conspicuous tails. The peak concentration of LBC-3B was almost twice that of LBC-3. The curve for LBC-3B is characterized by a sudden sink (0.11 mg/L) at 27 minutes and a distinct secondary peak (0.21 mg/L) at 82 minutes after starting the experiment. The curve at LBC-3 also shows a small sink near its peak at 93 minutes after injection. The rhodamine WT centroids were at 46.79 minutes for LBC-3B and 118.86 minutes for LBC-3. Hence the travel time of the rhodamine WT center of mass from LBC-3B to LBC-3 was 72.07 minutes. The comparison between the superimposed normalized (C/C_o) time-concentration plots (Figure 3.17) shows that the areas under the rhodamine WT curves at both locations are greater than those of nitrate.

The time-concentration plots (Figure 3.18) for propane in August are somewhat different than those observed in January and June. Curves for both LBC-3B and -3 do not seem to have reached a stable plateau concentration. Instead, for both the curves, there was a distinct change from a steep to a relatively gentler slope. The flexure points of the curves occurred after 33 minutes at LBC-3B and after 90 minutes at LBC-3. Another distinguishable difference between the propane plot of August and the previous test is that the concentration curve for LBC-3 seems to be diminished relative to that of -3B.

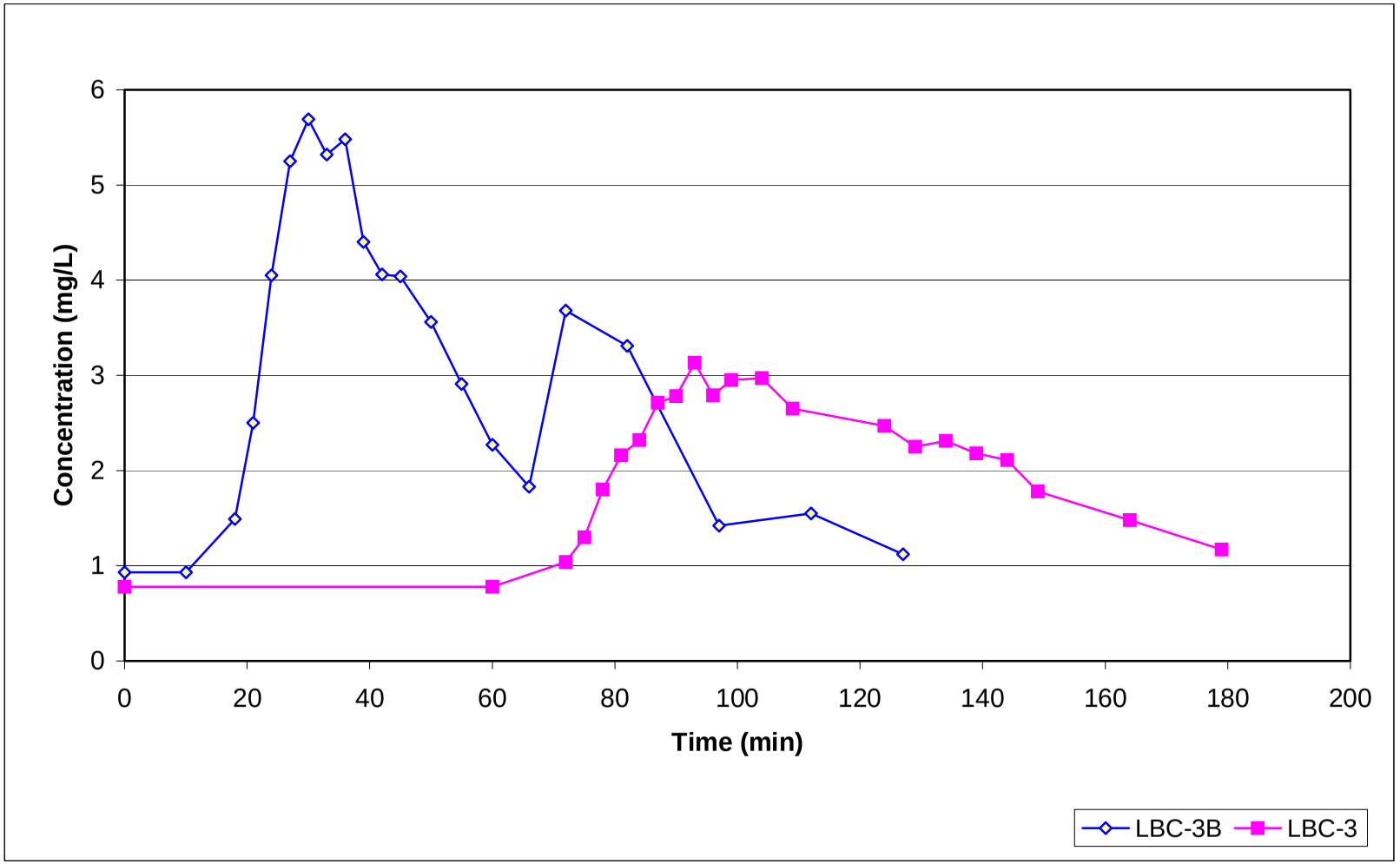

Figure 3.15: Time-concentration plot for nitrate (NO_3^--N) at LBC-3B and -3, August 2002.

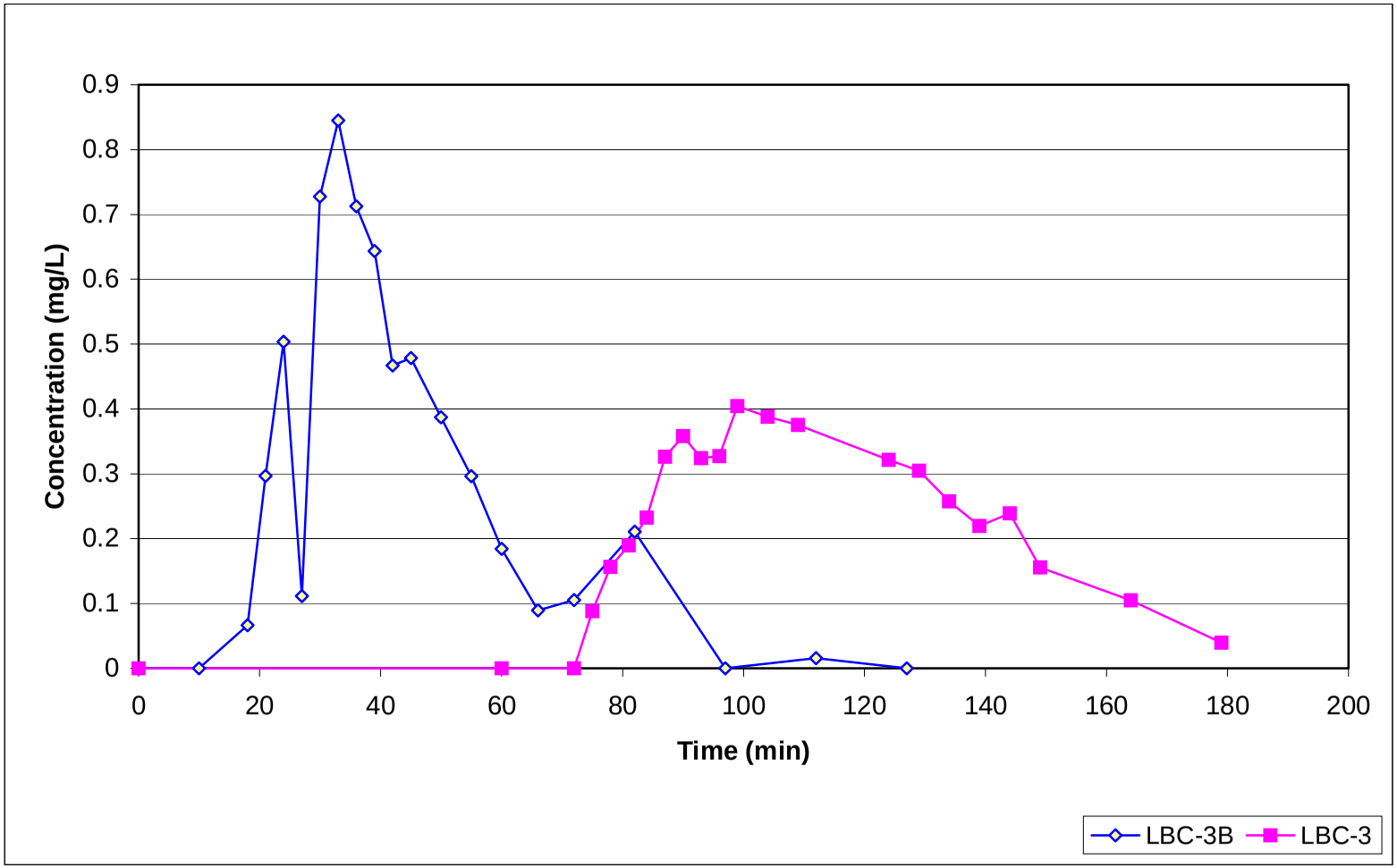

Figure 3.16: Time-concentration plot for rhodamine WT at LBC-3B and -3, August 2002

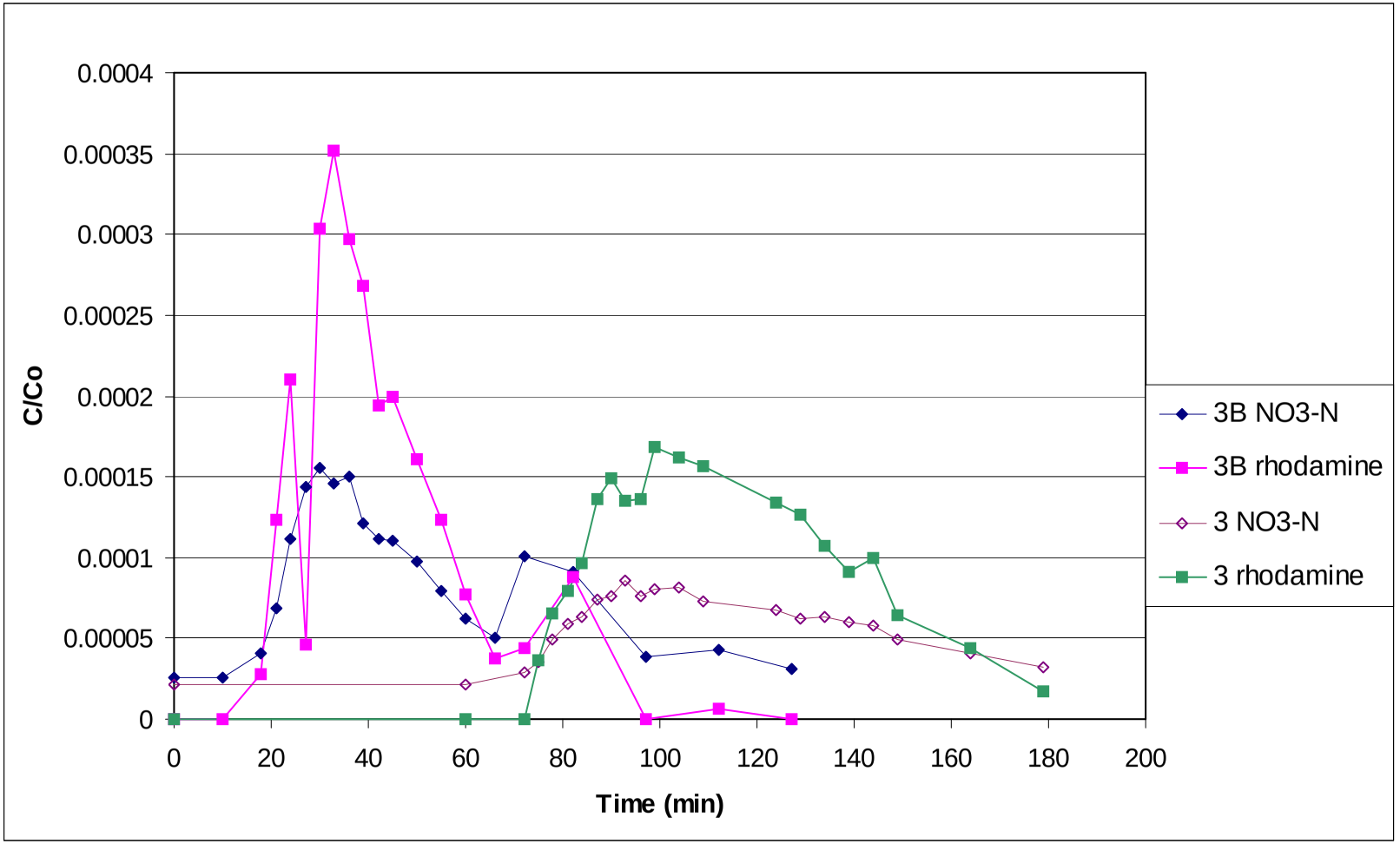

Figure 3.17: Time- normalized concentration plot for nitrate and rhodamine WT at LBC-3B and -3, August 2002.

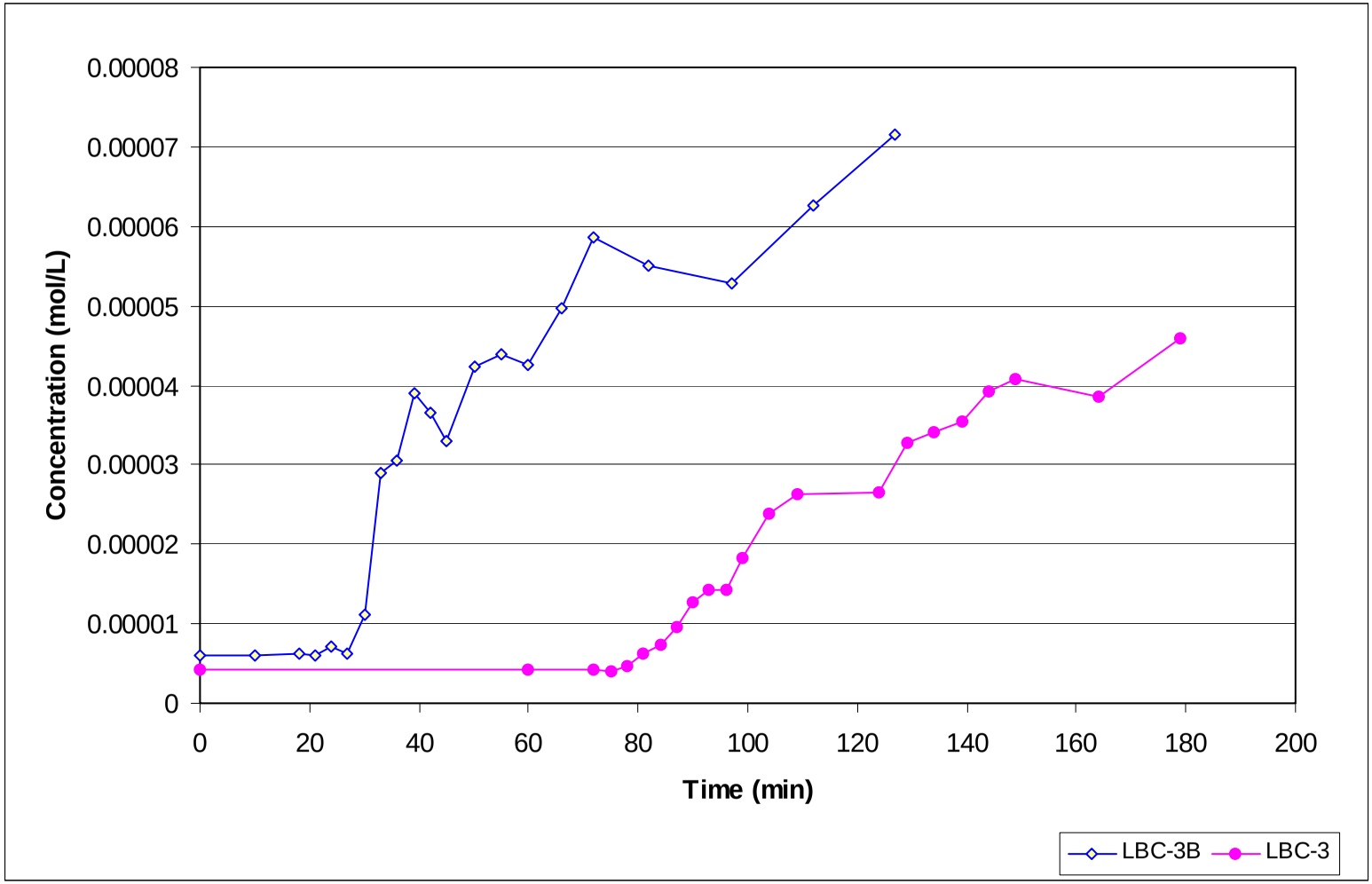

Figure 3.18: Time-concentration plot for propane at LBC-3B and -3, August 2002.

3.4 October 2002

The stream was gaged on October 13. Discharge ranged from 0.028 m^3/s to 0.039 m^3/s, with the highest value at LBC-3B and lowest at LBC-4 (Table 3.1; Figure 3.1). The values were lower than all the monitored periods except January 2002. The concentrations of ^{99}Tc and TCE were for the lowest among all the monitored periods. The ^{99}Tc concentrations ranged from 18.3 to 32.7 pCi/L (Table 3.2; Figure 3.2). The highest value was observed at LBC-2 and the lowest at LBC-3B. The values for the other locations were similar. The TCE concentrations gradually decreased downstream from 18 μg/L at LBC-4 to 5.4 μg/L at LBC-1 (Table 3.3; Figure 3.3).

The fall tracer test was started at 10:15 AM on October 14. Sampling of tracers in the stream was discontinued after 131 minutes at LBC-3B and after 169 minutes at LBC-3. The air and stream temperatures at the injection location were 12.7°C and 12.5°C, respectively (Figure 3.4). As in August, only sodium nitrate and rhodamine WT were used as solute tracers. The nitrate (NO_3^--N) time-concentration plot (Figure 3.19) peaked 31 minutes at LBC-3B and 111 minutes at LBC-3 after starting the experiment. The peak concentration at LBC-3B was more than twice that of LBC-3. The highest concentrations were 7.37 mg/L at LBC-3B and 3.59 mg/L at LBC-3. The curves for both the sampling locations were close to symmetrical. As for June and August, the nitrate concentration curve for LBC-3B is steeper than for LBC-3. Both the curves showed short tailing. The curve at LBC-3 did not return to the background concentration within the time of the experiment. Secondary peaks were observed at 69 minutes (1.51 mg/L) at LBC-3B and at 149 minutes (1.74 mg/L) at LBC-3. The centroid was at 36.28 minutes for LBC-3B and 122.65 minutes for LBC-3. Hence the travel time of the nitrate center of mass from LBC-3B to LBC-3 was 86.37 minutes.

Rhodamine WT concentrations (Figure 3.20) peaked 28 minutes at LBC-3B and 111 minutes at LBC-3 after starting the experiment. The peak concentration was 0.92 mg/L at LBC-3B and 0.46 mg/L at LBC-3. The time-concentration plots for both LBC-3B and LBC-3 are generally symmetrical, although the curve for LBC-3 shows a longer tail. Like nitrate, the rhodamine WT concentrations did not return to the background values before the end of the experiment. No prominent secondary peak was observed in any of the curves. The centroid was

at 37.67 minutes for LBC-3B and 122.08 minutes for LBC-3. Hence the travel time of the rhodamine WT center of mass from LBC-3B to -3 was 84.41 minutes.

The superimposed normalized (C/C_o) time-concentration plots (Figure 3.21) show larger areas under the rhodamine WT curves than under the nitrate curves. The peak concentrations of rhodamine WT were about twice those of nitrate at both the sampling locations.

The propane time-concentration plots (Figure 3.22) were distinct and much less noisy than observed in the previous monitored periods. The curve for LBC-3B reached a relative plateau concentration at about 1.5×10^{-4} moles/L after 76 minutes. For LBC-3, the concentration curve seems to increase with a constant slope, which suggests that a plateau was not reached before discontinuation of monitoring.

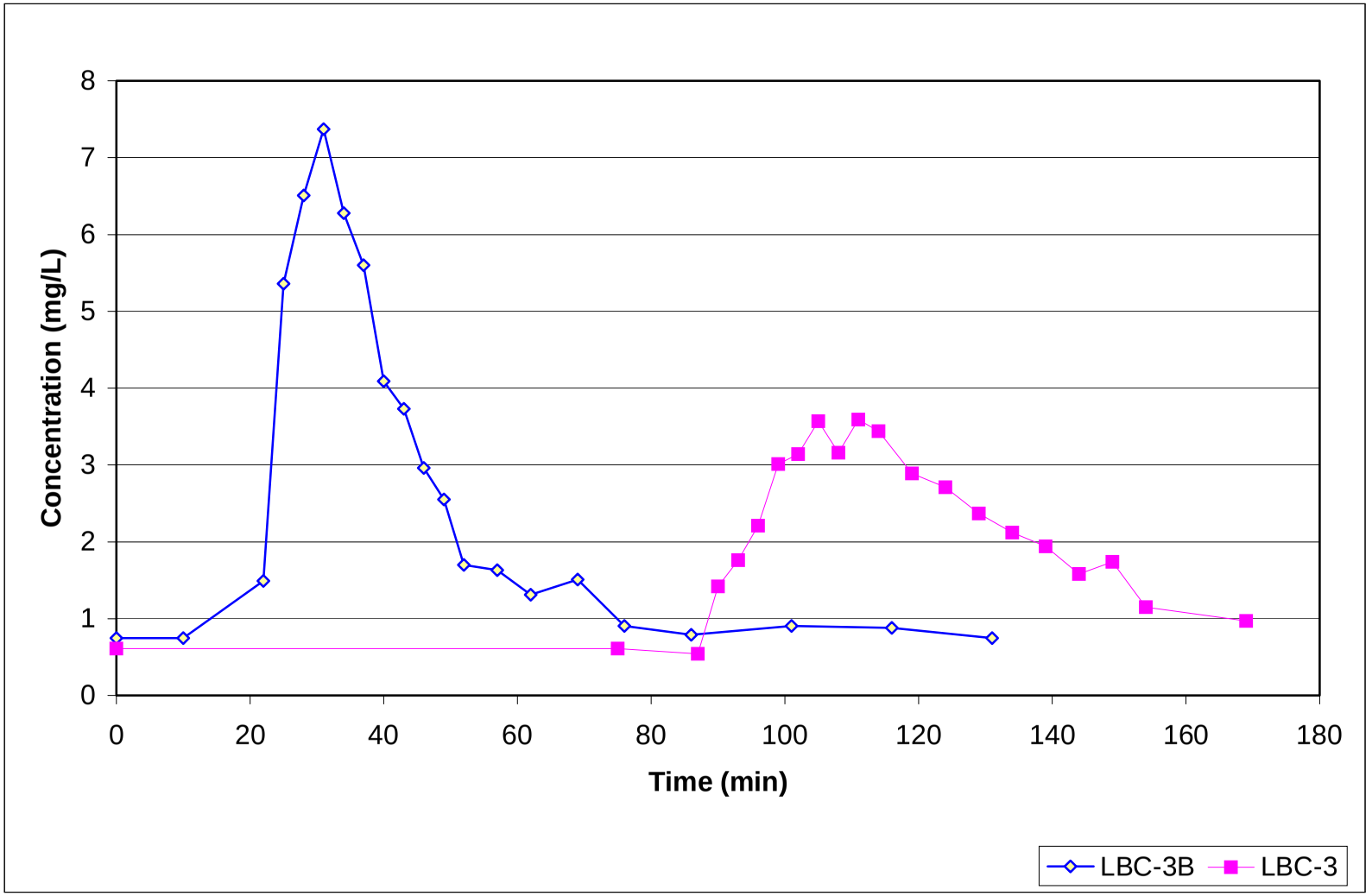

Figure 3.19: Time-concentration plot for nitrate (NO_3^--N) at LBC-3B and -3, October 2002.

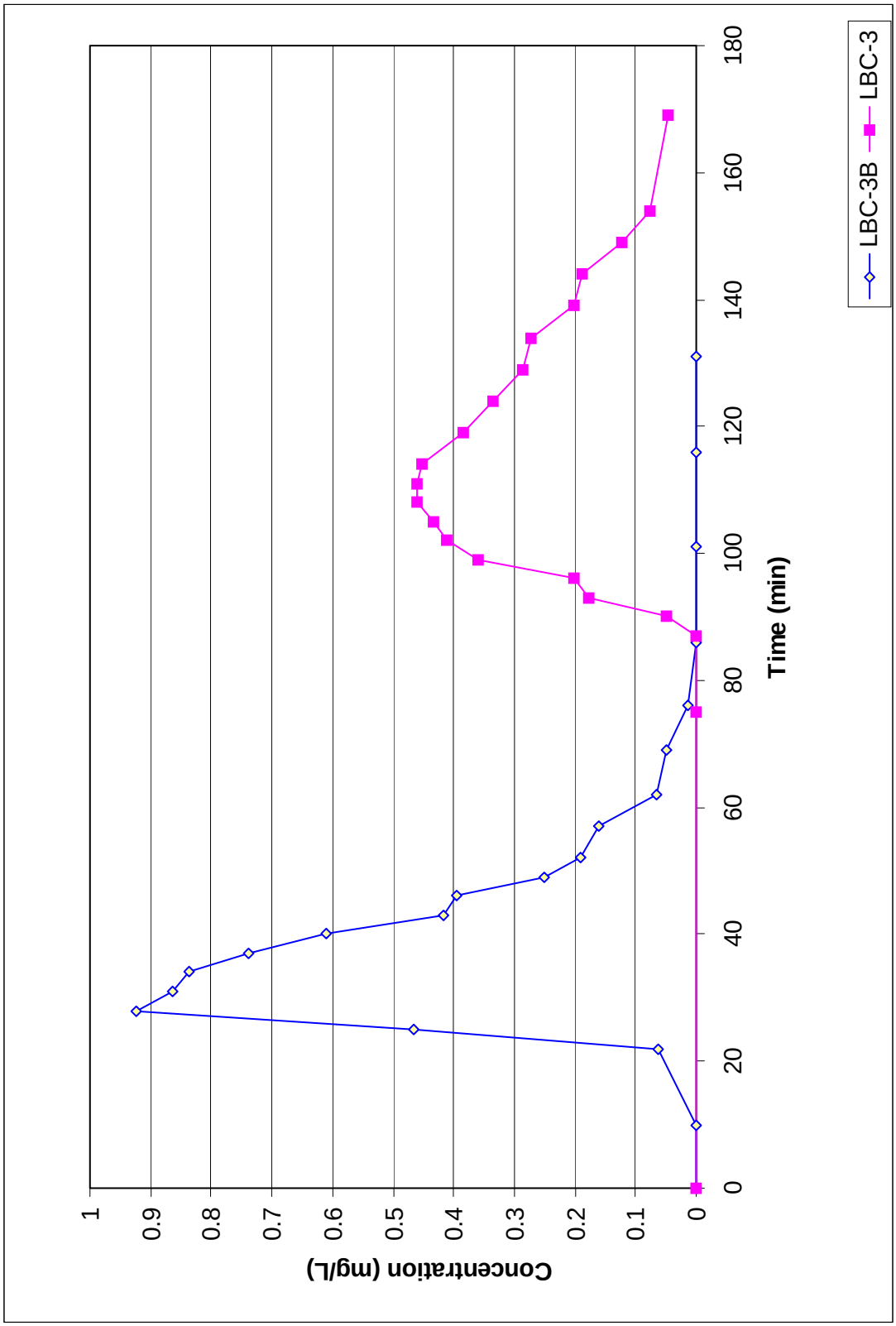

Figure 3.20: Time-concentration plot for rhodamine WT at LBC-3B and -3, October 2002.

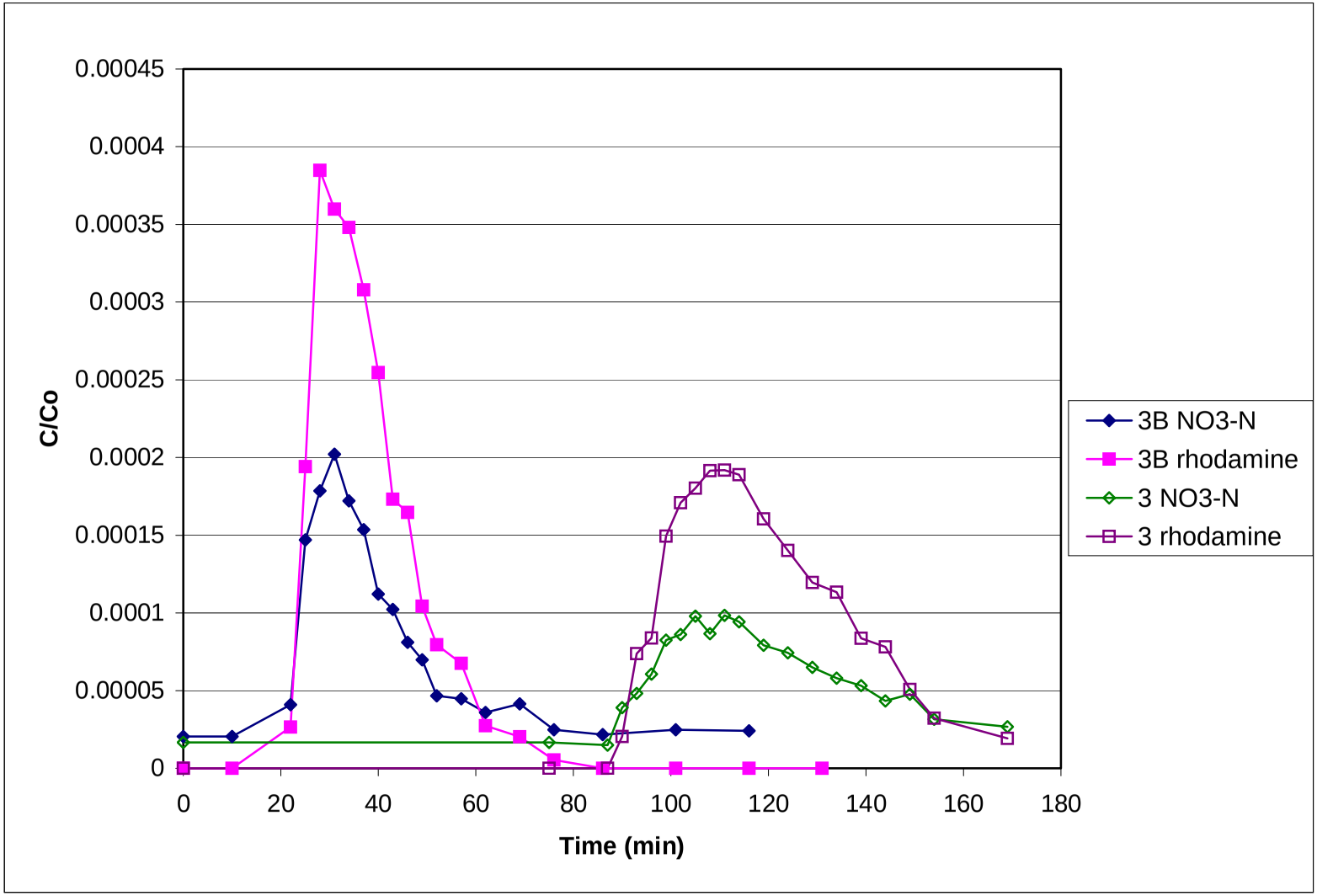

Figure 3.21: Time- normalized concentration plot for nitrate and rhodamine WT at LBC-3B and -3, October 2002.

Figure 3.22: Time-concentration plot for rhodamine WT at LBC-3B and -3, October 2002.

3.5 January 2003

The stream was gaged on January 7. Stream discharge was exceptionally high for January, (higher than the flow of any other monitored periods). Discharge (Table 3.1; Figure 3.1) ranged from 0.055 m^3/s to 0.12 m^3/s, with the highest value at LBC-1. Except at LBC-1, the discharge was found to be almost identical in the other gaged locations. Concentrations of both ^{99}Tc and TCE are comparable to the concentrations recorded in the preceding winter (January 2002). The values of ^{99}Tc ranged from 22.6 to 26.2 pCi/L, excluding the abnormal value of 78.8 pCi/L at LBC-4 (Table 3.2; Figure 3.2). The abnormality may have resulted from contamination of the sample or some seepage at the location with an abnormally high ^{99}Tc concentration. Otherwise, the concentration of ^{99}Tc was highest at LBC-3 and lowest at LBC-1. TCE concentrations varied from 15 μg/L at LBC-4 and -3B to 7.8 μg/L at LBC-1 with concentration gradually decreasing downstream (Table 3.3; Figure 3.3).

The experiment started at 10:00 A.M. on January 8. Monitoring was discontinued after 89 minutes at LBC-3B and after 136 minutes at LBC-3 after the start of the experiment. Propane injection was discontinued 136 minutes after starting injection. The air temperature was 8.4°C and stream temperature was 6.6°C (Figure 3.4). Sodium nitrate and rhodamine WT were again used as slug tracers. Nitrate concentrations (Figure 3.23) peaked at 24 minutes at LBC-3B and 62 minutes at LBC-3. The peak concentration at LBC-3 was more than half than that of LBC-3B. The highest concentrations were 5.11 mg/L at LBC-3B and 3.23 mg/L at LBC-3. The peak concentration at LBC-3B was significantly lower than in October. The curve for LBC-3B is more symmetrical and steeper than at LBC-3. Both the curves show relatively short tails. The curve at LBC-3 approached the background concentration by the end of the test. A secondary peak is not prominent for either curve. The centroid was at 28.87 minutes for LBC-3B and 70.89 minutes for LBC-3. Hence the travel time of the nitrate center of mass from LBC-3B to LBC-3 was 42.02 minutes.

The maximum concentration of rhodamine WT (Figure 3.24) was a little less than in October and about three times less than that observed in January 2002. The

concentrations peaked at 0.69 mg/L 24 minutes after tracer injection at LBC-3B and at 0.40 mg/L after 62 minutes at LBC-3. Like nitrate, the difference between the peak values at LBC-3B and -3 was less than in previous monitored periods. The rhodamine WT curves at both locations are less symmetric than nitrate, with longer tailing for LBC-3. No secondary peak was observed for either curve. The centroid was at 26.76 minutes for LBC-3B and at 71.03 minutes at LBC-3. The center of mass travel time from LBC-3B to LBC-3 was 44.27 minutes.

Visual comparison of the superimposed normalized (C/C_o) time-concentration plots (Figure 3.25) shows that peaks for the two tracers (nitrate and rhodamine WT) at LBC-3B and -3 occurred at the same time. However, the peak concentrations for rhodamine WT were almost twice of nitrate. Similarly, the areas under the concentration curves for rhodamine WT were much more than for nitrate.

The time-concentration plots for propane (Figure 3.26) in January 2003 show that both LBC-3B and -3 seemed to have reached stable plateau concentrations, in contrast to the August and October tests. The plateau concentrations were reached at 48 minutes at LBC-3B and at 100 minutes at LBC-3. These concentrations were 4.78×10^{-5} moles/L and 4.28×10^{-5} moles/L for LBC-3B and –3, respectively.

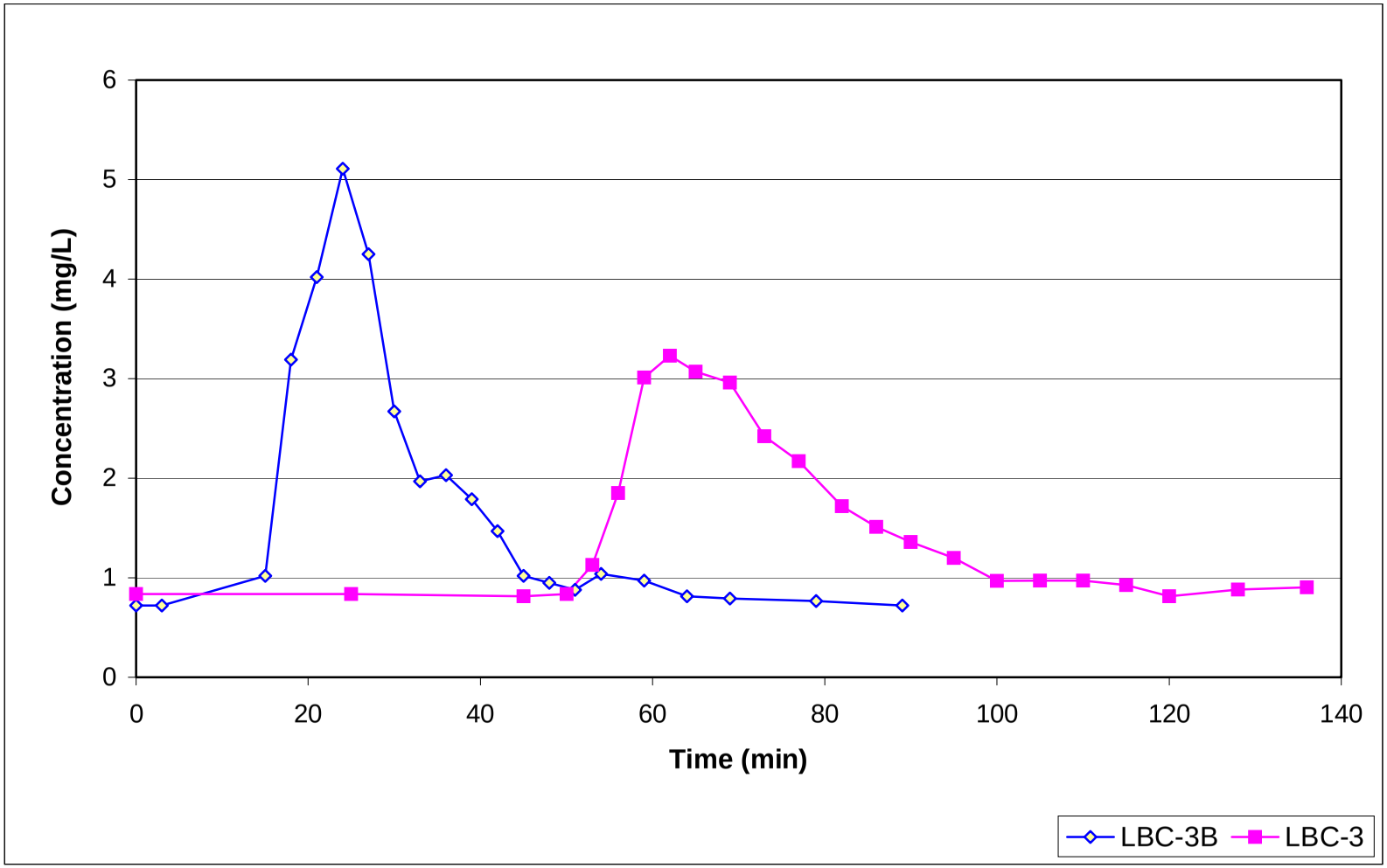

Figure 3.23: Time-concentration plot for nitrate (NO_3^--N) at LBC-3B and -3, January 2003.

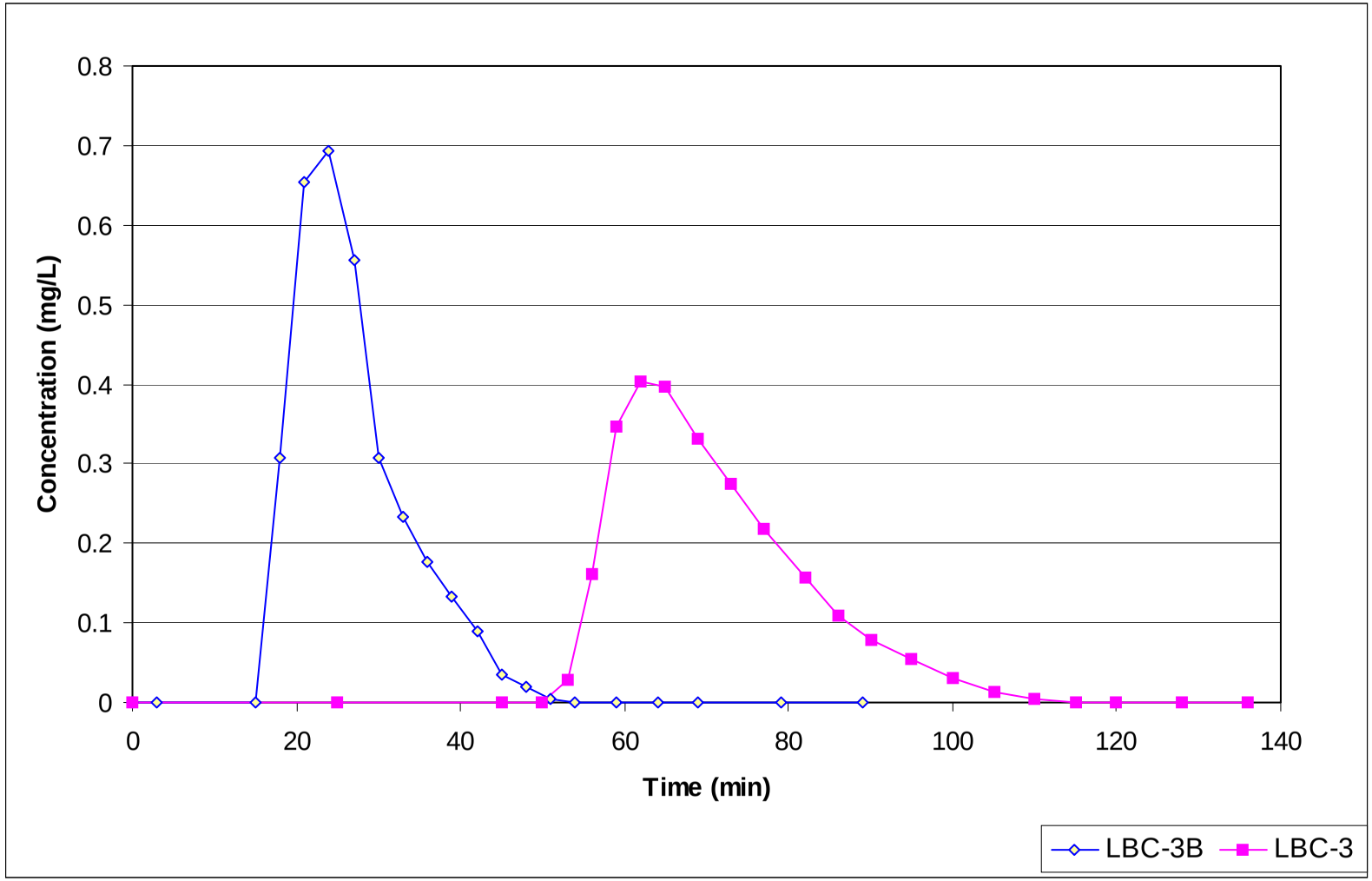

Figure 3.24: Time-concentration plot for rhodamine WT at LBC-3B and -3, January 2003.

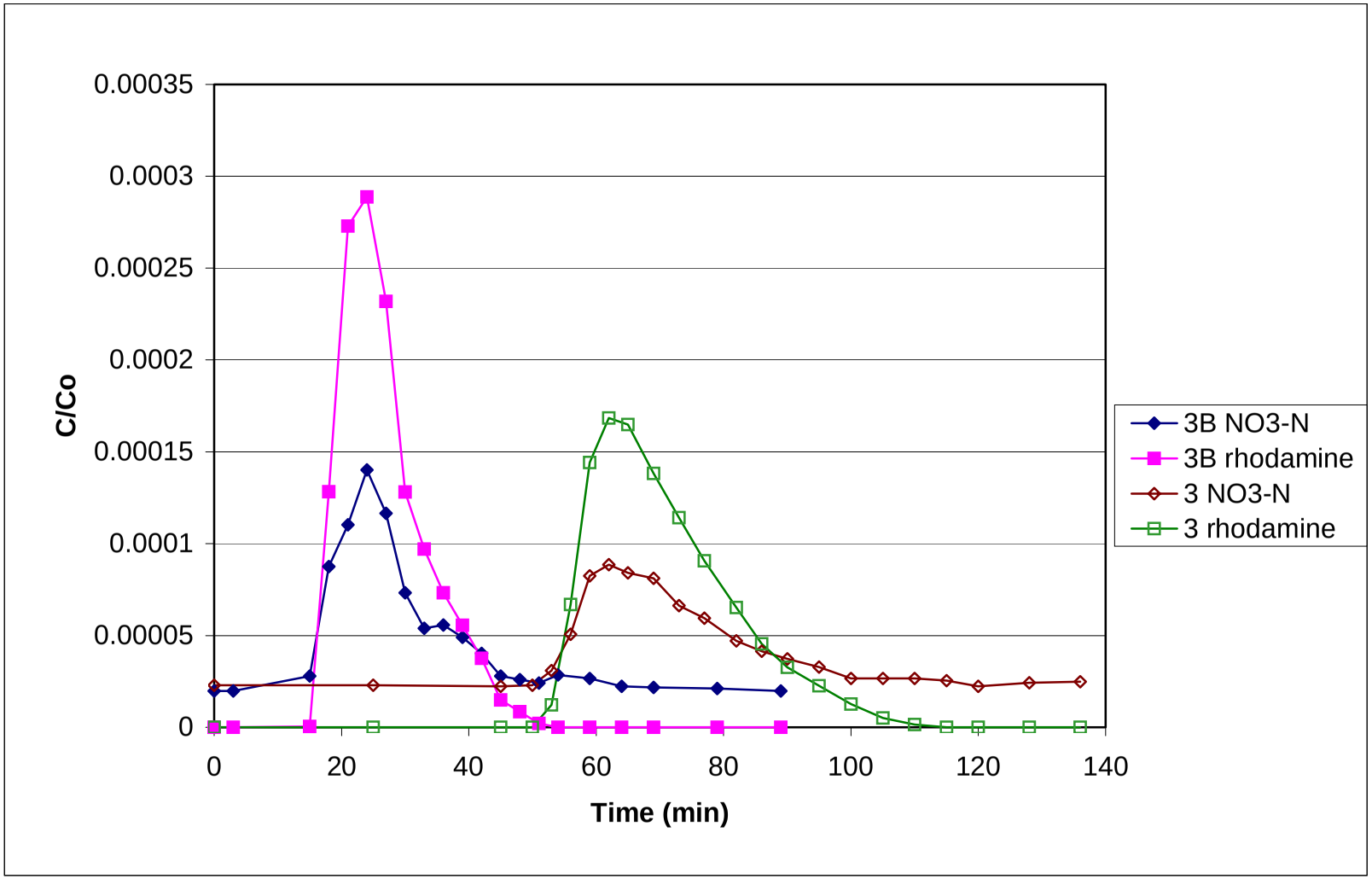

Figure 3.25: Time-normalized concentration plot for nitrate and rhodamine WT at LBC-3B and -3, January 2003.

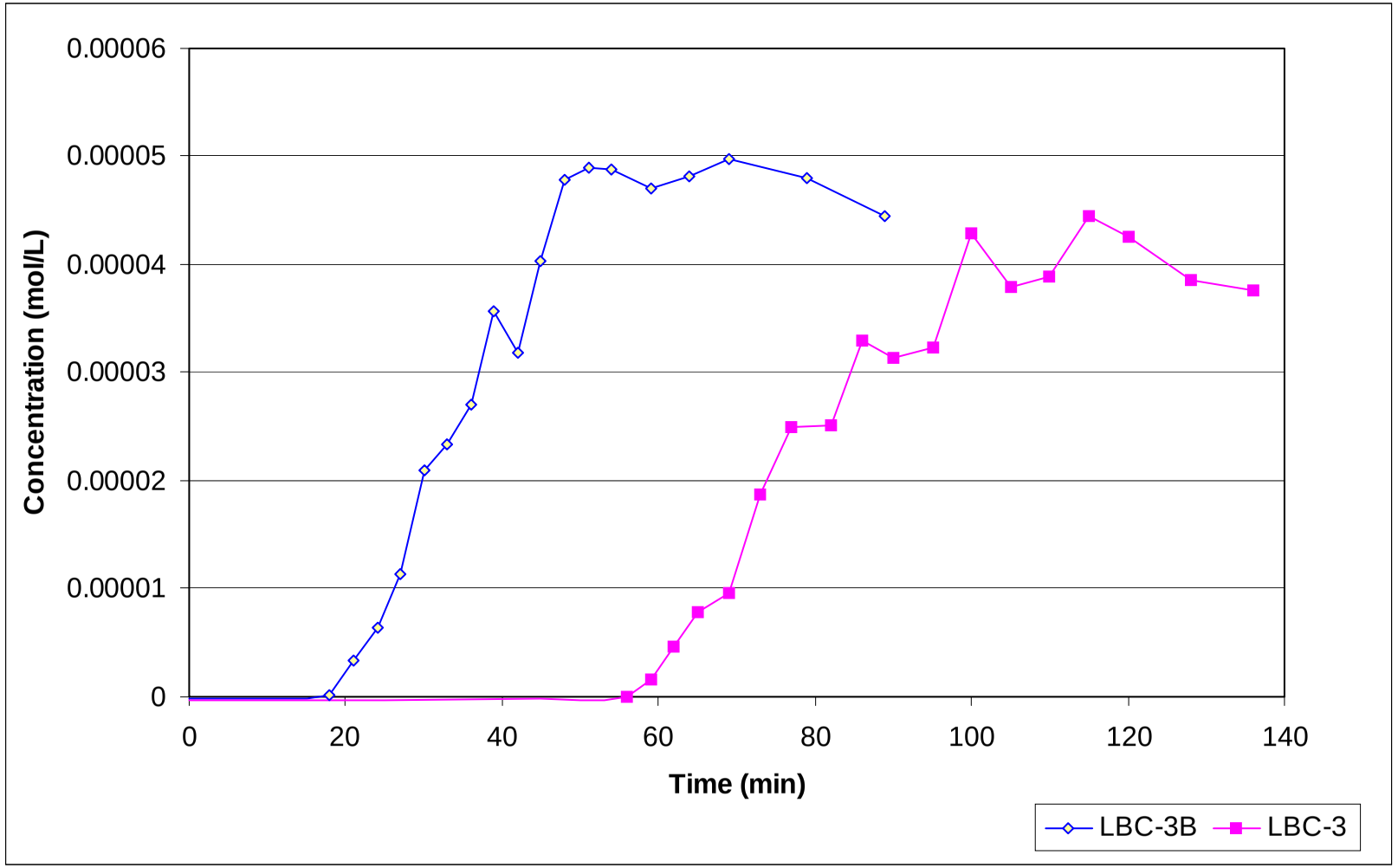

Figure 3.26: Time-concentration plot of propane at LBC-3B and -3, January 2003.

Chapter 4
Discussion

4.1 Simulation Results and Comparison with Field Values

Estimated parameter values obtained from OTIS-P for the 231-m long reach from LBC-3B to -3 have a wide range for a 95% confidence level (Table 4.1). During OTIS (forward) simulations, the parameter values were varied within their respective ranges. The values obtained by visual best fit to field data during sensitivity analyses are more representative than the OTIS-P estimates which were obtained by non-linear least-squares fit. There were two problems. First, simulating nitrate values for June, August, and October 2002 yielded poor convergence, probably because of the high background concentrations of nitrate in the stream. Second, the values estimated for the slug tracers in August and propane in June did not seem to converge. The best fit for August was able to give a more acceptable value for rhodamine WT than for nitrate.

The values of stream cross-sectional areas estimated from most OTIS-P simulations (and all OTIS simulations) are significantly lower than the values measured during gaging (Table 4.2; Figure 4.2). AREA values range from 0.53 to 0.80 m^2. Most of the values seem to cluster around 0.53 to 0.63 m^2. This discrepancy may result from the fact that the OTIS model assumes one-dimensional (longitudinal) transport of solutes, while in reality the transport of tracers in Little Bayou Creek is three-dimensional. However, because the stream reach has been channelized, transport is probably more one-dimensional than in a natural (meandering) stream.

Dispersion coefficient (DISP) values generally vary with discharge, as expected. For the slug tracers, the OTIS values range from 0.015 to 0.29 m^2/s (Table 4.2). Values for nitrate are higher than for rhodamine WT and bromide in most cases, although for January 2003 the values for nitrate and rhodamine WT are identical. For propane, the values range from 0.07 in October to 0.60 m^2/s in January 2003. The values for August are unusually high relative to discharge.

The OTIS-P modeling estimated the secondary storage zone area (AREA2) values for the slug tracers to cluster around 10^{-3} m^2, while the storage zone exchange coefficient (ALPHA)

values range from 10^{-5} to 10^{-3} s^{-1} (Table 4.2). The values of AREA2 are slightly higher for rhodamine WT in August and October (in the range of 10^{-1} m^2 and 10^{-2} m^2, respectively). These values imply that with the presumption of one-dimensional transport, the effects of AREA2 and ALPHA are insignificant for solute movement in the 231-m stretch of Little Bayou Creek, i.e., none of the tracer solutes have been substantially retained in the storage areas of the hyporheic zone or banks during most of the monitored periods. In October the storage zones were found to be larger relative to other times, which may explain the reason of very short tailings of the slug tracer curves. These estimated values are also in accord with the streambed morphology between LBC-4 and LBC-3. The channelization of Little Bayou Creek resulted in the replacement of the original streambed sediment by a thin veneer of fine to medium sand overlying sandy clay. Consequently, secondary storage of solutes along the flow path and reactions in the hyporheic zone are likely to be minimal.

The values of the first-order decay coefficient (LAMBDA) estimated for propane range from 1.90 to 7.86 d^{-1} (Table 4.4). LAMBDA varies with temperature, which is consistent with volatilization of propane (Figure 4.1). The relatively high value in January 2003 relative to January 2002 may have resulted from the higher temperature or increased discharge (Schwarzbach et al., 1993). These coefficients are about one order of magnitude smaller than those reported by Genereux and Hemond (1992) for the West Fork of Walker Branch, a small stream in eastern Tennessee. However, discharge values along Little Bayou Creek are about two orders of magnitude higher. One possible explanation for the apparent discrepancy is greater turbulence along the West Fork of Walker Branch because of that stream's higher gradient (0.037, versus approximately 0.0015 for Little Bayou Creek downstream of LBC-4) and more irregular (bedrock) channel. Volatilization coefficients of TCE were calculated from the propane values by using the TCE/propane ratio (0.79 $^{+}$/- 0.21) of Smith et al. (1980). The values ranged from 1.50 d^{-1} in January 2002 to 6.23 d^{-1} to June 2002.

Volatilization coefficients of TCE between LBC-3B and -3 were also calculated using a first-order decay equation with upstream and downstream concentrations of TCE and rhodamine WT travel-time data. The calculated and simulated values of the volatilization coefficient are

similar (within a factor of two, with agreement worst for August). The volatilization rates were least in January 2002 and greatest in June 2002, as expected.

The results of the best-fit OTIS simulations for LBC-3 are plotted with the field values (Figure 4.4 through 4.7). In most cases the centroids of the simulated curves for the slug tracers lag slightly behind the observed values. This lag may reflect the fact that transport of the solutes was controlled by the total discharge (surface and hyporheic flow) of the stream, while the simulations were done with surface discharge values only. In most cases, both the simulated and observed propane curves reach stable concentrations almost at the same time. The difference between simulated and observed values for January 2002 may in part reflect analytical errors in gas chromatography. The error was probably caused by the use of an inappropriate injecting needle and the inexperience of the author.

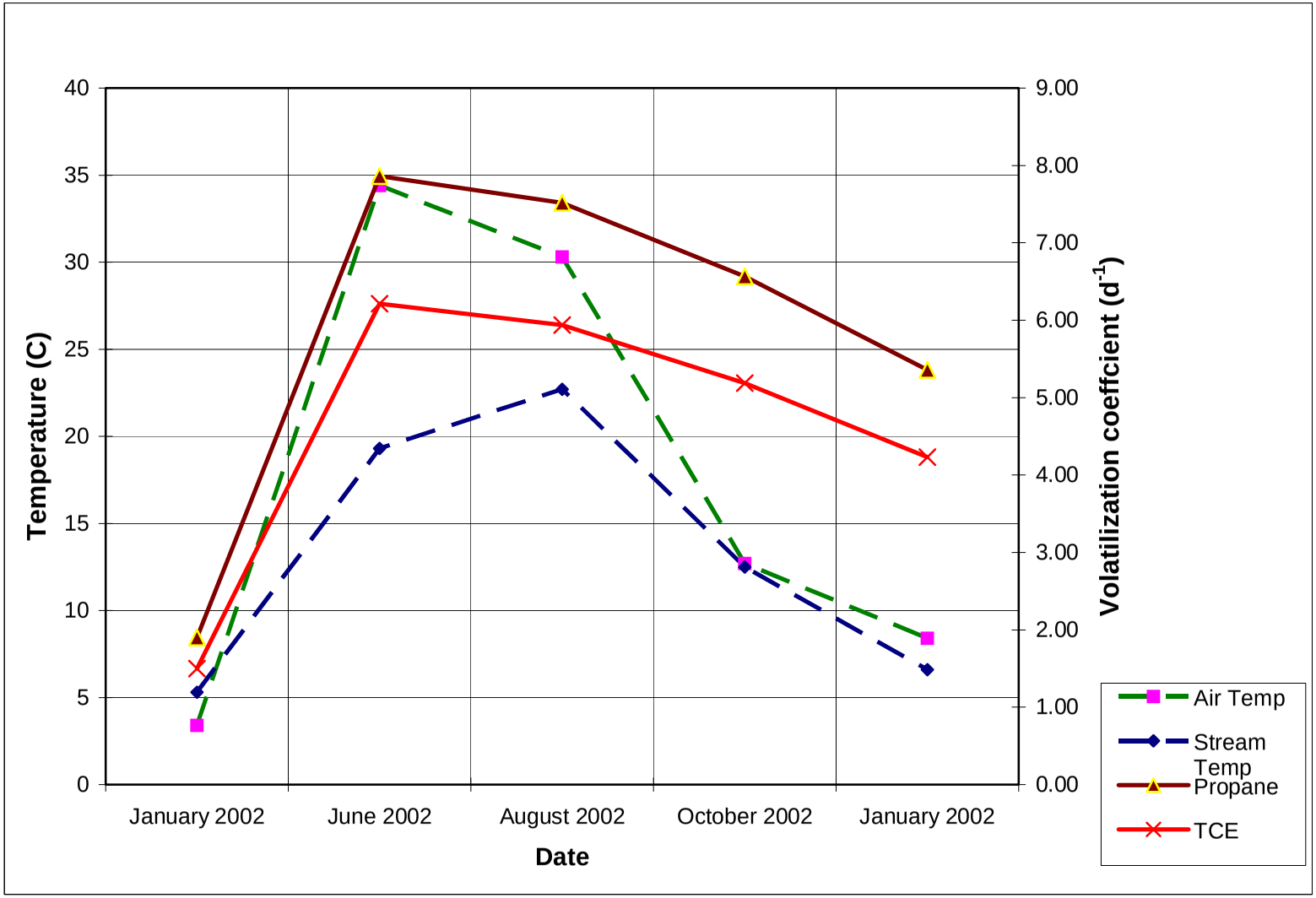

Figure 4.1: Volatilization coefficients of propane and TCE found from OTIS-P at ambient temperature.

Table 4.1: Range of estimated parameter values (for 95% of confidence level) for slug tracers by OTIS-P.

Season	Tracer	DISP (m^2/s)	AREA (m^2)	AREA2 (m^2)
January 2002	*Rhodamine*	-0.124 to 0.236	0.472 to 0.587	-0.101 to 0.104
	Bromide	-0.969 to 0.190	0.515 to 0.568	-0.529E-01to 0.577E-01
June	*Rhodamine*	-0.351 to 0.891	0.423 to 0.808	-0.224 to 0.239
	Bromide	-0.251 to 0.732	0.451 to 0.730	-0.175 to 0.177
	Nitrate	-0.175 to 0.177	-7.48 to 8.59	-8.16 to 8.16
August	*Rhodamine*	-0.142 to 0.889	0.413 to 0.762	-0.387 to 0.565
	Nitrate	-225 to 228	-129 to130	-129 to 129
October	*Rhodamine*	-0.245 to 0.791	0.422 to 0.687	-0.426E-01 to 0.677E-01
	Nitrate	-0.126 to 0.345	-3.93 to 2.38	-0.626E-01 to 0.577E-01
January 2003	*Rhodamine*	0.189 to 0.387	.608 to 0.637	-0.787 to 0.965E–01
	Nitrate	0.186 to 0.395	0.606 to 0.636	-0.133 to 0.162

Table 4.2: Estimated parameter values for slug tracers by OTIS-P.

Season	Tracer	DISP (m^2/s)	AREA (m^2)	AREA2 (m^2)	Alpha (s^{-1}) (fixed)	Gaged Area (m^2)
January 2002	*Rhodamine*	0.06 (**0.015**)	0.53 (**0.57**)	1.70E-03	1.00E-05	
	Bromide	0.09	0.54	2.30E-03	1.00E-05	1.14
June	*Rhodamine*	0.27 (**0.15**)	0.62	7.50E-03	1.00E-04	
	Bromide	0.24 (**0.16**)	0.59	7.00E-03	1.00E-05	1.27
	Nitrate	0.21	0.56	1.70E-03	1.00E-04	
August	*Rhodamine*	0.44 (**0.24**)	0.72	1.3E-1(**0.62**)	9.00E-06 (**1.00E-05**)	
	Nitrate	1.42	0.8	1.90E-03	1.00E-03	1.08
October	*Rhodamine*	0.15	0.59	7.50E-02	1.00E-05	
	Nitrate	0.06 (**0.23**)	1.93 (**0.60**)	7.50E-02	0	0.92
January 2003	*Rhodamine*	0.29	0.62	9.00E-2	1.00E-05	
	Nitrate	0.29	0.62	1.43E-2	1.00E-05	1.19

where
DISP = dispersion coefficient
AREA = main channel cross-sectional area
AREA2 = secondary storage zone cross-sectional area
ALPHA = storage zone exchange coefficient
Gaged area = main channel cross-sectional area calculated from gaging data
(OTIS best-fit values are in bold and within parentheses).

Table 4.3: Range of estimated parameter values (for 95% of confidence level) for propane by OTIS-P.

Season	DISP	AREA (m^2)	LAMBDA (s^{-1}) (m^2)
January 2002	-0.942E-01 to 0.429	0.533 to 0.662	-0.125E-04 to 0.575
June	0.132 to 0.516	0.529 to 0.653	0.914E-04 0.915E-04
August	0.979E-01 to 0.917	0.606 to 0.720	0.624E-04 to 0.111E-03
October	-0.214 to 0.329	0.610 to 0.458	0.486E-04 to 0.105E-03
January 2003	0.126 to 1.07	0.617 to 0.687	0.402E-04 to 0.841E-04

Table 4.4: Estimated parameter values for propane by OTIS-P.

Season	DISP (m^2/s)	AREA (m^2)	LAMBDA (d^{-1})	First order decay coefficient of TCE (d^{-1}) [(*0.79 of LAMBDA)]	Gaged Area (m^2)
January 2002	0.17	0.60	1.90	1.50	1.14
June	0.32	0.60	7.86	6.21	1.27
August	0.51	0.66	7.52	5.94	1.08
October	0.07	0.56	6.57	5.19	0.92
January 2003	0.6	0.65	5.36	4.23	1.19

where
DISP = dispersion coefficient
AREA = main channel cross-sectional area
LAMBDA = first order decay coefficient
Gaged area = main channel cross-sectional area calculated from gaging data

Table 4.5: Volatilization coefficient and volatilization rate of TCE obtained from OTIS-P and first-order decay equation.

Season	k (/min) [1]	k (/min) [2]	R [μg/(L*min)] [1]	R [μg/(L*min)] [2]
January 2002	1.60E-03	1.00E-03	2.79E-02	1.88E-02
June	5.20E-03	4.30E-03	2.94E-01	2.46E-01
August	2.30E-03	4.10E-03	7.55E-02	1.36E-01
October	3.20E-03	3.60E-03	5.40E-02	6.13E-02
January 2003	3.20E-03	2.90E-03	4.85E-02	4.41E-02

where
k [1]: volatilization coefficient of TCE calculated from first order decay equation
k [2]: volatilization coefficient calculated from first order decay coefficient value (LAMBDA) of propane from OTIS-P simulation
R [1]: volatilization rate of TCE calculated using value of k [1]
R [2]: volatilization rate of TCE calculated using value of k [2].

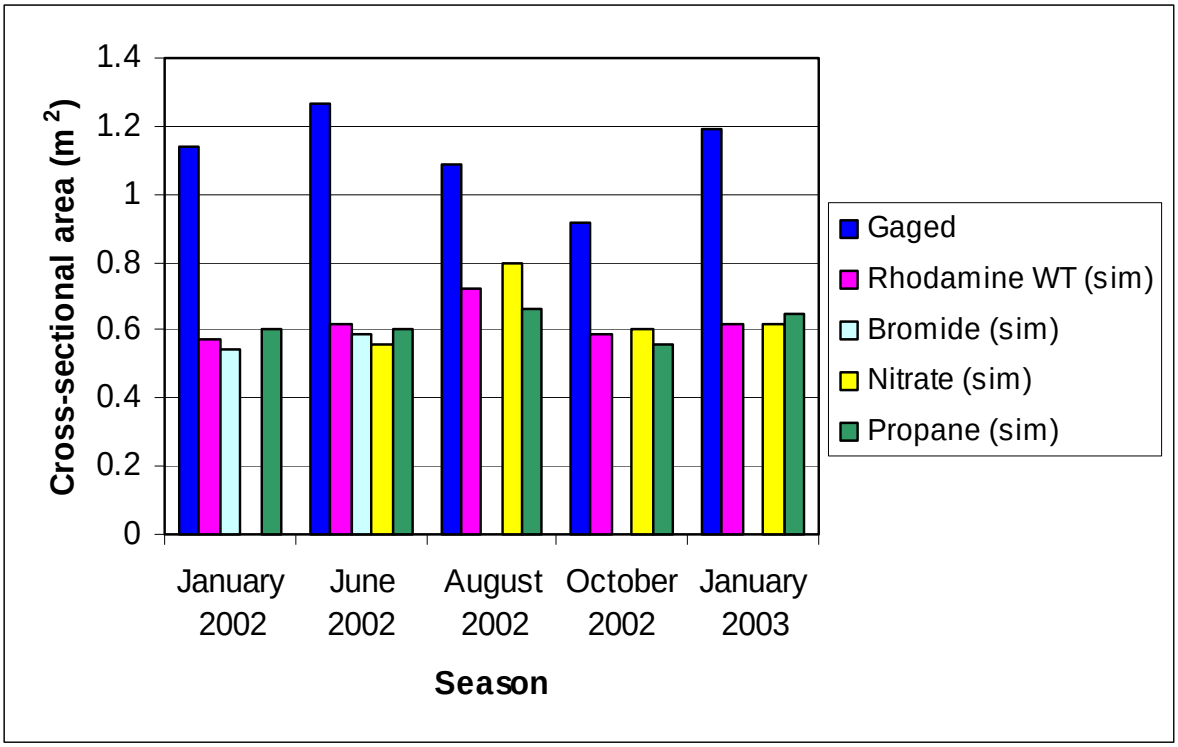

Figure 4.2: Comparison of gaged value and simulation value of stream cross sectional area at LBC-3.

4.2 Trends of Tracer Curves

One of the main priorities of the present study is identification of the transport and fate of the different tracers injected into the stream. Breakthrough curves generally complied with the expected trends. For slug tracers (bromide, nitrate and rhodamine WT), the concentrations peaked and then tailed off. For continuous injection of propane, the curves tended to approach steady concentrations.

For the slug input tracers, the curves at the first sampling location (LBC–3B) peaked more sharply than the curves at the downstream sampling location (LBC–3). Similarly, for propane, the curves at LBC-3 approached steady state more quickly than those at LBC-3B. As the gas was transported downstream, its concentration was depleted by volatilization. Incidentally, for most of the monitored periods and for many of the slug tracers, secondary peaks were observed in the curves at LBC–3B. These peaks may be attributed to in-stream transient storage in stagnation zones (Figure 3.9) between the injection point and the sampling point. Such secondary peaks were not visible at the downstream sampling location probably because of the relatively large distance between LBC–3B and –3, along which dispersion compensated for the lag time of the solutes for the second peak at the upstream sampling point.

In January 2002, the surface discharge was lower than during other monitoring periods, which led to relatively long travel times and less dilution, as evident from relatively high concentrations of rhodamine WT. The fact that both bromide and rhodamine WT had almost identical travel times from LBC–3B to -3 suggests that both of them behaved similarly and conservatively during transport.

Transport of the slug tracers was fastest in June 2002 (Figure 4.3). The curves for bromide, nitrate, and rhodamine WT were similar in shape, but the normalized peak bromide concentration was greater than for the other tracers. Although rhodamine WT is susceptible to photodegradation and nitrate can be biodegraded under anaerobic conditions in the hyporheic zone, the similar shapes and center of mass travel times suggests that rhodamine WT and nitrate were not attenuated relative to bromide. The curves for propane stabilized and then started to

increase again. This may have been caused by mismanagement in regulating the discharge pressure of the propane near the end of the experiment.

In August, the field values obtained for slug tracers seem to be noisy. The propane curves never seem to have attained steady state values, perhaps because of the relatively high stream temperature. Another cause may have been the use of a flow meter, which was used with the diffuser to control the propane discharge and ultimately was found not to function properly.

October had a very low discharge rate, almost comparable to January 2002. As a result, travel times were longest in October. The trends of the slug tracer curves were similar to those of the previous monitored periods. The fact that the propane curve for LBC-3 did not reach steady state was probably due to a combination of the long travel time and early termination of sampling.

January 2003 had the highest discharge rate, which resulted in the second shortest travel times (after June). The short tailing of the curves was probably due to the high discharge. Both the propane curves stabilized at similar concentrations.

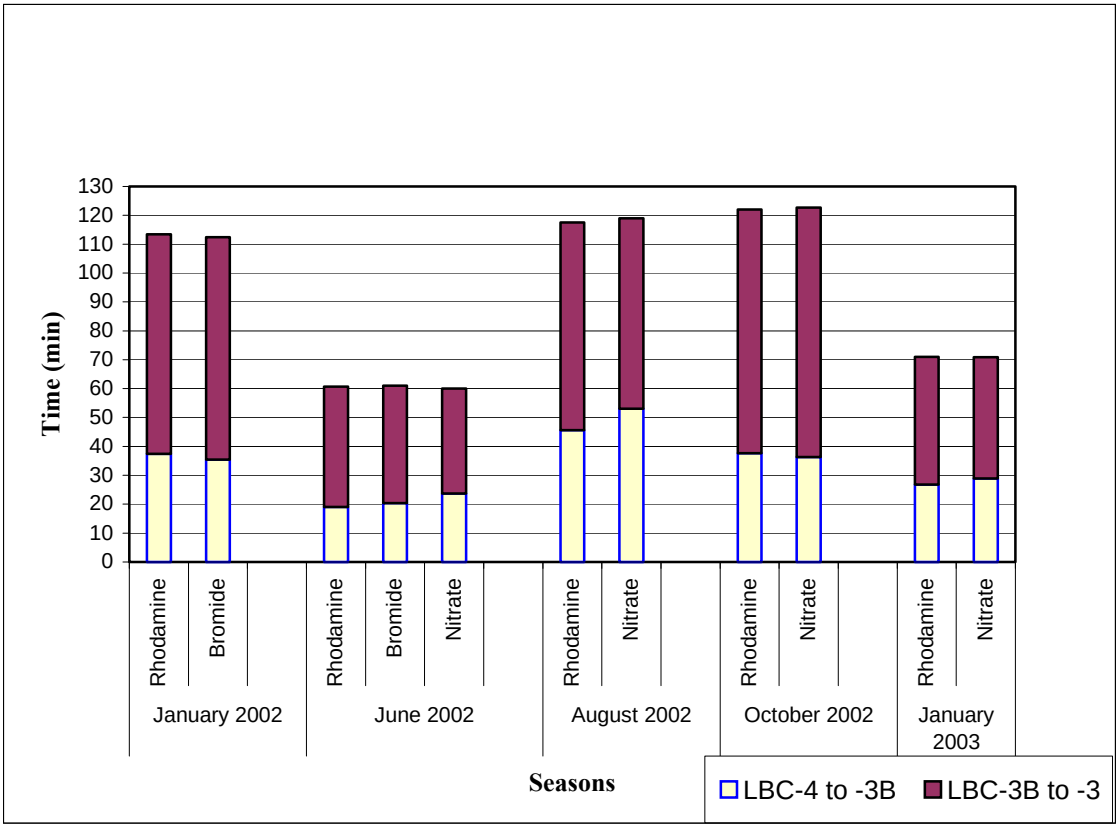

Figure 4.3: Comparison of travel time for different slug tracers.

4.3 Stream Discharge and Ground Water–Stream Interactions

Discharge of Little Bayou Creek was highest in January 2003, followed by June, August, October, and January of 2002. Fryar et al. (2000) noted that flow peaked during late winter and decreased to a minimum in early autumn. The unusually high discharge in January 2003 reflects the fact that the last 4 months of 2002 were the 15th wettest September-December period in Kentucky in the past century. Precipitation at the Paducah National Weather Service office for the period (47.7 cm) was 7.9 cm above normal (University of Kentucky Agricultural Weather Center, http://wwwagwx.ca.uky.edu, unpublished data, 2003). In order to assess the effects of inaccuracy in stream gaging, an error calculation was made for LBC-3B in January 2002. The measured value was 0.03 m^3; by varying the depth and velocity by factors of 0.05 to 0.01, the values ranged from 0.024 m^3 to 0.035 m^3 (-20% to + 17%).

Efforts were also made to determine the total discharge (surface and hyporheic flow) of the stream by using an empirical equation from Kilpatrick and Cobb (1985) (mentioned in Chapter 2) with slug tracer values. The results are summarized in Tables 4.6 and 4.7. The values of discharge obtained from the calculations differed by factors of 2 to 4 times between the three tracers (Figure 4.8). The values closest to the gaged discharge values were obtained by using the values of bromide, while values obtained by using rhodamine WT seemed to be least plausible. Discharge values obtained from gaging were almost always less than those obtained from tracers. This suggests that there is significant flow in the hyporheic zone.

Table 4.6: Comparison of gaged values of surface discharge at LBC-3B with total discharge values calculated using Kilpatrick and Cobb's (1985) equation.

Seasons	Gaged value (m^3/s)	Bromide (m^3/s)	Nitrate (m^3/s)	Rhodamine WT (m^3/s)
January 2002	0.03	0.105	NA	0.048
June	0.06	0.105	0.224	0.227
August	0.04	NA	0.077	0.059
October	0.04	NA	0.105	0.072
January 2003	0.07	NA	0.187	0.146

Table 4.7: Comparison of gaged values of surface discharge at LBC-3 with total discharge values calculated using Kilpatrick and Cobb's (1985) equation.

Seasons	Gaged value (m^3/s)	Bromide (m^3/s)	Nitrate (m^3/s)	Rhodamine WT (m^3/s)
January 2002	0.03	0.073	NA	0.025
June	0.06	0.065	0.104	0.147
August	0.04	NA	0.101	0.056
October	0.03	NA	0.133	0.073
January 2003	0.07	NA	0.179	0.146

4.4 Contaminant Flux and Attenuation

Concentrations of contaminants in stream water were seasonally variable and seemed to vary with the discharge. The concentrations peaked in June, when the discharge was almost double that of the other monitored periods. The minimum concentrations occurred in January 2002, when the surface discharge was lowest. Thus the increase in ground water inflow increased the concentrations of TCE and ^{99}Tc in the stream during the late spring, whereas contaminant concentrations decreased with discharge in January 2002. The disconnect between contaminant concentrations (low) and stream flow (high) in January 2003 suggests increased interflow following the wet fall.

TCE and ^{99}Tc fluxes (Figures 4.9 and 4.10) show two different trends. Values > 0 represent apparent effluxes of contaminants (mass loss from the stream), whereas values < 0 represent influxes. TCE fluxes are mostly clustered between 0 and 400 μg and generally increase downstream. TCE fluxes tended to be greatest during the summer months, consistent with increased temperature and thus increased volatilization. In contrast to TCE, ^{99}Tc fluxes tend to cluster around zero, which suggests that ^{99}Tc is conservative.

Assuming ^{99}Tc is conservative and its concentrations in inflowing ground water vary with those of TCE, as observed by Clausen et al. (1992), the ratio of TCE to ^{99}Tc can be used to examine the relative attenuation of TCE with increasing distance downstream. The TCE/^{99}Tc ratio (Figure 4.11) generally decreased from about 0.8 at LBC–4 to about 0.2 at LBC–1. The ratio actually increases in most cases between LBC-4 and LBC-3B, which suggests a process by which ^{99}Tc is attenuated relative to TCE or the inflow of ground water relatively enriched in ^{99}Tc. However, a comparison of absolute concentrations suggests that most changes in ^{99}Tc between LBC-4 and LBC-3B may be within analytical error. As noted previously, the ^{99}Tc result for LBC-4 from January 2003 is suspect.

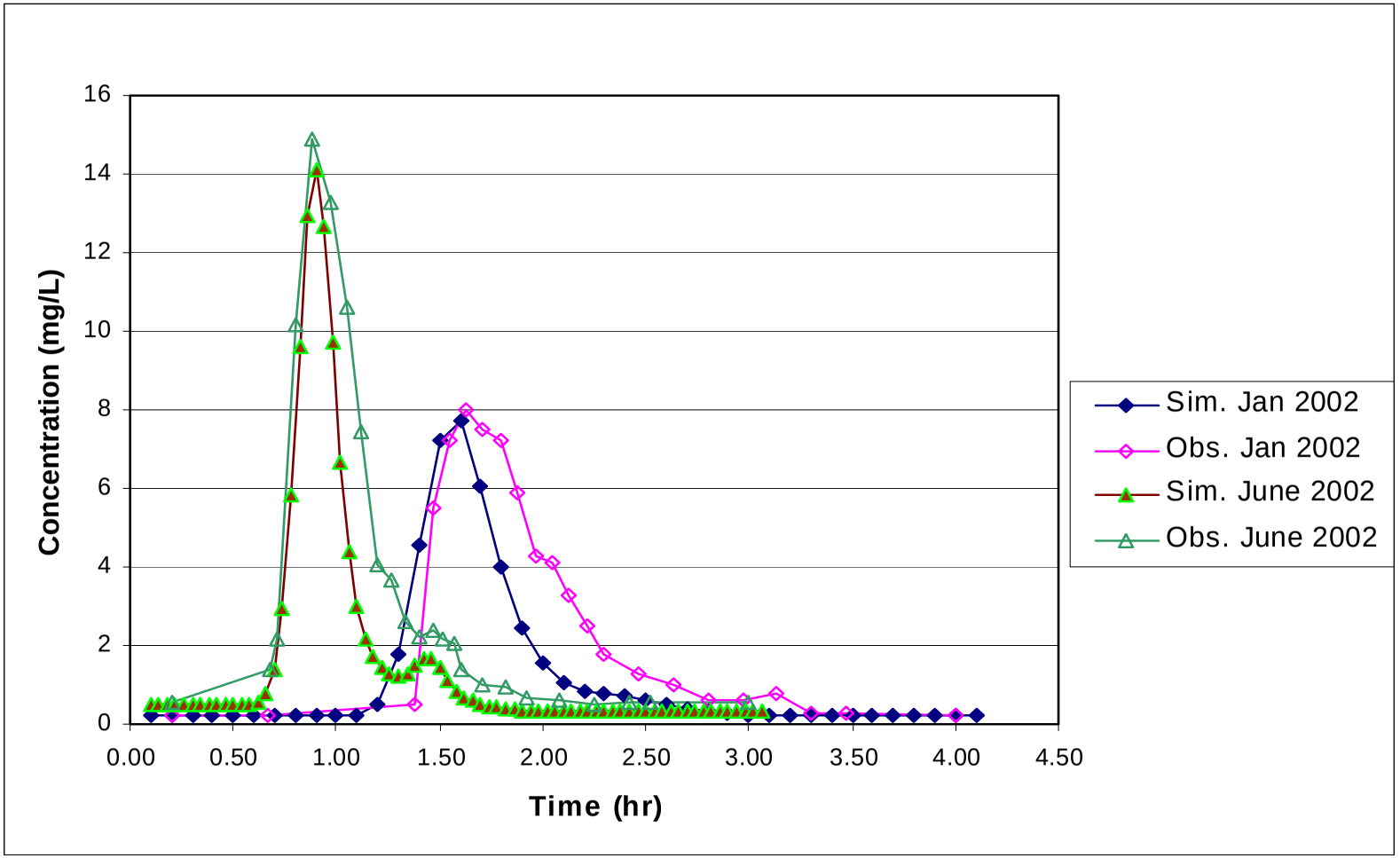

Figure 4.4: Simulated and observed concentration plot at LBC-3 for bromide.

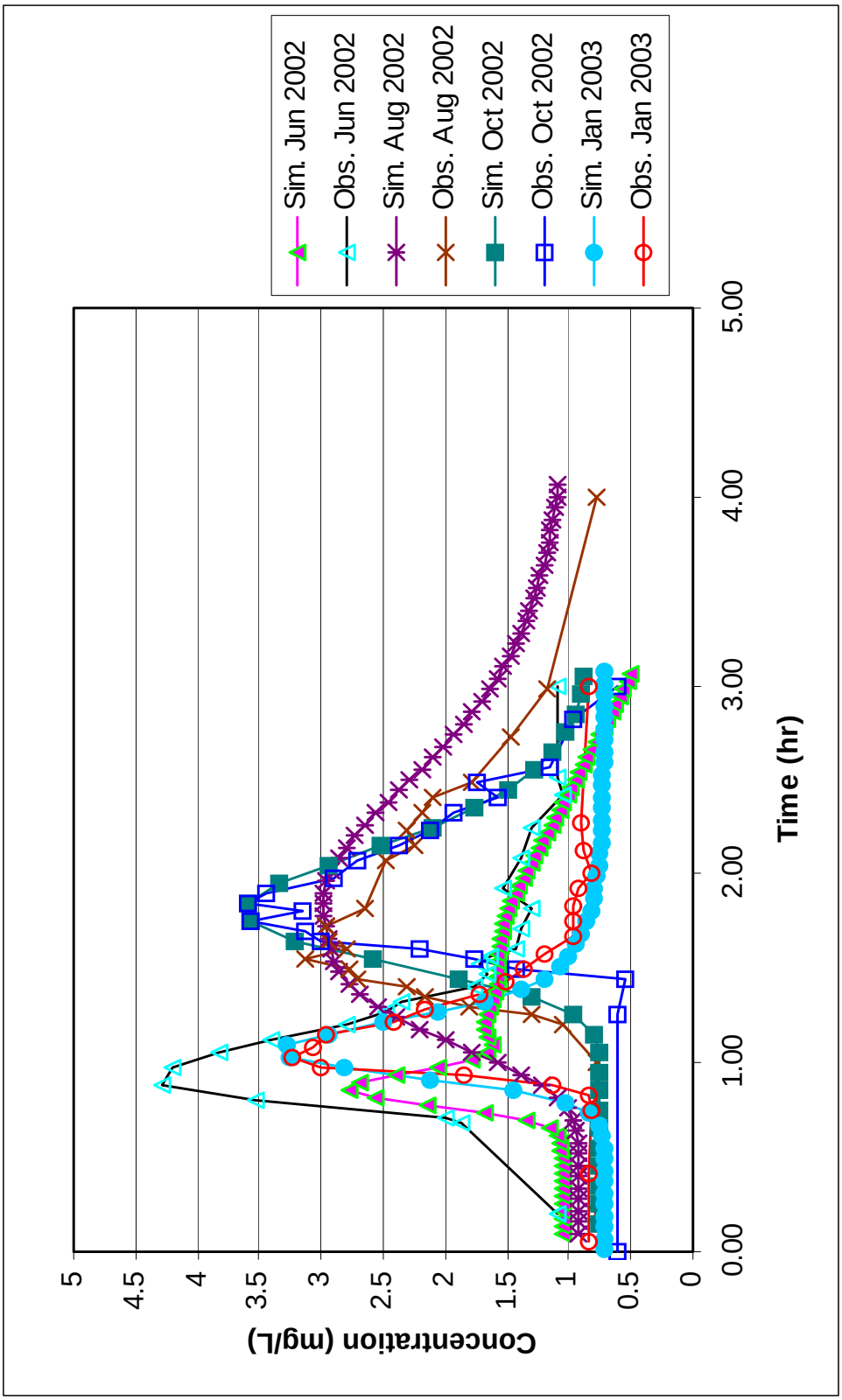

Figure 4.5: Simulated and observed concentration plot at LBC-3 for nitrate.

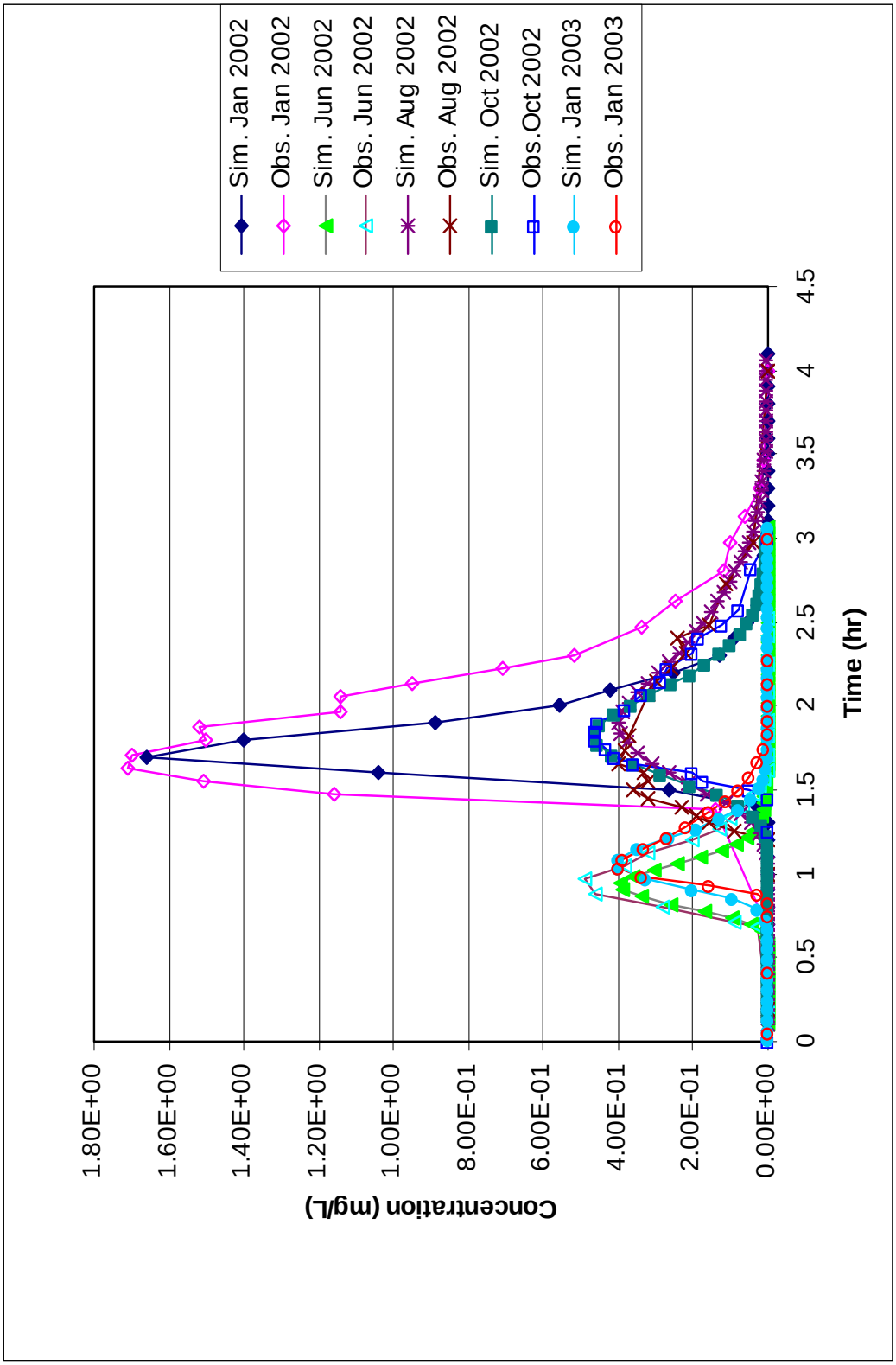

Figure 4.6: Simulated and observed concentration plot at LBC-3 for rhodamine WT.

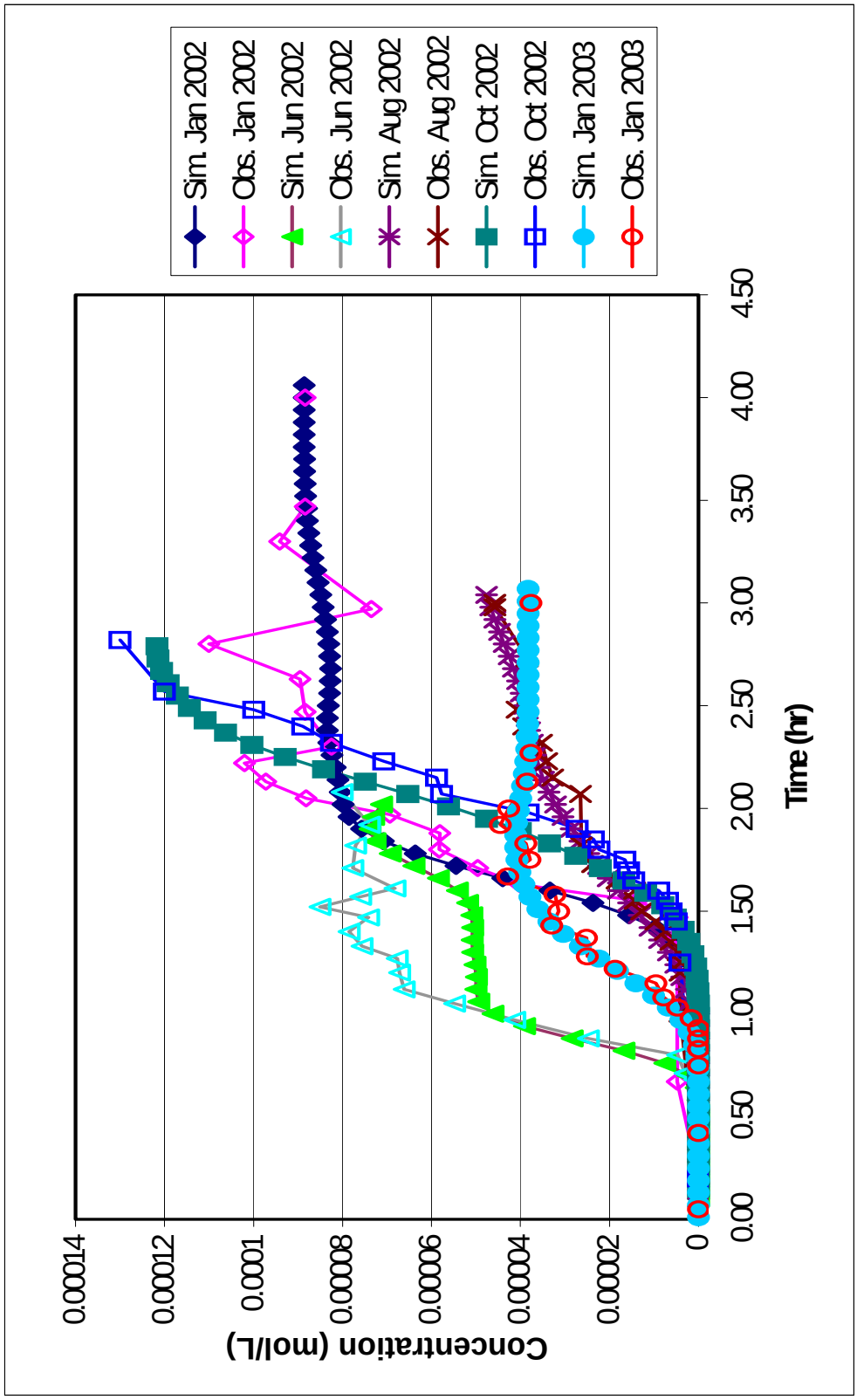

Figure 4.7: Simulated and observed concentration plot at LBC-3 for propane.

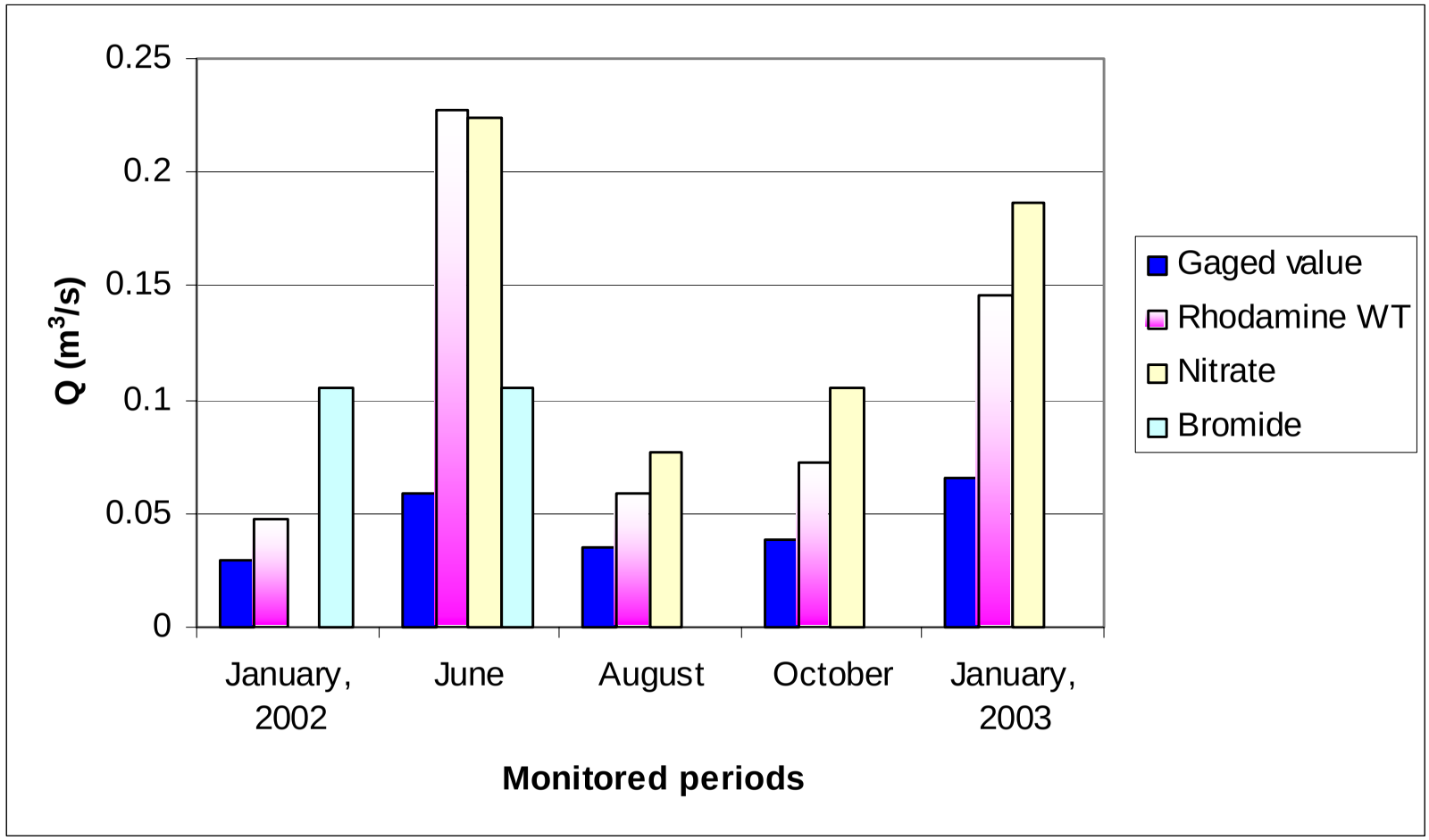

Figure 4.8: Comparison of total discharge values obtained by different slug tracers with gaged discharge values at LBC-3B

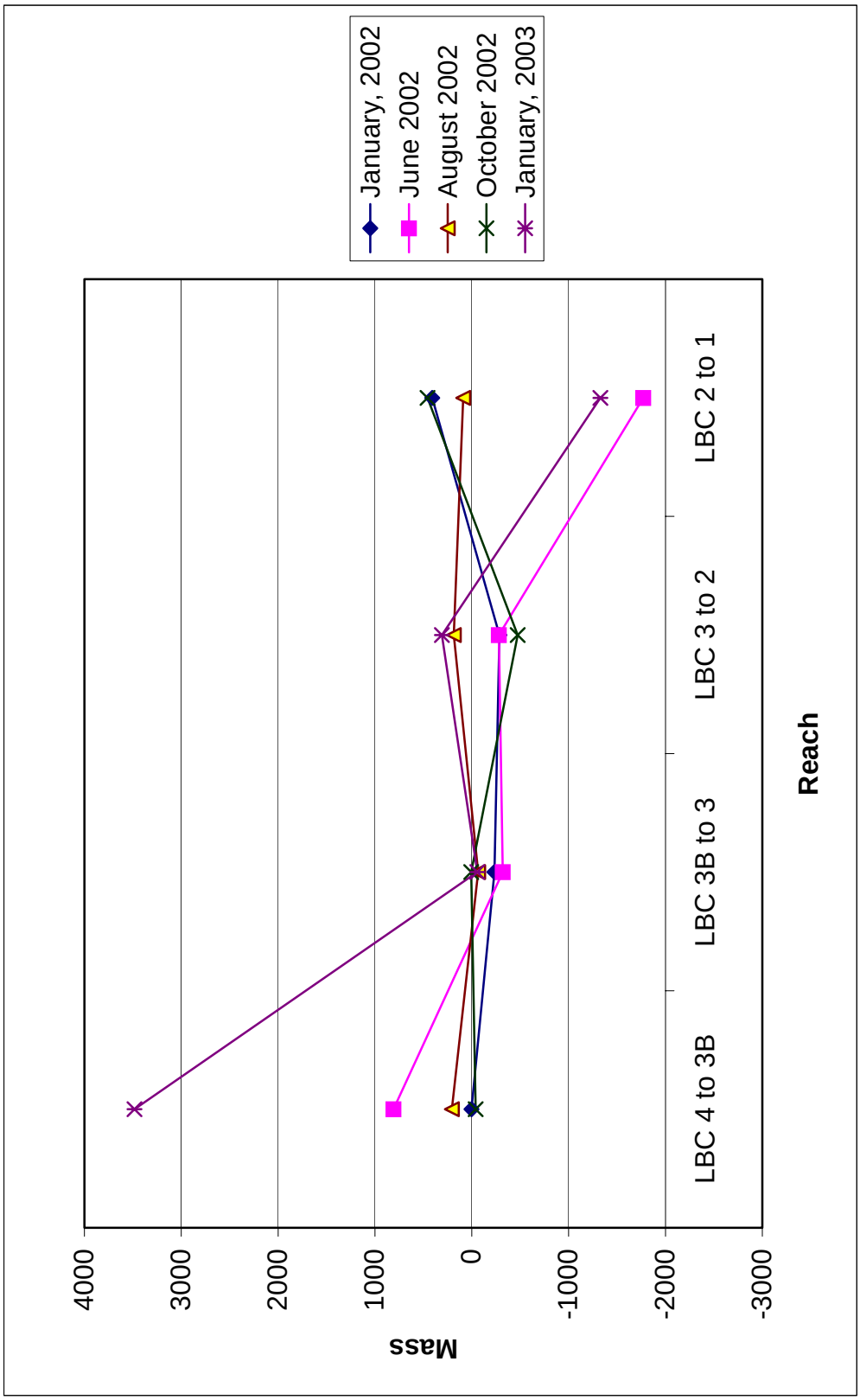

Figure 4.9: ^{99}Tc flux loss (pCi) along each reach.

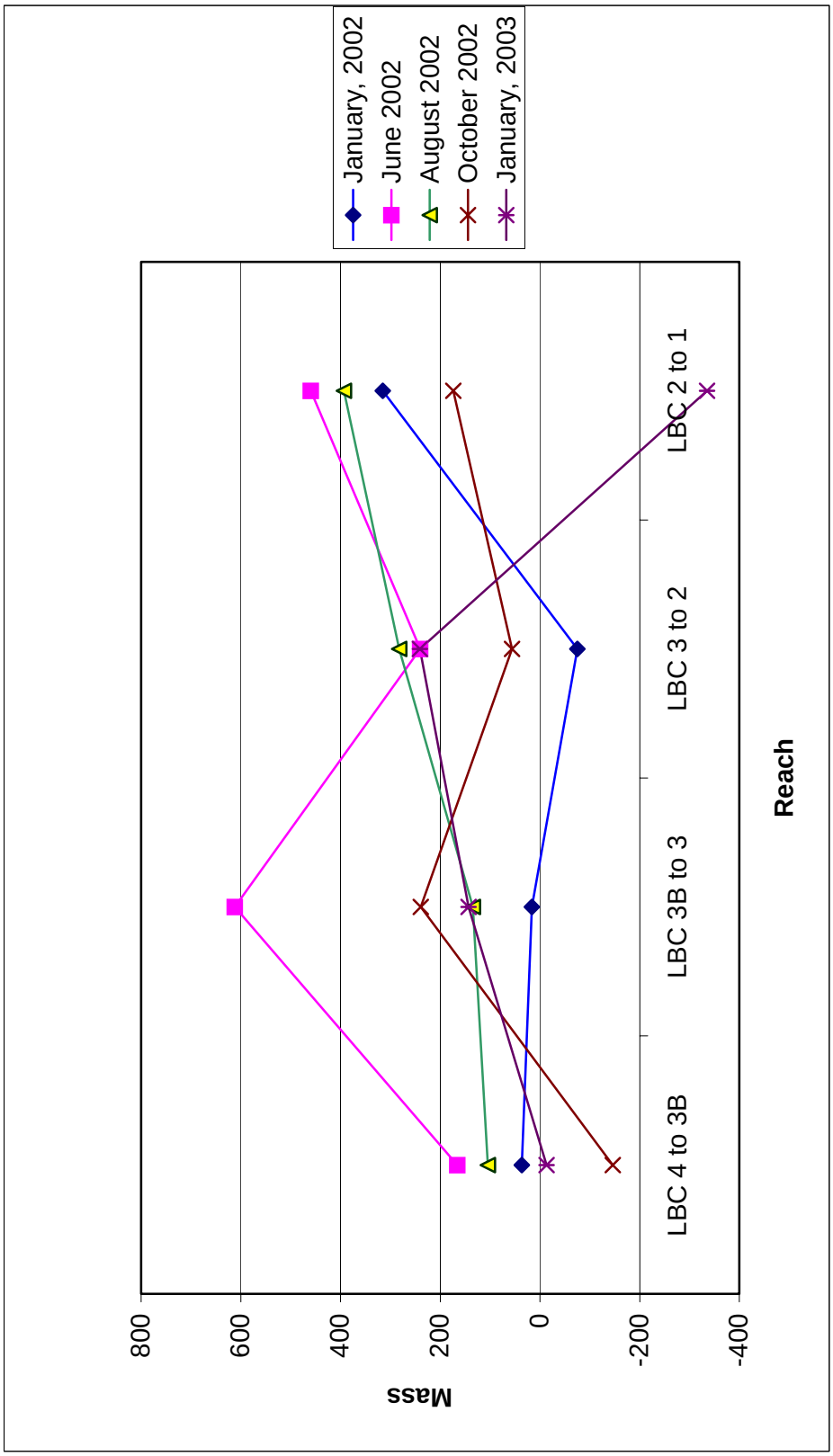

Figure 4.10: TCE flux loss (µg) along each reach.

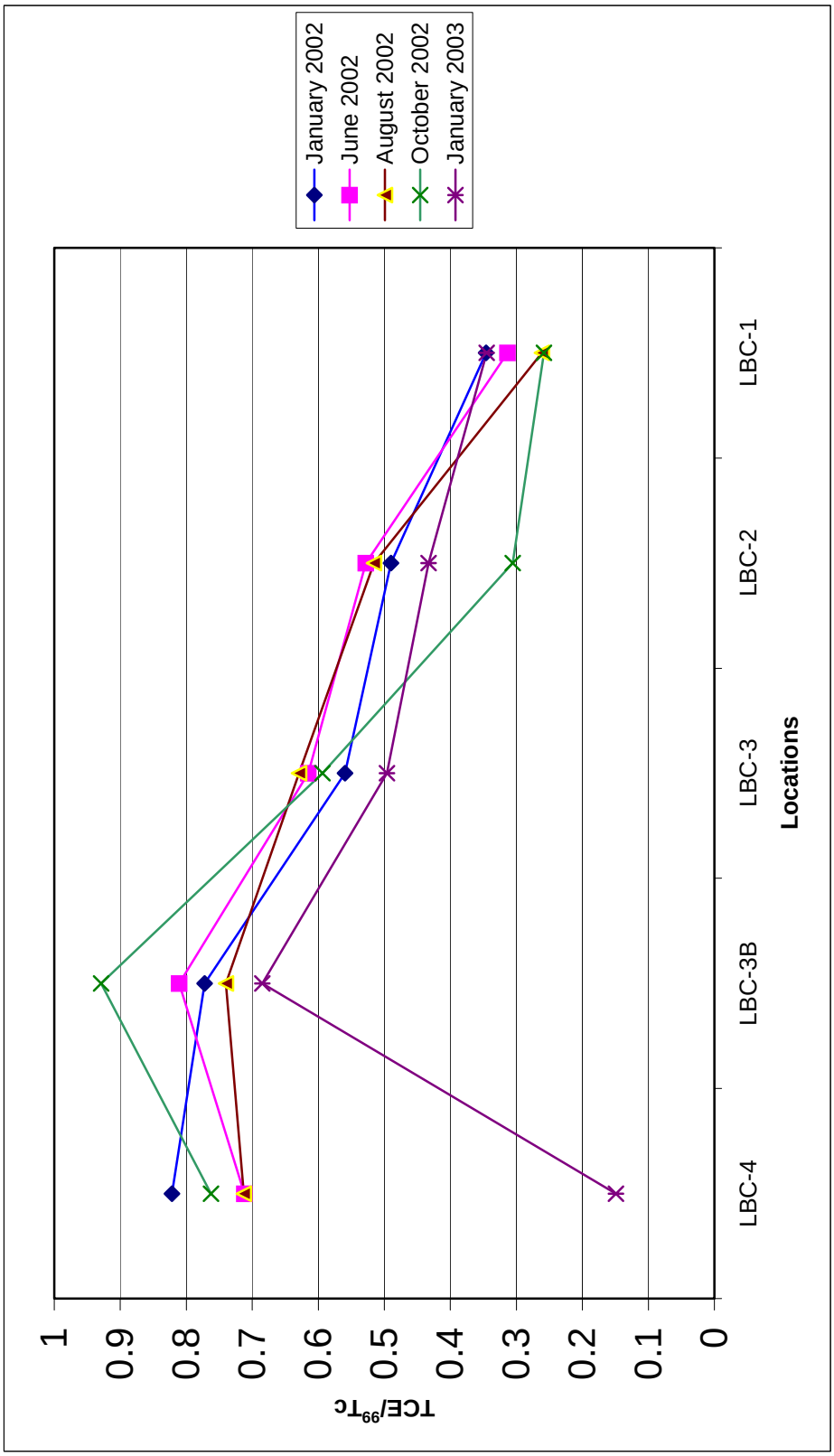

Figure 4.11: TCE/^{99}Tc (µg/pCi) ratio along each reach.

Chapter 5
Conclusions

Stream gaging, contaminant monitoring and tracer tests at Little Bayou Creek were conducted in January 2002(winter), June 2002 (late spring-early summer), August 2002 (summer), October 2002 (fall) and January 2003 (winter). Stream flow was high in January 2003 and June 2002 and low in January 2002 and October 2002. The discharge for August was between these values. The high discharge values in January 2003 probably resulted from from the preceding, extremely wet fall. TCE concentrations gradually decreased downstream from LBC-4 to LBC-1, whereas ^{99}Tc did not show any distinct trend of concentration change. Contaminant concentrations were highest in June 2002 and lowest in January 2002.

Comparison of the slug tracers bromide, nitrate and rhodamine WT showed that concentrations tended to peak at similar time. Center-of-mass travel times for the different slug tracers for each monitoring period were similar and were highest in October and lowest in June. During several of the monitoring periods, prominent secondary peaks were observed in the slug tracer curves for LBC-3B, while such peaks were absent or indistinct in the curves for LBC-3. These secondary peaks probably resulted from transient stagnation zones within the reach from LBC-4 to –3B. The continuously injected tracer propane tended plateau (except for both locations in August and for LBC-3 in October). The plateau concentration was highest in October and lowest in January 2003.

Simulation modeling (excluding the data from August, which did not converge) with the tracer test data and stream discharge values indicates that the dispersion coefficients for the tracers were highest in January 2003 (highest flow regime) and lowest in January 2002 (lowest flow regime). Probably because of the presumption of one-dimensional transport in the model, the effective channel cross sectional areas for all the monitored periods were lower than the gaged cross sectional areas. The secondary storage zone areas and storage zone exchange coefficients were insignificant for solute transport. The volatilization coefficients of TCE calculated from modeled values of the first-order decay coefficient for propane were close to the volatilization coefficient values calculated from TCE concentrations. The volatilization

coefficients calculated for propane and TCE varied with ambient temperature. Considering the channel morphology and good fit of the simulation and field data, transport of solute in Little Bayou Creek is dominantly one-dimensional.

Monitoring and modeling data suggest that ^{99}Tc is not attenuated along the studied reach except by dilution. Tracer tests with nitrate indicate ^{99}Tc is not immobilized by reduction in the hyporheic zone. Instead, the input of contaminated ground water during wet seasons may increase the contaminant concentration in the stream water between LBC-4 and 3B. TCE is attenuated along the flow path from LBC-4 to -1 by dilution and volatilization, which increased with ambient temperature and with discharge. Rhodamine WT data suggest that hydrophobic sorption of TCE to the stream bed sediments is not significant. This result is consistent with the lack of secondary storage, since sorption would be likely to occur in low-flow or stagnant zones.

APPENDIX A

Analytical Data for the Tracers for Each Monitoring Period

Table A-1: Concentration of bromide at LBC-3B, January 2002.

Proceeding time (min)	Concentration (mg/L)	Normalized concentration (C/Co)
0	0	0
16	0.2	1.03E-05
18	0.6	3.09E-05
23	10.3	5.30E-04
28	12.3	6.30E-04
33	9.2	4.70E-04
38	4	2.10E-04
43	3.1	1.60E-04
48	1.7	8.76E-05
53	1.4	7.21E-05
58	1.2	6.18E-05
63	0.6	3.09E-05
68	0.6	3.09E-05
73	0.4	2.06E-05
78	1.3	6.70E-05
83	0.7	3.60E-05
88	0.4	2.06E-05
95	0.4	2.06E-05
105	0.3	1.55E-05
115	0.2	1.03E-05

Table A-2: Concentration of bromide at LBC-3, January 2002.

Proceeding time (min)	Concentration (mg/L)	Normalized concentration (C/Co)
0	0	0
40	0.2	1.03E-05
83	0.5	2.58E-05
88	5.5	2.83E-04
93	7.2	3.70E-04
98	8	4.12E-04
103	7.5	3.86E-04
108	7.2	3.70E-04
113	5.9	3.00E-04
118	4.3	2.20E-04
123	4.1	2.10E-04
128	3.3	1.70E-04
133	2.5	1.30E-04
138	1.8	9.27E-05
148	1.3	6.70E-05
158	1	5.15E-05
168	0.6	3.09E-05
178	0.6	3.09E-05
188	0.8	4.12E-05
198	0.3	1.55E-05
208	0.3	1.55E-05

Table A-3: Concentration of rhodamine WT at LBC-3B, January 2002.

Proceeding time (min)	Concentration (mg/L)	Normalized concentration (C/Co)
0	0	0
16	0	0
18	0.0299	9.97E-06
23	1.3344	4.45E-04
28	2.0443	6.81E-04
33	1.632	5.44E-04
38	1.1795	3.93E-04
43	0.6401	2.13E-04
48	0.5042	1.68E-04
53	0.5233	1.74E-04
58	0.2166	7.22E-05
63	0.1499	5.00E-05
68	0.1191	3.97E-05
73	0.0856	2.85E-05
78	0.0365	1.22E-05
83	0.0327	1.09E-05
88	0.0199	6.63E-06
95	0.0157	5.23E-06
105	0.0153	5.10E-06
115	0	0

Table A-4: Concentration of rhodamine WT at LBC-3, January 2002.

Proceeding time (min)	Concentration (mg/L)	Normalized concentration (C/Co)
0	0	-7.67E-06
40	0	-7.67E-06
83	0.144	4.81E-05
88	1.168	3.89E-04
93	1.518	5.06E-04
98	1.711	5.70E-04
103	1.709	5.70E-04
108	1.505	5.02E-04
113	1.521	5.07E-04
118	1.145	3.82E-04
123	1.142	3.81E-04
128	0.956	3.19E-04
133	0.710	2.37E-04
138	0.526	1.75E-04
148	0.341	1.14E-04
158	0.253	8.43E-05
168	0.122	4.07E-05
178	0.106	3.54E-05
188	0.055	1.84E-05
198	0.018	5.87E-06
208	0.009	3.03E-06

Table A-5: Concentration of propane at LBC-3B, January 2002.

Proceeding time (min)	C_g (mol/L)	C_w (mol/L)	$C_i = C_g + C_w$ (mol/L)
0	4.44E-06	1.65E-07	4.60E-06
16	4.44E-06	1.65E-07	4.60E-06
18	4.44E-06	1.65E-07	4.60E-06
23	2.82E-05	1.05E-06	2.92E-05
28	5.16E-05	1.92E-06	5.35E-05
33	1.01E-04	3.77E-06	2.00E-04
38	1.01E-04	4.56E-06	1.01E-04
43	1.02E-04	4.53E-06	1.00E-04
48	8.02E-05	2.97E-06	8.31E-05
53	5.70E-05	2.12E-06	5.91E-05
58	8.18E-05	3.03E-06	8.48E-05
63	8.18E-05	3.01E-06	8.43E-05
68	1.00E-04	4.08E-06	1.00E-04
73	9.41E-05	3.48E-06	9.75E-05
78	1.01E-04	3.81E-06	1.01E-04
83	7.25E-05	2.68E-06	7.51E-05
88	6.85E-05	2.53E-06	7.09E-05
95	1.00E-04	3.96E-06	1.01E-04
105	8.18E-05	3.03E-06	8.48E-05
115	9.46E-05	3.50E-06	9.81E-05

Table A-6: Concentration of propane at LBC-3, January 2002.

Proceeding time (min)	**C_g (mol/L)**	**C_w (mol/L)**	**$C_i = C_g + C_w$ (mol/L)**
0	4.63E-06	1.71E-07	4.80E-06
40	4.63E-06	1.71E-07	4.80E-06
83	4.64E-06	1.72E-07	4.81E-06
88	4.63E-06	1.71E-07	4.80E-06
93	1.33E-05	4.94E-07	1.38E-05
98	3.86E-05	1.43E-06	4.02E-05
103	4.78E-05	1.77E-06	4.96E-05
108	5.62E-05	2.08E-06	5.83E-05
113	5.60E-05	2.08E-06	5.81E-05
118	6.69E-05	2.48E-06	6.94E-05
123	8.51E-05	3.15E-06	8.82E-05
128	9.38E-05	3.48E-06	9.73E-05
133	9.84E-05	3.65E-06	1.02E-04
138	7.95E-05	2.95E-06	8.25E-05
148	8.52E-05	3.16E-06	8.84E-05
158	8.64E-05	3.20E-06	8.96E-05
168	1.08E-04	3.99E-06	1.12E-04
178	7.09E-05	2.63E-06	7.35E-05
188	9.87E-05	3.66E-06	1.02E-04
198	9.07E-05	3.36E-06	9.41E-05
208	8.52E-05	3.16E-06	8.84E-05

Table A-7: Concentration of bromide at LBC-3B, June 2002.

Proceeding time (min)	Concentration (mg/L)	Normalized concentration (C/Co)
0	0.50	1.29E-05
8	0.50	1.29E-05
11	1.55	3.99E-05
15	30.90	7.96E-04
20	8.11	2.09E-04
25	2.86	7.37E-05
28	1.97	5.07E-05
31	1.61	4.15E-05
34	1.52	3.91E-05
37	1.11	2.86E-05
40	0.93	2.40E-05
43	0.57	1.47E-05
46	1.31	3.37E-05
49	3.89	1.340E-04
52	0.59	1.52E-05
55	0.49	1.26E-05
58	0.90	2.32E-05
61	0.42	1.08E-05
64	0.43	1.11E-05
67	0.51	1.31E-05
70	0.33	8.50E-06

Table A-8: Concentration of bromide at LBC-3, June 2002.

Proceeding time (min)	Concentration (mg/L)	Normalized concentration (C/Co)
0	0.53	1.36E-05
41	1.41	3.63E-05
43	2.18	5.61E-05
48	10.14	2.61E-04
53	14.89	3.83E-04
58	13.30	3.43E-04
63	10.60	2.73E-04
67	7.42	1.91E-04
72	4.07	1.05E-04
76	3.67	9.45E-05
80	2.59	6.67E-05
84	2.23	5.74E-05
88	2.37	6.10E-05
91	2.19	5.64E-05
94	2.04	5.25E-05
97	1.41	3.63E-05
103	0.99	2.55E-05
109	0.94	2.42E-05
115	0.69	1.78E-05
125	0.61	1.57E-05
135	0.48	1.24E-05
145	0.58	1.49E-05
155	0.53	1.36E-05

Table A-11: Concentration of nitrate at LBC-3B, June 2002.

Proceeding time (min)	Concentration (mg/L)	Normalized concentration (C/Co)
0	1.06	2.91E-05
8	1.06	2.91E-05
11	1.21	3.32E-05
15	4.83	1.32E-04
20	2.26	6.20E-05
25	1.39	3.81E-05
28	1.18	3.24E-05
31	1.81	4.96E-05
34	1.79	4.91E-05
37	1.71	4.69E-05
40	1.62	4.44E-05
43	1.59	4.36E-05
46	1.66	4.55E-05
49	1.55	4.25E-05
52	1.54	4.22E-05
55	1.55	4.25E-05
58	1.63	4.47E-05
61	1.55	4.25E-05
64	1.53	4.20E-05
67	1.56	4.28E-05
70	1.54	4.22E-05

Table A-12: Concentration of nitrate at LBC-3, June 2002.

Proceeding time (min)	Concentration (mg/L)	Normalized concentration (C/Co)
0	1.10	3.02E-05
41	1.88	5.15E-05
43	2.00	5.48E-05
48	3.53	9.68E-05
53	4.29	1.18E-04
58	4.21	1.15E-04
63	3.83	1.05E-04
67	3.41	9.35E-05
72	2.80	7.68E-05
76	2.47	6.77E-05
80	2.35	6.44E-05
84	1.77	4.85E-05
88	1.65	4.52E-05
91	1.72	4.72E-05
94	1.63	4.47E-05
97	1.43	3.92E-05
103	1.38	3.78E-05
109	1.31	3.59E-05
115	1.53	4.20E-05
125	1.38	3.78E-05
135	1.31	3.59E-05
145	1.05	2.88E-05
155	1.10	3.02E-05

Table A-9: Concentration of rhodamine WT at LBC-3B, June 2002.

Proceeding time (min)	Concentration (mg/L)	Normalized concentration (C/Co)
0	0	0
8	0	0
11	0.126	4.21E-05
15	1.071	3.57E-04
20	0.340	1.13E-04
25	0.088	2.94E-05
28	0.062	2.05E-05
31	0.040	1.33E-05
34	0.034	1.14E-05
37	0	0
40	0	0
43	0	0
46	0	0
49	0	0
52	0	0
55	0	0
58	0	0
61	0	0
64	0	0
67	0	0
70	0	0

Table A-10: Concentration of rhodamine WT at LBC-3, June 2002.

Proceeding time (min)	Concentration (mg/L)	Normalized concentration (C/Co)
0	0	0
41	0.029	9.50E-06
43	0.089	2.98E-05
48	0.278	9.27E-05
53	0.461	1.54E-04
58	0.488	1.63E-04
63	0.375	1.25E-04
67	0.317	1.06E-04
72	0.202	6.74E-05
76	0.127	4.23E-05
80	0.095	3.18E-05
84	0.069	2.31E-05
88	0.036	1.21E-05
91	0.024	8.00E-06
94	0.014	4.77E-06
97	0.005	1.63E-06
103	0	0
109	0	0
115	0	0
125	0	0
135	0	0
145	0	0
155	0	0

Table A-13: Concentration of propane at LBC-3B, June 2002.

Proceeding time (min)	C_g (mol/L)	C_w (mol/L)	$C_i = C_g + C_w$ (mol/L)
0	0	0	0
8	0	0	0
11	0	0	0
15	3.86E-05	1.43E-06	4.00E-05
20	6.66E-05	2.47E-06	6.91E-05
25	6.73E-05	2.49E-06	6.98E-05
28	5.93E-05	2.20E-06	6.15E-05
31	5.81E-05	2.15E-06	6.03E-05
34	5.83E-05	2.16E-06	6.05E-05
37	5.32E-05	1.97E-06	5.51E-05
40	6.23E-05	2.31E-06	6.46E-05
43	7.05E-05	2.61E-06	7.31E-05
46	5.46E-05	2.02E-06	5.66E-05
49	6.09E-05	2.26E-06	6.31E-05
52	5.67E-05	2.10E-06	5.88E-05
55	6.12E-05	2.27E-06	6.35E-05
58	6.41E-05	2.38E-06	6.65E-05
61	6.07E-05	2.25E-06	6.30E-05
64	6.93E-05	2.57E-06	7.19E-05
67	8.05E-05	2.98E-06	8.35E-05
70	9.67E-05	3.58E-06	1.01E-04

Table A-14: Concentration of propane at LBC-3, June 2002.

Proceeding time (min)	**C_g (mol/L)**	**C_w (mol/L)**	**$C_i = C_g + C_w$ (mol/L)**
0	0	0	0
41	8.36E-07	3.10E-08	8.67E-07
43	2.91E-06	1.08E-07	3.02E-06
48	4.51E-06	1.67E-07	4.67E-06
53	2.40E-05	8.88E-07	2.49E-05
58	3.98E-05	1.47E-06	4.13E-05
63	5.28E-05	1.96E-06	5.48E-05
67	6.38E-05	2.36E-06	6.62E-05
72	6.48E-05	2.40E-06	6.72E-05
76	6.53E-05	2.42E-06	6.77E-05
80	7.29E-05	2.70E-06	7.56E-05
84	7.57E-05	2.80E-06	7.85E-05
88	7.16E-05	2.65E-06	7.42E-05
91	8.21E-05	3.04E-06	8.52E-05
94	7.32E-05	2.71E-06	7.59E-05
97	6.57E-05	2.44E-06	6.82E-05
103	7.50E-05	2.78E-06	7.77E-05
109	7.44E-05	2.76E-06	7.71E-05
115	7.14E-05	2.64E-06	7.40E-05
125	7.72E-05	2.86E-06	8.01E-05
135	7.03E-05	2.61E-06	7.29E-05
145	7.95E-05	2.94E-06	8.24E-05
155	8.67E-05	3.21E-06	8.99E-05

Table A-15: Concentration of nitrate at LBC-3B, August 2002.

Proceeding time (min)	Concentration (mg/L)	Normalized concentration (C/Co)
0	0.93	2.55E-05
10	0.93	2.55E-05
18	1.49	4.08E-05
21	2.50	6.85E-05
24	4.05	1.00E-04
27	5.25	1.00E-04
30	5.69	1.56E-04
33	5.32	1.46E-04
36	5.48	1.50E-04
39	4.40	1.21E-04
42	4.06	1.11E-04
45	4.04	1.11E-04
50	3.56	9.76E-05
55	2.91	7.98E-05
60	2.27	6.22E-05
66	1.83	5.02E-05
72	3.68	1.01E-04
82	3.31	9.08E-05
97	1.42	3.89E-05
112	1.55	4.25E-05
127	1.12	3.07E-05

Table A-16: Concentration of nitrate at LBC-3, August 2002.

Proceeding time (min)	Concentration (mg/L)	Normalized concentration (C/Co)
0	0.78	2.14E-05
60	0.78	2.14E-05
72	1.04	2.85E-05
75	1.30	3.56E-05
78	1.80	4.94E-05
81	2.16	5.92E-05
84	2.32	6.36E-05
87	2.71	7.43E-05
90	2.78	7.62E-05
93	3.13	8.58E-05
96	2.79	7.65E-05
99	2.95	8.09E-05
104	2.97	8.14E-05
109	2.65	7.27E-05
124	2.47	6.77E-05
129	2.25	6.17E-05
134	2.31	6.33E-05
139	2.18	5.98E-05
144	2.11	5.79E-05
149	1.78	4.88E-05
164	1.48	4.06E-05
179	1.17	3.21E-05

Table A-17: Concentration of rhodamine WT at LBC-3B, August 2002.

Proceeding time (min)	Concentration (mg/L)	Normalized concentration (C/Co)
0	0	0
10	0	0
18	0.067	2.78E-05
21	0.297	1.24E-04
24	0.503	2.10E-04
27	0.112	4.65E-05
30	0.728	3.03E-04
33	0.845	3.52E-04
39	0.644	2.68E-04
42	0.467	1.95E-04
45	0.478	1.99E-04
50	0.387	1.61E-04
55	0.297	1.24E-04
60	0.184	7.68E-05
66	0.090	3.73E-05
72	0.106	4.40E-05
82	0.211	8.78E-05
97	0	0
112	0.016	6.58E-06
127	0	0

Table A-18: Concentration of rhodamine WT at LBC-3, August 2002.

Proceeding time (min)	Concentration (mg/L)	Normalized concentration (C/Co)
0	0	0
60	0	0
72	0	0
75	0.088	3.68E-05
78	0.156	6.52E-05
81	0.189	7.89E-05
84	0.233	9.69E-05
87	0.327	1.36E-04
90	0.358	1.49E-04
93	0.324	1.35E-04
96	0.327	1.36E-04
99	0.404	1.69E-04
104	0.388	1.62E-04
109	0.375	1.56E-04
124	0.322	1.34E-04
129	0.305	1.27E-04
134	0.258	1.07E-04
139	0.219	9.14E-05
144	0.239	9.96E-05
149	0.156	6.48E-05
164	0.105	4.38E-05
179	0.040	1.66E-05

Table A-19: Concentration of propane at LBC-3B, August 2002.

Proceeding time (min)	**C_g (mol/L)**	**C_w (mol/L)**	**$C_i = C_g + C_w$ (mol/L)**
0	5.71E-06	2.11E-07	5.92E-06
10	5.71E-06	2.11E-07	5.92E-06
18	6.06E-06	2.24E-07	6.28E-06
21	5.79E-06	2.15E-07	6.00E-06
24	6.87E-06	2.55E-07	7.13E-06
27	6.05E-06	2.24E-07	6.27E-06
30	1.07E-05	3.98E-07	1.11E-05
33	2.79E-05	1.03E-06	2.89E-05
36	2.94E-05	1.09E-06	3.05E-05
39	3.77E-05	1.40E-06	3.91E-05
42	3.52E-05	1.31E-06	3.65E-05
45	3.17E-05	1.18E-06	3.29E-05
50	4.08E-05	1.51E-06	4.23E-05
55	4.23E-05	1.57E-06	4.39E-05
60	4.10E-05	1.52E-06	4.26E-05
66	4.78E-05	1.77E-06	4.96E-05
72	5.66E-05	2.10E-06	5.87E-05
82	5.32E-05	1.97E-06	5.51E-05
97	5.09E-05	1.89E-06	5.28E-05
112	6.03E-05	2.24E-06	6.26E-05
127	6.90E-05	2.56E-06	7.16E-05

Table A-20: Concentration of propane at LBC-3, August 2002.

Proceeding time (min)	**C_g (mol/L)**	**C_w (mol/L)**	**$C_i = C_g + C_w$ (mol/L)**
0	3.99E-06	1.48E-07	4.14E-06
60	3.99E-06	1.48E-07	4.14E-06
72	3.99E-06	1.48E-07	4.14E-06
75	3.82E-06	1.41E-07	3.96E-06
78	4.41E-06	1.63E-07	4.57E-06
81	5.98E-06	2.22E-07	6.21E-06
84	7.20E-06	2.67E-07	7.46E-06
87	9.25E-06	3.43E-07	9.59E-06
90	1.23E-05	4.56E-07	1.28E-05
93	1.38E-05	5.12E-07	1.43E-05
96	1.39E-05	5.13E-07	1.44E-05
99	1.76E-05	6.53E-07	1.83E-05
104	2.30E-05	8.51E-07	2.38E-05
109	2.54E-05	9.39E-07	2.63E-05
124	2.55E-05	9.45E-07	2.65E-05
129	3.17E-05	1.17E-06	3.28E-05
134	3.29E-05	1.22E-06	3.41E-05
139	3.41E-05	1.26E-06	3.53E-05
144	3.79E-05	1.40E-06	3.93E-05
149	3.94E-05	1.46E-06	4.08E-05
164	3.71E-05	1.37E-06	3.85E-05
179	4.42E-05	1.64E-06	4.58E-05

Table A-21: Concentration of nitrate at LBC-3B, October 2002.

Proceeding time (min)	Concentration (mg/L)	Normalized concentration (C/Co)
0	0.75	2.05E-05
10	0.75	2.05E-05
22	1.49	4.09E-05
25	5.36	1.47E-04
28	6.51	1.79E-04
31	7.37	2.02E-04
34	6.28	1.72E-04
37	5.60	1.54E-04
40	4.09	1.12E-04
43	3.73	1.02E-04
46	2.96	8.12E-05
49	2.55	6.99E-05
52	1.70	4.66E-05
57	1.63	4.47E-05
62	1.31	3.59E-05
69	1.51	4.14E-05
76	0.90	2.48E-05
86	0.79	2.17E-05
101	0.90	2.48E-05
116	0.88	2.41E-05
131	0.75	2.05E-05

Table A-22: Concentration of nitrate at LBC-3, October2002.

Proceeding time (min)	Concentration (mg/L)	Normalized concentration (C/Co)
0	0.61	1.67E-05
75	0.61	1.67E-05
87	0.54	1.49E-05
90	1.42	3.89E-05
93	1.76	4.83E-05
96	2.21	6.06E-05
99	3.01	8.25E-05
102	3.14	8.61E-05
105	3.57	9.79E-05
108	3.16	8.66E-05
111	3.59	9.84E-05
114	3.44	9.43E-05
119	2.89	7.92E-05
124	2.71	7.43E-05
129	2.37	6.50E-05
134	2.12	5.81E-05
139	1.94	5.32E-05
144	1.58	4.33E-05
149	1.74	4.77E-05
154	1.15	3.15E-05
169	0.97	2.67E-05

Table A-23: Concentration of rhodamine WT at LBC-3B, October 2002.

Proceeding time (min)	Concentration (mg/L)	Normalized concentration (C/Co)
0	0	0
10	0	0
22	0.064	2.65E-05
25	0.466	1.94E-04
28	0.923	3.85E-04
31	0.864	3.60E-04
34	0.835	3.48E-04
37	0.739	3.08E-04
40	0.611	2.55E-04
43	0.416	1.73E-04
46	0.395	1.65E-04
49	0.250	1.04E-04
52	0.191	7.96E-05
57	0.162	6.75E-05
62	0.066	2.74E-05
69	0.049	2.03E-05
76	0.013	5.29E-06
86	0	4.17E-08
101	0	0
116	0	0
131	0	0

Table A-24: Concentration of rhodamine WT at LBC-3, October 2002.

Proceeding time (min)	Concentration (mg/L)	Normalized concentration (C/Co)
0	0	0
75	0	0
87	0	0
90	0.049	2.04E-05
93	0.177	7.38E-05
96	0.202	8.40E-05
99	0.359	1.50E-04
102	0.410	1.71E-04
105	0.433	1.80E-04
108	0.460	1.92E-04
111	0.461	1.92E-04
114	0.453	1.89E-04
119	0.385	1.61E-04
124	0.336	1.40E-04
129	0.287	1.20E-04
134	0.272	1.13E-04
139	0.201	8.38E-05
144	0.188	7.82E-05
149	0.122	5.08E-05
154	0.077	3.22E-05
169	0.046	1.92E-05

Table A-25: Concentration of propane at LBC-3B, October 2002.

Proceeding time (min)	**C_g (mol/L)**	**C_w (mol/L)**	**$C_i = C_g + C_w$ (mol/L)**
0	4.98E-06	1.84E-07	5.16E-06
10	4.98E-06	1.84E-07	5.16E-06
22	5.25E-06	1.95E-07	5.45E-06
25	8.56E-06	3.17E-07	8.87E-06
28	3.00E-05	1.11E-06	3.11E-05
31	2.69E-05	9.98E-07	2.79E-05
34	3.85E-05	1.43E-06	3.99E-05
37	4.35E-05	1.61E-06	4.51E-05
40	4.48E-05	1.66E-06	4.65E-05
43	4.96E-05	1.84E-06	5.14E-05
46	5.79E-05	2.15E-06	6.01E-05
49	7.36E-05	2.73E-06	7.63E-05
52	8.86E-05	3.28E-06	9.19E-05
57	1.03E-04	3.80E-06	1.06E-04
62	1.24E-04	4.60E-06	1.29E-04
69	1.47E-04	5.46E-06	1.53E-04
76	1.54E-04	5.71E-06	1.60E-04
86	1.55E-04	5.74E-06	1.61E-04
101	1.62E-04	6.00E-06	1.68E-04
116	1.63E-04	6.05E-06	1.69E-04
131	1.55E-04	5.75E-06	1.61E-04

Table A-26: Concentration of propane at LBC-3, October 2002.

Proceeding time (min)	**C_g (mol/L)**	**C_w (mol/L)**	**$C_i = C_g + C_w$ (mol/L)**
0	3.98E-06	1.47E-07	4.13E-06
75	3.98E-06	1.47E-07	4.13E-06
87	4.82E-06	1.79E-07	5.00E-06
90	5.94E-06	2.20E-07	6.16E-06
93	6.70E-06	2.48E-07	6.95E-06
96	8.62E-06	3.19E-07	8.94E-06
99	1.41E-05	5.23E-07	1.46E-05
102	1.52E-05	5.62E-07	1.57E-05
105	1.59E-05	5.91E-07	1.65E-05
108	2.16E-05	8.00E-07	2.24E-05
111	2.27E-05	8.43E-07	2.36E-05
114	2.63E-05	9.75E-07	2.73E-05
119	3.69E-05	1.37E-06	3.83E-05
124	5.56E-05	2.06E-06	5.77E-05
129	5.68E-05	2.10E-06	5.89E-05
134	6.82E-05	2.53E-06	7.07E-05
139	7.95E-05	2.95E-06	8.25E-05
144	8.58E-05	3.18E-06	8.89E-05
149	9.94E-05	3.68E-06	1.03E-04
154	1.16E-04	4.28E-06	1.20E-04
169	1.33E-04	4.93E-06	1.38E-04

Table A-27: Concentration of nitrate at LBC-3B, January 2003.

Proceeding time (min)	Concentration (mg/L)	Normalized concentration (C/Co)
0	0.72	1.98E-05
3	0.72	1.98E-05
15	1.02	2.80E-05
18	3.19	8.75E-05
21	4.02	1.10E-04
24	5.11	1.40E-04
27	4.25	1.17E-04
30	2.67	7.32E-05
33	1.97	5.40E-05
36	2.03	5.57E-05
39	1.79	4.91E-05
42	1.47	4.03E-05
45	1.02	2.80E-05
48	0.95	2.60E-05
51	0.88	2.41E-05
54	1.04	2.85E-05
59	0.97	2.67E-05
64	0.81	2.23E-05
69	0.79	2.17E-05
79	0.77	2.11E-05
89	0.72	1.98E-05

Table A-28: Concentration of nitrate at LBC-3, January 2003.

Proceeding time (min)	Concentration (mg/L)	Normalized concentration (C/Co)
0	0.84	2.29E-05
25	0.84	2.29E-05
45	0.81	2.23E-05
50	0.84	2.29E-05
53	1.13	3.10E-05
56	1.85	5.07E-05
59	3.01	8.25E-05
62	3.23	8.86E-05
65	3.07	8.42E-05
69	2.96	8.12E-05
73	2.42	6.64E-05
77	2.17	5.95E-05
82	1.72	4.72E-05
86	1.51	4.14E-05
90	1.36	3.73E-05
95	1.20	3.29E-05
100	0.97	2.66E-05
105	0.97	2.67E-05
110	0.97	2.67E-05
115	0.93	2.54E-05
120	0.81	2.23E-05
128	0.88	2.42E-05
136	0.90	2.48E-05

Table A-29: Concentration of rhodamine WT at LBC-3B, January 2003.

Proceeding time (min)	Concentration (mg/L)	Normalized concentration (C/Co)
0	0	0
3	0	0
15	0.001	3.75E-07
18	0.308	1.28E-04
21	0.655	2.73E-04
24	0.693	2.89E-04
27	0.557	2.32E-04
30	0.308	1.28E-04
33	0.233	9.71E-05
36	0.176	7.32E-05
39	0.133	5.55E-05
42	0.090	3.77E-05
45	0.036	1.48E-05
48	0.020	8.50E-06
51	0.005	2.08E-06
54	0	0
59	0	0
64	0	0
69	0	0
79	0	0
89	0	0

Table A-30: Concentration of rhodamine WT at LBC-3, January 2003.

Proceeding time (min)	Concentration (mg/L)	Normalized concentration (C/Co)
0	0	0
25	0	0
45	0	0
50	0	0
53	0.029	1.23E-05
56	0.160	6.68E-05
59	0.346	1.44E-04
62	0.404	1.68E-04
65	0.396	1.65E-04
69	0.332	1.38E-04
73	0.274	1.14E-04
77	0.218	9.07E-05
82	0.157	6.53E-05
86	0.109	4.55E-05
90	0.079	3.27E-05
95	0.054	2.26E-05
100	0.030	1.27E-05
105	0.012	5.08E-06
110	0.004	1.54E-06
115	0	0
120	0	0
128	0	0
136	0	0

Table A-31: Concentration of propane at LBC-3B, January 2003.

Proceeding time (min)	C_g (mol/L)	C_w (mol/L)	$C_i = C_g + C_w$ (mol/L)
0	0	0	0
3	0	0	0
15	0	0	0
18	1.06E-07	3.92E-09	1.10E-07
21	3.18E-06	1.18E-07	3.30E-06
24	6.11E-06	2.26E-07	6.34E-06
27	1.10E-05	4.08E-07	1.14E-05
30	2.02E-05	7.50E-07	2.10E-05
33	2.25E-05	8.32E-07	2.33E-05
36	2.61E-05	9.67E-07	2.71E-05
39	3.44E-05	1.27E-06	3.57E-05
42	3.06E-05	1.14E-06	3.18E-05
45	3.89E-05	1.44E-06	4.03E-05
48	4.62E-05	1.71E-06	4.79E-05
51	4.72E-05	1.75E-06	4.89E-05
54	4.71E-05	1.74E-06	4.88E-05
59	4.53E-05	1.68E-06	4.70E-05
64	4.65E-05	1.72E-06	4.82E-05
69	4.79E-05	1.78E-06	4.97E-05
79	4.63E-05	1.72E-06	4.80E-05
89	4.30E-05	1.59E-06	4.46E-05

Table A-32: Concentration of propane at LBC-3, January 2003.

Proceeding time (min)	C_g (mol/L)	C_w (mol/L)	$C_i = C_g + C_w$ (mol/L)
0	0	0	0
25	0	0	0
45	0	0	0
50	0	0	0
53	0	0	0
56	0	0	0
59	1.57E-06	5.80E-08	1.62E-06
62	4.49E-06	1.66E-07	4.65E-06
65	7.57E-06	2.80E-07	7.85E-06
69	9.25E-06	3.43E-07	9.59E-06
73	1.80E-05	6.67E-07	1.87E-05
77	2.41E-05	8.94E-07	2.50E-05
82	2.43E-05	9.00E-07	2.52E-05
86	3.19E-05	1.18E-06	3.30E-05
90	3.03E-05	1.12E-06	3.14E-05
95	3.11E-05	1.15E-06	3.22E-05
100	4.14E-05	1.53E-06	4.29E-05
105	3.65E-05	1.35E-06	3.79E-05
110	3.75E-05	1.39E-06	3.88E-05
115	4.29E-05	1.59E-06	4.45E-05
120	4.10E-05	1.52E-06	4.26E-05
128	3.71E-05	1.38E-06	3.85E-05
136	3.63E-05	1.35E-06	3.77E-05

Table A-33: ^{99}Tc flux (in pCi) loss along each of the reaches of Little Bayou Creek.

Reaches	January 2002	June	August	October	January 2003
LBC 2 to 1	407.50	-1770.05	87.97	458.06	-1328.46
BC 3 to 2	-285.25	-279.93	185.97	-472.40	307.37
LBC-3B to 3	-233.81	-319.51	-63.97	6.048	-57.45
LBC 4 to 3B	3.01	807.67	206.01	-38.33	3483.45

Table A-34: TCE loss (in μg) along each of the reaches of Little Bayou Creek.

Reaches	January 2002	June	August	October	January 2003
LBC 2 to 1	314.99	459.18	392.90	173.78	-335.26
LBC-3 to 2	-75.31	239.85	282.08	55.88	240.96
LBC-3B to 3	16.42	611.88	134.20	239.07	142.93
LBC 4 to 3B	36.59	165.72	104.31	-145.98	-13.36

APPENDIX B

Matlab Program for Centroid Calculation

User defined Matlab function **centroid.m** (modified by Veeraganesh. Yalla and Abhijit Mukherjee from Johnson, 1995) [http://web.ccr.jussieu.fr/ccr/Documentation/Calcul/matlab5v11/docs/ftp.mathworks.com/pub/contrib/v4/misc/centroid.m]. Before executing, save under the present work directory

```
function [x0,y0] = centroid(x,y)
% CENTROID Center of mass of a polygon.
%    [X0,Y0] = CENTROID(X,Y) Calculates centroid
%    (center of mass) of planar polygon with vertices
%    coordinates X, Y.
%    Z0 = CENTROID(X+i*Y) returns Z0=X0+i*Y0 the same
%    as CENTROID(X,Y).


% Algorithm:
%  X0 = Int{x*ds}/Int{ds}, where ds - area element
%  so that Int{ds} is total area of a polygon.
%    Using Green's theorem the area integral can be
%  reduced to a contour integral:
%  Int{x*ds} = -Int{x^2*dy}, Int{ds} = Int{x*dy} along
%  the perimeter of a polygon.
%    For a polygon as a sequence of line segments
%  this can be reduced exactly to a sum:
%  Int{x^2*dy} = Sum{ (x_{i}^2+x_{i+1}^2+x_{i}*x_{i+1})*
%  (y_{i+1}-y_{i})}/3;
%  Int{x*dy} = Sum{(x_{i}+x_{i+1})(y_{i+1}-y_{i})}/2.
%    Similarly
%  Y0 = Int{y*ds}/Int{ds}, where
%  Int{y*ds} = Int{y^2*dx} =
%  = Sum{ (y_{i}^2+y_{i+1}^2+y_{i}*y_{i+1})*
%  (x_{i+1}-x_{i})}/3.

 % Handle input .....................
if nargin==0, help centroid, return, end
if nargin==1
```

```
  sz = size(x);
  if sz(1)==2      % Matrix 2 by n
    y = x(2,:); x = x(1,:);
  elseif sz(2)==2  % Matrix n by 2
    y = x(:,2); x = x(:,1);
  else
    y = imag(x);
    x = real(x);
  end
end

 % Make a polygon closed ..............
x = [x(:); x(1)];
y = [y(:); y(1)];

 % Check length .......................
l = length(x);
if length(y)~=l
  error(' Vectors x and y must have the same length')
end

 % X-mean: Int{x^2*dy} ................
del = y(2:l)-y(1:l-1);
v = x(1:l-1).^2+x(2:l).^2+x(1:l-1).*x(2:l);
x0 = v'*del;

 % Y-mean: Int{y^2*dx} ................
del = x(2:l)-x(1:l-1);
v = y(1:l-1).^2+y(2:l).^2+y(1:l-1).*y(2:l);
y0 = v'*del;

 % Calculate area: Int{y*dx} ..........
a = (y(1:l-1)+y(2:l))'*del;
tol= 2*eps;
if abs(a)<tol
  disp(' Warning: area of polygon is close to 0')
  a = a+sign(a)*tol+(~a)*tol;
end
 % Multiplier
a = 1/3/a;

 % Divide by area .....................
x0 = -x0*a;
y0 =  y0*a;

if nargout < 2, x0 = x0+i*y0; end
```

Matlab program **t-centroid.m** to calculate centroid for three sets of tracer concentration data in MS-Excel worksheet. Authors : Veeraganesh Yalla and Abhijit Mukherjee (2002)

```
A= xlsread('c:\matlab6p1\bin\win32\file.xls); % reading the excel file
X =A(:,1);% reading the sampling time
B= A(:,2);% reading the 2nd column entries
C= A(:,3);% reading the 3rd column entries
D= A(:,4);% reading the 4th column entries
reading the 7th column entries

[a1,b1]=centroid(X,B) % centroid of graph of second column
%
 [a2,b2]=centroid(X,C)% centroid of graph of third column
%
 [a3,b3]=centroid(X,D)% centroid of graph of fourth column
%
```

APPENDIX C

Sample OTIS and OTIS-P Input Files

Input files used for simulation of propane, January 2003:

Control file (used for both OTIS and OTIS-P)

```
###############################################################################
#
#                         OTIS-P control file
#
#
#    line              name of the:
#    ----              --------------
#     1                parameter file
#     2                flow file
#     3                data file
#     4                STARPAC input file
#     5                parameter output file
#     6                STARPAC output file
#     7                solute output file
#     8                sorption output file (ISORB=1 only)
#
###############################################################################
paramsP.inp
qp.inp
datap.inp
starp.inp
params.out
star.out
propaneJan3.out
```

Parameter file (used for both OTIS and OTIS-P)

```
#########################################################################
#
#                       Parameter file, Jan03
#
#   2002 Little Bayou Creek Tracer Injection
#   Conservative Transport of Propane
#
#   Parameter Values from:
#
#   January03 test run.
#
#########################################################################
Mukherjee and Fryar, LBC Rhodamine
 1            |      PRTOPT
 0.10         |      PSTEP  [hour]
 0.02         |      TSTEP  [hour]
 0.01         |      TSTART [hour]
 3.00         |      TFINAL [hour]
 0.0          |      XSTART [L]
 0.0          |      DSBOUND [(L/sec)CU]
  1           |      NREACH
#############################################################
#
#  Physical Parameters for each reach
#
#NSEG RCHLEN       DISP         AREA2        ALPHA
#         |            |            |            |
#####*############*############*############*##############
350  350.0        0.63          0.009        0
#############################################################
#
# Number of Solutes and flags for decay and sorption
#
# NSOLUTE (col.1-5) IDECAY(col.6-10) ISORB(col.11-15)
#
#    |    |
#####*####*#################################################
1    1    0
#############################################################
#
#  Decay Coefficients (IDECAY=1, only)
#
#                    for I = 1, NREACH
#
#LAMBDA       LAMBDA2
#            |
##############*################################################
0.23e-3       0.23e-3
#############################################################
#
#  Sorption Parameters (ISORB=1, only)
#
```

```
#                    for I = 1, NREACH
#
#LAMHAT       LAMHAT2      RHO          KD           CSBACK
#            |            |            |            |
##############################################################
##############################################################
#  Print Information
#*####*#######################################################
1     0               NPRINT (col.1-5)  IOPT (col.6-10)
 241.0               (PRTLOC  for I = 1, NPRINT)
##############################################################
#
#  Boundary Conditions
#
#####*########################################################
22   3             NBOUND (col.1-5)  IBOUND (col.6-10)
########################################################
#                for I = 1,NBOUND
#
#USTIME       USBC (for i=1,NSOLUTE)
#            |            |            |
#####*########*#########################################
     0.03     0.00
     0.05     0.00
     0.25     0.00
     0.30     1.1e-7
     0.35     3.3e-6
     0.40     6.34e-6
     0.45     1.14e-5
     0.50     2.1e-5
     0.55     2.33e-5
     0.60     2.71e-5
     0.65     3.57e-5
     0.70     3.18e-5
     0.75     4.03e-5
     0.80     4.79e-5
     0.85     4.89e-5
     0.90     4.88e-5
     0.98     4.7e-5
     1.07     4.82e-5
     1.15     4.97e-5
     1.32     4.8e-5
     1.48     4.46e-5
     3.00     4.46e-5
```

Flow File (used for both OTIS and OTIS-P)

```
#########################################################################
#
#                        Steady flow file
#
#   2002 Rhodamine slug (Mukherjee and Fryar, 2002)
#
#########################################################################
0.00                 QSTEP [hour]
0.06                 QSTART [L^3/second]
#############################################################
#            for I = 1, NREACH
#
#QLATIN       QLATOUT      AREA         (CLATIN J=1,NSOLUTE)
#            |            |            |            |
#############################################################
0.00         0.00         0.43         0.00
```

Data File (used only for OTIS-P)

```
#########################################################################
#
#                         OTIS-P data file
#
#
#    line     for J = 1, NREACH
#    ----
#     1       N - Number of observations for reach J.
#     2-N+1   TIME (time-variable) or DIST (steady-state) associated
#             with each observation (col. 1-15) and CONC (col. 16-30).
#
#
#     Little Bayou Creek Propane - Jan,2003
#     Mukherjee and Fryar
#
#########################################################################
#
#  Site 1, (LBC #3)
#
24
     0.05        0.00
     0.42        0.00
     0.75        0.00
     0.83        0.00
     0.88        0.00
     0.93        0.00
     0.98        1.62e-6
     1.03        4.65e-6
     1.08        7.85e-6
     1.15        9.59e-6
     1.22        1.87e-5
     1.28        2.50e-5
     1.37        2.52e-5
     1.43        3.30e-5
     1.50        3.14e-5
     1.58        3.22e-5
     1.67        4.29e-5
     1.75        3.79e-5
     1.83        3.88e-5
     1.92        4.45e-5
     2.00        4.26e-5
     2.13        3.85e-5
     2.27        3.77e-5
     3.00        3.77e-5
```

STARPAC File (used only for OTIS-P)

```
#############################################################################
#
#
#                     STARPAC Parameter Input File
#               Little Bayou Creek Propane - Jan, 2003
#                       Mukherjee and Fryar
#
#
#############################################################################
#
#  Record Types 1-4, Integer values in Columns 1-5
#  -----------------------------------------------
#  IWEIGHT   Weight Revision Option
#  IVAPRX    Variance/Covariance Option
#  MIT       Maximum Number of Iterations
#  NPRT      STARPAC Print Option
#
0
1
100
22222
#
#  Record Types 5-7, Double precision values in Columns 1-13
#  ----------------------------------------------------------
#  DELTA     Maximum Scaled Change, First Iteration
#  STOPP     Stopping Value for Parameter Convergence
#  STOPSS    Stopping Value for Sum of Square Convergence
#
1.0
1.D-5
1.D-5
#
# For each of the ten model parameters, enter IFIXED (Integer, Col. 1-5)
# and SCALE (Floating Point, Col 6-18).
#
#IFXD SCALE
#    |                 | IFIXED and SCALE for:
#----*-----------------------------------------
0    0.0D0             | Dispersion Coefficient, DISP
0    0.0D0             | Main Channel Cross-Sectional Area, AREA
1    0.0D0             | Storage Zone Cross-Sectional Area, AREA2
1    0.0D0             | Storage Zone Exchange Coefficient, ALPHA
0    0.0D0             | Main Channel First-Order Decay Coefficient, LAMBDA
1    0.0D0             | Storage Zone First-Order Decay Coefficient, LAMBDA2
1    0.0D0             | Mass of Accessible Sediment/Volume Water, RHO
1    0.0D0             | Distribution Coefficient, KD
1    0.0D0             | Main Channel Sorption Rate Coefficient, LAMHAT
1    0.0D0             | Storage Zone Sorption Rate Coefficient, LAMHAT2
```

References

Allen-King, R.M., Groenevelt, H., Warren, C.J. and Mackay, D.M., 1996. Nonlinear chlorinated-solvent sorption in four aquitards. Journal of Contaminant Hydrology, vol. 22, p. 203-221.

Anders, E., 1960. Radiochemistry of technetium. USAEC Report NAS-NS-3021. National Technical Information Service. Springfield, Virginia.

Atkins, H.L., 1970. Pathways of an artificial element in the body. USAEC Report BNL-50285. National Technical Information Service, Springfield, Virginia.

ATSDR, 2001. Public health assessment: Paducah Gaseous Diffusion Plant (USDOE), Paducah, McCracken County, Kentucky. Prepared by Energy Section, Federal Facilities Assessment Branch, Division of Health Assessment and Consultation, Agency for Toxic Substances and Disease Registry, Atlanta, Georgia.

Avanzino, R.J., and Kennedy, V.C., 1993. Long-term frozen storage of stream water samples for dissolved orthophosphate, nitrate plus nitrite, and ammonia analysis. Water Resources Research, vol. 29, no. 10, p. 3357-3362.

Avery, C., Yeskis, D., and Bolen, W., 1991. Interaction of ground water with Rock River near Byron, Illinois. Eos Transactions, American Geophysical Union, vol. 72, no. 4, p. 185.

Bencala, K.E., and Walters, R.A., 1983. Simulation of solute transport in a mountain pool-and-riffle stream−A transient model. Water Resources Research, vol. 19, no. 3, p. 718-724.

Boggs, M.J., and Adams, E.E., 1992. Field study of dispersion in a heterogeneous aquifer, 4. Investigation of adsorption and sampling bias. Water Resources Research, vol. 28, no. 12, p. 3325-3336.

Bourg, A.C.M., Degranges, P., Mouvet, C., and Sauty, J.P., 1993. Migration of chlorinated hydrocarbon solvents through Coventry sandstone rock columns. Journal of Hydrology, vol. 149, p. 183-207.

Butler, D. L., 1999. Assessment of potential trichloroethene biodegradation in wetland soils, McCracken County, Kentucky. Unpublished MS thesis, University of Kentucky, 121 p.

Carey, D.I., and Stickney, J.F., 2001. Ground water resources of McCracken County, Kentucky. Kentucky Geological Survey, University of Kentucky, Open-File Report OF-01-79, 22 p.

CH2M Hill, 1990. Results of the site investigation, Phase I, at the Paducah Gaseous Diffusion Plant, Paducah, Kentucky. Report KY/SUB 13 B-97777 CP-03/1991.

CH2M Hill Southeast Inc., 1992. Results of the site investigation, Phase II, at the Paducah Gaseous Diffusion Plant, Paducah, Kentucky. Document KY/SUB/13B-97777C P-03/1991/1, prepared for the U.S. Department of Energy under contract DE-AC05-76OR00001.

Chapelle, F.H., 1993. Ground-Water Microbiology and Geochemistry. John Wiley and Sons, New York, 424 p.

Clausen, J.L., Douthitt, J.W., Davis, K.R., and Phillips, B.E., 1992. Report of the Paducah Gaseous Diffusion Plant ground water investigation phase III. Document KY/E-150, prepared by Martin Marietta Energy Systems, Inc., for the U.S. Department of Energy, 147 p.

Clausen, J.L., Sturchio, N.C., Heraty, L.J., Huang, L., and Abrajano, T., 1997. Evaluation of natural attenuation processes for trichloroethylene and technetium-99 in the Northeast and Northwest Plumes at the Paducah Gaseous Diffusion Plant, Paducah, Kentucky. A report by Lockheed Martin Energy Systems, Inc., for the U.S. Department of Energy, 65 p.

Clausen, J.L., Zutman, J.L., and Farrow, N.D., 1993. Characterization of the Northwest Plume utilizing a driven discrete-depth sampling system: Document KY/ER-22, prepared by the

Uranium Enrichment Organization, managed by Martin Marietta Energy Systems, for the U.S. Department of Energy under DOE contract no. DE-AC05-76OR00001.

Clausen, J.L., Zutman, J.L., Pickering, D.A., and Farrow, N.D., 1995. Final report on drive-point characterization of the Northwest Plume at the Paducah Gaseous Diffusion Plant. Document KY/ER-66, Martin Marietta Energy Systems Inc., Paducah Gaseous Diffusion Plant, Paducah, Kentucky.

Conant, B., 2001. A PCE plume discharging to a river: Investigation of flux, geochemistry, and biodegradation in the stream bed. Unpublished PhD dissertation, University of Waterloo, Waterloo, 543 p.

Davis, K.R., 1996. The McNairy Formation in the area of the Paducah Gaseous Diffusion Plant. Document KY/EM-148, prepared by Environmental Management and Enrichment Facilities, managed by Lockheed Martin Energy Systems for the U.S. Department of Energy under DOE contract no. DE-AAC05-76OR00001.

Davis, R.W., Lambert, T.W., and Hansen, A.J. Jr., 1973. Subsurface geology and ground-water resources of the Jackson Purchase region, Kentucky. U.S. Geological Survey Water-Supply Paper 1987, 66 p.

Daqing, C., and Eriksen, T.E., 1996, Reduction of pertechnetate in solution by heterogeneous electron transfer from Fe (II)-containing geological material. Environmental Science and Technology, vol. 30, p. 2263-2269

Donaldson, J.R., and Tryon, P.V., 1990. User's guide to STARPAC−The standards, time series, and regression package. National Institute of Standards and Technology Internal Report NBSIR 86-3448.

Etienne, N.M.P., 1999. Assessing potential biodegradation of trichloroethene in deep sediments at the Paducah Gaseous Diffusion Plant, Kentucky. Unpublished MS thesis, University of Kentucky, 128 p.

Etienne, N.M.P., Butler, D.L., Fryar, A.E., and Coyne, M.S., 2001. Trichloroethene biodegradation potential in wetland soils and palaeowetlands sediments. Bioremediation Journal, vol. 5, issue 1, p. 27-50.

Evaldi, R.D., and McClain, D.L., 1989. Stream flow, specific-conductance, and temperature data for Bayou and Little Bayou Creeks near Paducah, Kentucky, August 15 and 16, 1989. U.S. Geological Survey Open-File Report 89-582, 19 p.

Finch, W.I., 1967. Geologic map of part of the Joppa Quadrangle, McCracken County, Kentucky, U.S. Geological Survey Map GQ-652, 1 sheet.

Fryar, A.E., 1997. Subsurface degradation and sorption of chloroethenes in the vicinity of the Paducah Gaseous Diffusion Plant. Report prepared for the Federal Facilities Oversight Unit, Kentucky Water Resources Research Institute, University of Kentucky, 46 p.

Fryar, A.E., Wallin, E.J., and Brown, D.L., 2000. Spatial and temporal variability in seepage between a contaminated aquifer and tributaries to the Ohio River. Ground Water Monitoring & Remediation, vol. 20, no. 3, p. 129-146.

Fusillo, T., Sargent, B., Waler, R., and Ellis, W., 1991. Investigation of the discharge of ground water containing volatile organic compounds into a stream at Picatinny Arsenal, New Jersey. Eos, Transactions, American Geophysical Union, vol. 72, no. 4, p. 185-186.

Genereux, D.P., and Hemond, H.F., 1990. Naturally occurring radon−222 as a tracer for streamflow generation: steady state methodology and field example. Water Resources Research, vol. 26, no. 12, p. 3065-3075.

Genereux, D.P., and Hemond, H.F., 1992. Determination of gas exchange rate constants for a small stream on Walker Branch watershed, Tennessee. Water Resources Research, vol. 28, no. 9, p. 2365-2374.

Grant, R.S., and Skavroneck, S., 1980. Comparison of tracer methods and predictive equations for determination of stream reaeration coefficients on three small streams in Wisconsin. U.S. Geological Survey Water Resources Investigation Report 80-19, 43 p.

Hopkins, G.D., and McCarty, P.L., 1993. A field evaluation of in situ aerobic cometabolism of trichloroethylene and three dichloroethylene isomers using phenol and toluene as the primary substrates. Environmental Science & Technology, vol. 29, p. 1628-1637.

Imbrigiotta, T.E., Ehlke, T., Wilson, B.H., and Wilson, J.T., 1996. Natural attenuation of a trichloroethene plume at Picatinny Arsenal, New Jersey. In Symposium on Natural Attenuation of Chlorinated Organics in Ground Water, USEPA Report /540/R-96/509, p. 83-89.

Jacobs EM Team, 1999. Transport modeling results for the Northeast Plume interim remedial action and the Northwest Plume at the Paducah Gaseous Diffusion Plant, Paducah, Kentucky, Report prepared for the U.S. Department of Energy under contract no. DE-AC05-98OR22700, 100 p.

Jacobs Engineering Group, Inc., 1995. Technical memorandum for interim remedial action of the Northeast Plume at the Paducah Gaseous Diffusion Plant, Paducah, Kentucky. Report prepared for the U.S. Department of Energy under contract no. DE-AC05-93OR22028.

Kilpatrick, F.A., and Cobb, E.D., 1985. Measurement of discharge using tracers. U.S. Geological Survey Techniques of Water-Resources Investigations Book 3, Chapter A16,
52 p.

Kilpatrick, F.A., Rathbun, R.E., Yotsukura, N., Parker, G.W., and Delong, L.L., 1987. Determination of stream reaeration coefficients by use of tracers. U.S. Geological Survey Open-File Report 87-245, 52 p.

Kilpatrick, F.A., and Wilson, J.F., 1989. Measurement of time of travel in streams by dye tracing. Geological Survey Techniques of Water-Resources Investigations Book 3, Chapter A9, 27 p.

Kim, H., and Hemond, H.F., 1998. Natural discharge of volatile organic compounds from contaminated aquifers to surface waters. Journal of Environmental Engineering, vol. 124, no. 8, p. 744-751.

Kimball, B.A., Runkel, R.L., and Gerner, L.J., 2001. Quantification of mine-drainage inflows to Little Cottonwood Creek, Utah, using a tracer-injection and synoptic-sampling study. Environmental Geology, vol. 40, p. 1390-1404.

Kolata, D.R., Treworgy, J.D., and Masters, J.M., 1981. Structural framework of the Mississippi Emabayment of southern Illinois. Illinois State Geological Survey Circular 516, 38 p.

Langston, C.J., McIntyre, J., and Street, R., 1998. Investigation of the shallow subsurface near the Paducah Gaseous Diffusion Plant using SH-wave seismic methods. Society of Exploration Geophysicists, 1998 Technical Program, Expanded Abstracts, vol. 1, p. 878-880.

Larkin, R.G., and Sharp, J.M., 1992. On the relationship between river-basin geomorphology, aquifer hydraulics, and ground-water flow direction in alluvial aquifers. Geological Society of America Bulletin, vol. 104, no. 12, p. 1608-1620.

LaSage, D.M. and Fryar, A.E., 2000. Quantifying discharge of contaminated ground water into a first-order stream, McCracken County, Kentucky. In Program and Abstracts, 45th Annual Midwest Ground Water Conference, p. 47.

Lloyd, J.R., Sole, V.A., Van Praagh, J.R., and Lovley D.R., 2000. Direct and Fe (II)–mediated reduction of technetium by Fe(III)–reducing bacteria. Applied and Environmental Microbiology, vol. 66, no. 9, p. 3743-3749.

Marcher, M.V., and Stearns, R.G., 1962. Tuscaloosa Formation in Tennessee. Geological Society of America Bulletin, vol. 73, p. 1365-1386.

McGrain, P., and Currens, J.C., 1978. Topography of Kentucky. Kentucky Geological Survey Series 10, Special Publication 25, 76 p.

Meyer, R.E., Arnold, W.D., and Case, F.I., 1989. Thermodynamics of technetium related to nuclear waste disposal: Solubilities of Tc(IV) oxides and the electrode potential of the Tc(VII)/Tc(IV)-oxide couple. Division of Engineering, Office of Nuclear Regulatory Research, U.S., Nuclear Regulatory Commission, Washington, D.C.

Nelson, M.J.K., Montgomery, S.O., Mahaffey, W.R., Pritchard, P.H., 1987. Biodegradation of trichlorothylene and involvement of an aromatic biodegradative pathway. Applied and Environmental Microbiology, vol. 55, p. 2819-2826.

Olive, W.W., 1966. Geological Maps of Heath Quadrangle, McCracken and Ballard counties, Kentucky. U.S. Geological Survey Map GQ-561, 1 sheet.

Olive, W.W., 1980. Geological maps of Jackson Purchase Region, Kentucky. U.S. Geological Survey

Pignolet, L., Auvray, F., Fonsny, K., Capot, F., and Moureau, Z., 1989. Role of various microorganisms on Tc behavior in sediments. Health Physics, vol. 57, no. 5, p. 791-800.

Plumb, R.H., and Pitchford, A.M., 1985. Volatile organic scans: Implications of ground water monitoring. In Proceedings of the NWWA/API Conference on Petroleum Hydrocarbons and

Organic Chemicals in Ground Water. National Water Well Association, Dublin, Ohio, p. 207-223.

Rantz, S.E., 1982. Measurement and computation of streamflow, vol. 1: Measurement of stage and discharge. U.S. Geological Survey Water-Supply Paper 2175, 22 p.

Runkel, R.L., 1998. One-dimensional transport with inflow and storage (OTIS): A solute transport model for streams and rivers. U.S. Geological Survey Water Resources Investigation Report no. 98-4018, 73 p.

Runkel, R.L., and Broshears, R.E., 1991. One-dimensional transport with inflow and storage (OTIS): A solute transport model for small streams. University of Colorado, CADSWES Technical Report 91-01, 85 p.

Schaumburg, F.D., 1990. Banning trichloroethylene: responsible reaction or overkill? Environmental Science and Technology, vol. 24, no.1, p. 17-22.

Schwalb, H.R., 1969. Paleozoic geology of the Jackson Purchase Region, Kentucky, with reference to petroleum possibilities. Kentucky Geological Survey Series 10. Report of Investigations 10.

Schwarzenbach, R.P., Gschwend, P.M., and Imboden, D.M., 1993. Environmental Organic Chemistry. Wiley-Interscience, New York, 681 p.

Seaman, J.C., Bertsch, P.M., and Miller, W.P., 1995. Ionic tracer movement through highly weathered sediments. Journal of Contaminant Hydrology, vol. 20, p. 127-143.

Smith, J.H., Bomberg, D.C., and Haynes, D.L., 1980. Prediction of volatilization rates of high-volatility chemicals from natural water bodies. Environmental Science and Technology, vol. 14, p. 1332-1337.

Sweat, C.J., 2000. The role of organic carbon in natural attenuation of a trichloroethene-contaminated aquifer system, Paducah, Kentucky. Unpublished MS thesis, University of Kentucky, 132 p.

Till, J.E., 1986. Source terms of technetium-99 from nuclear fuel cycle facilities. In The Behaviour of Technetium in the Environment. Desmet, S. and Myttenaere, C. (Eds.), Elsevier, New York, p. 1-19.

USDOE, 1996. Phase I Paducah Gaseous Diffusion Plant Waste Area Group 6 industrial hydrological study: Document DOE/OR/07-1478&D1, prepared by Oak Ridge National Laboratory and Environmental Management and Enrichment Facilities, managed by Lockheed Martin Energy Systems for the U.S. Department of Energy under DOE contract DE-AC05-96OR22464.

USEPA, 1985. Substances found at proposed and final NPL sites through update number three. Document NPL-U3-6-3, USEPA, Washington, D.C.

USEPA, 1986. Test methods for evaluating solid waste, physical/chemical methods, third edition.

Van Loon, L., Satalmans, M., Maes, M., Cremers, A., and Cogneau, M., 1986. Soil humic acid complexes of technetium: Synthesis and characterization. In The Behaviour of Technetium in the environment. Desmet, S. and Myttenaere, C. (Eds.), Elsevier, New York, p. 143-153

Vasudevan, D., Fimmen, R.L., and Francisco, A.B. 2001. Tracer-grade rhodamine WT: structure of constituent isomers and their sorption behavior. Environmental Science & Technology, vol. 35, no. 20, p. 4089-4096.

Vroblesky, D.A., Lorah, M.M., and Trimble, S.P., 1991. Mapping zones of contaminated ground water discharge using creek-bottom-sediment vapor samplers, Aberdeen Proving Ground, Maryland. Ground Water, vol. 29, p. 7-12.

Wallin, E.J., 1998. Ground-water/stream-water interactions in the vicinity of the Paducah Gaseous Diffusion Plant, McCracken County, Kentucky. Unpublished MS thesis, University of Kentucky, 111 p.

Wanninkhof, R., Mulholland, P.J., and Elwood, J.W., 1990. Gas-exchange rate for a first order stream determined with deliberate and natural tracers. Water Resources Research, vol. 26, no. 7, p. 1621-1630.

Westrick, J.J., Mello., J.W., and Thomas, R.F., 1984. The ground water supply survey. Journal of the American Water Works Association, vol. 76, no. 5, p. 52-59.

White, D.S., Elzinga, C.H., and Hendricks, S.P., 1987. Temperature patterns within the hyporheic zone of a northern Michigan river. Journal of the North American Benthological Society, vol. 6, no. 2, p. 85-91.

Wildung, R.E., McFadden, K.M., and Garland, T.R., 1979. Technetium sources and behavior in the environment. Journal of Environmental Quality, vol. 8, no. 2, p. 156-161.

Wilson, J.T., and Wilson, B.H., 1985. Biotransformation of trichloroethylene in soil. Applied and Environmental Microbiology, vol. 49, p. 242-243.

Winkler, A., Bruhl, H., Trapp, C.H., and Bock, W.D., 1988. Mobility of technetium in various rocks and defined combinations of natural minerals. Radiochimica Acta, vol. 44, no. 45, p. 183-186.

Winter, T.C., Harvey, J.W., Franke, O.L., and Alley, W.M., 1998. Ground water and surface water, a single resource. U.S. Geological Survey Circular 1139, 79 p.

Yotsukura, N., Stedfast, D.A., and Brutseart, W.H., 1983. An assessment of steady state propane gas method for reaeration coefficients−Cowaselon Creek, New York. U.S. Geological Survey Water Resources Investigation Report 83-4183, 95 p.

Vita

Personal Details
Name: Abhijit Mukherjee
Birth Date: 23rd February 1976
Birth Place: Calcutta, India
Father: Barindra Lal Mukherjee
Mother: Kajali Mukherjee

Education

- Bachelor of Science with Honors in Geology [B.Sc(Hons.)] from University of Calcutta, India, 1997
- Master of Science (M.Sc) in Geology from University of Calcutta, India, 1999
- Post Graduate diploma in software engineering from National Institute of Information Technology, India, 2000

Occupation

- Teaching Assistant in Geological Sciences, 2001-2003
- Research Assistant in Geological Sciences, summer 2002

Honors/Scholarships

- Research grant from Southeastern Section Geological Society of America, 2002
- Research support award, Graduate School, University of Kentucky, 2002
- Research support award, Department of Geological Sciences, University of Kentucky, Brown-McFarlan Fund, 2002
- Nominated for "International Man of the Year" by International Biographical Center, Cambridge, UK, 2001
- Selected as "One of the 2000 Outstanding Scientists and Intellectuals" by International Biographical Center, Cambridge, UK, 2001
- Nominated for "Young Scientist Award" by Indian Science Congress Association, 2001
- All India Rank 20th in GATE, Government of India, 2001
- Recipient of National Scholarship from Government of India for excellence in graduate study, 1999
- Recipient of Total Freedom Scholarship from National Institute of Information Technology (NIIT), India for software engineering study, 1997

Publications

- Mukherjee, A. and Fryar, A.E., 2003. Identification of natural attenuation of trichloroethene and technetium along Little Bayou Creek, Kentucky, by tracer tests. Geological Society of America Abstracts with Programs, vol. 35, no. 1.

- Mukherjee, A., and Fryar, A.E., 2003. Natural attenuation of trichloroethene and technetium along Little Bayou Creek, Kentucky. In Proceedings of Kentucky Water Resources Annual Symposium, Kentucky Water Resources Institute.
- Mukherjee, A., and Mitra, A.K., 2003. Geotechnical study of mass movements in a part of the eastern Himalayas. Journal of Indian Geology (in review).
- Mukherjee, A., 2002. Hydrogeological study on causes and effects and remediation of arsenic contamination of Bengal basin ground water. In Proceedings, 89th Session of Indian Science Congress, Earth System Sciences.
- Ghosh, A.R., and **Mukherjee, A**., 2002. Arsenic contamination and human health impacts in Burdwan district, West Bengal, India. Geological Society of America Abstracts with Programs vol. 34, no. 2.
- Mukherjee, A., 2001. Assessment of causal factors and suggested remedial measures for the landslides of the west slope of Kalimpong hills. In Proceedings, 88th Session of Indian Science Congress, Earth System Sciences.
- Mukherjee, A., 1999. Triggering the ages of ice. Breakthrough, vol. 8 no. 2.
- Mukherjee, A., 1995. March toward extinction. Scan, vol. 8.